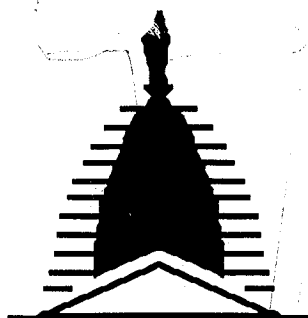NASA-CR-197155

NASw-4435

IN-05-CR

26134

159 p

UNIVERSITY of NOTRE DAME

NASA/USRA UNIVERSITY ADVANCED DESIGN PROGRAM 1993-1994

PROJECT CENTER MENTOR: NASA-AMES DRYDEN FLIGHT RESEARCH FACILITY

Icarus - Rewaxed

A HIGH SPEED, LOW-COST GENERAL AVIATION AIRCRAFT FOR "AEROWORLD"

April 1994

Department of Aerospace and Mechanical Engineering
University of Notre Dame
Notre Dame, IN 46556

Recent Future, Inc.

presents

ICARUS

Rewaxed

Team Leader: Bryan Farrens
Chief Engineer: Macy Hueckel
Director of Manufacturing: Dan Fulkerson
Propulsions Analyst: Matt Barents
Control Systems Analyst: Brian Capozzi
Structures Analyst: Keri Ramsey

"Fly High, Touch The Sun..."

TABLE OF CONTENTS

Appendices

LIST OF FIGURES

LIST OF TABLES

List of Nomenclature

AC	aerodynamic center
AR	aspect ratio
C_D	airplane drag coefficient
C_d	section drag coefficient
CG	center of gravity
$C_{L\alpha}$	3D lift curve slope
C_L, C_{Lmax}	Lift coefficient (aircraft)
C_l	section lift coefficient
$C_{l\beta}$	roll power coefficent due to sideslip
$C_{l\delta a}$	roll power coefficient due to aileron deflection
C_{Mo}	coefficent of moment curve intercept
$C_{M\alpha}$	coefficient of moment curve slope
$C_{M\delta e}$	elevator control power
$C_{n\beta}$	yawing moment coefficient
C_t	coefficient of thrust
E	modulus of elasticity
FAA	Federal Aviation Administration
FCC	Federal Communications Commision
FS	factor of safety
I	moment of inertia
J	advance ratio
K_g	gust alleviation factor
L/D	lift to drag ratio
L	lift
M	bending moment
MAC	mean aerodynamic chord
R	turn radius
R/C	rate of climb
RE	Reynold's Number
S_W, S_V, S_H	area of wing, vertical and horizontal tails
V, V_∞	velocity, shear
V_V	vertical volume ratio
W	weight
WMTO	maximum take-off weight

b	span
c	chord
e	Oswald efficiency
$i_{w,t}$	incidence angle of wing/tail
g	gravitational constant
$l_{t,v}$	moment arm from cg to 1/4 chord of tail
m_0	section lift curve slope
m	lift curve slope corrected for finite wing
n	load factor
$\bar{p}$	roll rate
q	dynamic pressure
t/c	airfoil thickness ratio
Γ	dihedral angle
ϕ	bank angle
α	angle of attack
δ	tip deflection
δ_a	aileron deflection
δ_e	elevator delection
δ_r	rudder deflection
ϕ	angle made by CG and tire
η	ratio of dynamic pressures
θ	angle made by AC and tire
σ	stress
ρ	density
τ	flap effectiveness factor

1.0 Executive Summary

Icarus Rewaxed is a single engine, 6 passenger, general aviation airplane. With a cruise velocity of 72 ft/s , the *Icarus* can compete with the performance of any other airplane in its class with an eye on economics and safety. It has a very competitive initial price ($3498.00) and cost per flight ($6.36 - 8.40). *Icarus* can serve all airports in Aeroworld with a takeoff distance of 25.4 feet and maximum range of 38000 feet. It is capable of taking off from an unprepared field with a grass depth of 3 inches.

Icarus has a low wing configuration and uses dihedral, rudder, and ailerons for roll control. A rudder/elevator combination provides yaw and pitch control. The "tail-dragger" landing gear incorporates a steerable tail wheel to facilitate ground control. The propulsion system uses an Astro-15 electric motor mounted at the nose of the aircraft. It incorporates the Zingali 10-8, 3 bladed propeller, and thirteen Panasonic batteries (1.2V, 1400 mah) for fuel.

With the two main design objectives of high speed and takeoff distance compatible with the Aeroworld airports, the wing design was of primary importance. A large wing was needed to satisfy the relatively short takeoff distance (28 feet), yet too large a wing hinders the other objective of high speed by creating drag. The current wing design balances these two considerations. This rectangular wing uses a DF-101 airfoil, has an area of 7.5 ft^2, and an Aspect Ratio of 7.2. High lift devices were considered for the wing design, but the increased manufacturing time and cost outweighed the potential benefits.

Structurally, the *Icarus* optimizes passenger safety while minimizing weight. All load bearing components are designed with a factor of safety of 1.4 . Weight minimization came from finding the most extreme loading condition and calculating the margin of safety. By designing the aircraft for this extreme

condition without over-designing, Recent Future, Inc. determined the smallest amount of structure needed for any expected flight condition or any reasonable extreme loading. The driving design objective of high cruise speed motivates this search for weight savings.

This need to supply strength with minimal weight was the motivating factor to explore materials that have not been previously used in Aeroworld. New materials include advanced graphite composites and high strength steel. Although the graphite outperformed all other materials in strength and stiffness for its weight, its high cost drove it out of consideration. Steel gave virtually the same performance as graphite at 25% of the cost. Thus, a thin-walled steel shaft is used as the main load bearing component: the wing spar. This new material represents a tremendous gain in structural strength over previous Aeroworld wooden designs. It also provides a slight savings in weight. The increased strength is of primary importance for this high speed aircraft, for potential gusts or maneuvers at cruise can dramatically increase the load factor.

The *Icarus* has the ability to take off from an unprepared field with three inch grass. This design requirement put a premium on the tail-dragger landing gear design. This gear must provide adequate clearance for the propeller, yet still be able to handle the stresses inherent in landing impact. The landing gear contributes over 35% of the total drag for the aircraft. With this in mind, the landing gear of the *Icarus* is designed to be structurally sound with a minimum amount cross-sectional area. Steel piano wire struts are used for the main gear. These struts are then attached to the steel wing spar to provide adequate strength, yet still cushion the plane on impact.

Another facet that sets the *Icarus* apart from existing airplanes in the Aeroworld market is the use of airfoil sections for the horizontal tail. Other companies have cited weight savings as a primary motivator for a flat plate design.

However, Recent Future's analysis shows that the structural and aerodynamic gains from airfoil shapes far outweigh the relatively minor (less than one ounce at the extreme) weight savings. The drag benefit from the aerodynamic horizontal tail shape helps maximize cruise velocity, and the structural benefits with the thicker spar allows the tail to handle the large load factors at the extreme of the flight envelope.

The main weakness in this design stems from the competing objectives of minimum takeoff distance and maximum flight speed. Maximum cruise velocity is the prime figure of merit for Recent Future, Inc., but this parameter could not be completely optimized because of the basic need for servicing the existing airports. Thus the large wing needed for takeoff hinders the performance in flight by creating excess drag. The long landing gear also lessens performance by exposing bluff body struts into the airflow.

Another potential weakness comes from the risk involved with trying a new wing spar design. Without a data base or previous examples, the wing design represents a break from the security of experience. There are technical hurdles inherent in using a steel shaft. The first possible problem comes from the fact that this shaft is tapered[1]. While this taper does not weaken the shaft, it does present a problem of positioning the airfoils. In order to maintain the desired shape of the wing, each airfoil will have to be individually fashioned and attached to the spar. This will increase manufacturing costs and may lessen wing effectiveness. The second potential weakness comes from the fact that the steel spar will not traverse the entire span of the wing. It is imperative, therefore, that the wood structure used to extend the wing to its desired length is capable of supporting all possible

---

[1] The shaft was purchased from a subcontractor -- *The Golf Pro* in Mishawaka, IN -- and its design is geared toward the needs of a good one wood.

loads. This design runs the risk of have a "weak link" position that would negate the strength benefits of the steel shaft.

Overall, *Icarus Rewaxed* fills the market need for a high-speed, low cost aircraft. It provides customers with a general aviation craft that can compete in the existing performance market with the added security of an advanced structure. With the use of advanced materials, the maneuvering capability of the *Icarus* is increased, as it can withstand greater load factors than previous aircraft. With the ability to service and reach all existing airports in Aeroworld, only the sky limits the *Icarus* owner.

Figure 1.1: Isometric View of *Icarus Rewaxed*
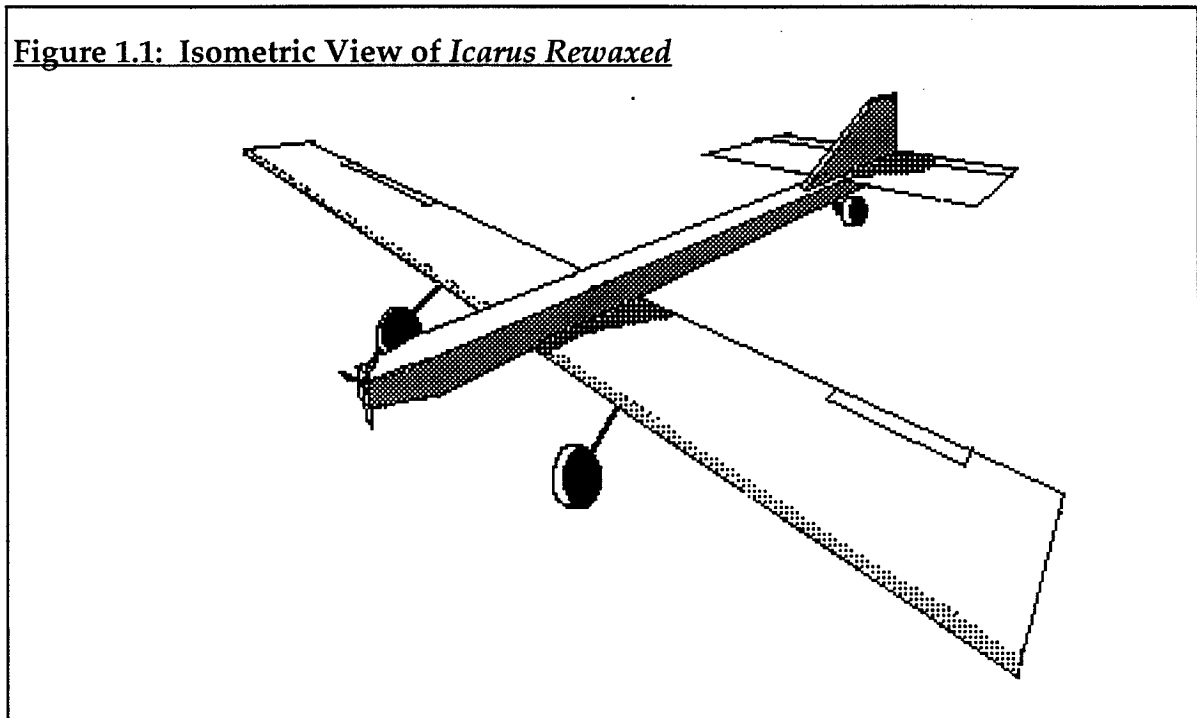
Table 1.1: Specification Summary

Fuselage		
	Total Length:	45 inches
	Payload Volume:	140 in^2
	Height:	2.75 inches
	Width:	3.5 inches

Wing		
	Airfoil Selection:	DF-101
	Wing Area:	7.5 ft^2
	Aspect Ratio:	7.2
	Span:	7.35 ft
	Chord:	12.25 in
	Dihedral:	5°
	Wing Incidence Angle:	1°
	Wing Sweep:	0°
	Estimated Airplane Clmax	0.95
	Stall Angle:	12°
	Aileron Size:	12" x 1"
	Max Aileron Deflection:	± 15°

Tail: Horizontal		
	Airfoil Selection:	SD8020
	Hor. Tail Area:	1.56 ft^2
	Aspect Ratio:	3.5
	Span:	28 inches
	Chord:	8 inches
	Incidence Angle:	-2°
	Elevator Size:	26" x 1"
	Max Elevator Deflection:	± 20°

Tail: Vertical		
	Flat Plate	
	Ver. Tail Area:	71.5 in^2
	Aspect Ratio:	1.05
	Root Chord:	9 inches
	End Chord:	5 inches
	Height:	11 inches
	Rudder Area:	11" x 4"
	Max Rudder Deflection:	± 30°

Propulsion		
	Motor:	Astro 15
	Propeller Designation:	Zingali 10-8
	Number of Blades:	3
	Number of Batteries:	13
	Battery Pack Voltage:	15.6 volts

Side View

Engine

Passenger Passenger

Speed Controller

Battery Battery
Battery Battery

Aileron Servo

Receiver & Power Pack

Rudder & Elevator Servo

Passenger Passenger Passenger Passenger

←—— **Wing Carrythrough** ——→

Top View

Engine

Passenger Passenger

Speed Controller

Battery Battery
Battery Battery
Battery Battery

AileronServo

Receiver

Power Pack

Elevator Servo

RudderServo

Passenger Passenger Passenger Passenger

←———————————————————— **Total Length 45 inches** ————————————————————→

Figure 1.2: Three View External Configuration

(scale: 1 inch = 1 foot)

1 - 7
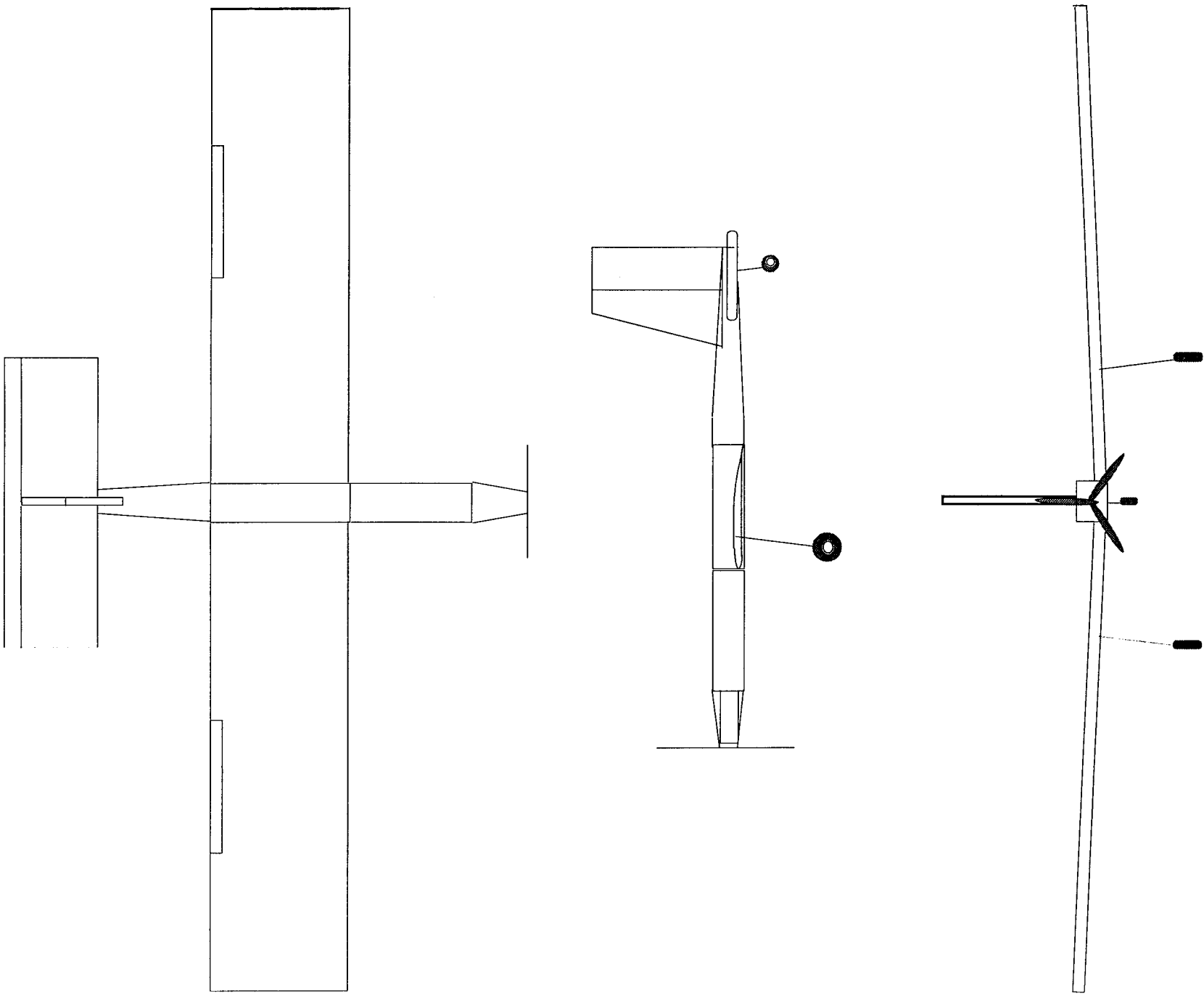
2.0 MISSION DEFINITION

The mission of the project undertaken by Recent Future, Incorporated is to design a low-cost, high-speed, general aviation aircraft to augment the current commercial fleet in Aeroworld (see Figure 2.1 & Table 2.1). The airplane is expected to minimize cost while demonstrating improved cruise speed over the current fleet.

Figure 2.1: Layout of Aeroworld Cities and Airports
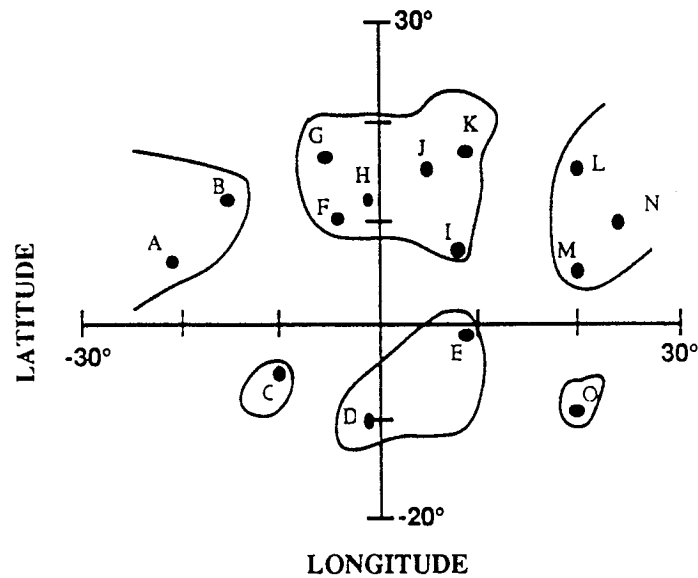
LONGITUDE

Table 2.1: Information of Aeroworld Cities

City	Longitude	Latitude	Runway Length Factor
A	-21	6	1
B	-15	12	0.8
C	-10	-5	0.7
D	-1	-10	1
E	9	-1	1
F	-4	10	1
G	-5	17	1
H	-1	12	1
I	8	7	1
J	5	15	1
K	9	17	1
L	20	15	1
M	20	5	1
N	24	10	1
O	20	-9	0.7

2.1 SUMMARY OF DESIGN REQUIREMENTS & OBJECTIVES

The following is a summary of the primary requirements and objectives imposed us by various external and internal agents. The requirements are imposed by three groups in particular Management [MI], Government [GI], and the Design Group [DI]. The objectives are set forth by the group as "performance guarantees" for the ultimate product of the design, the technology demonstrator.

2.2 REQUIREMENTS

- **Takeoff and Landing**

  The aircraft must be able to takeoff and land under its own power as well as takeoff from an "unmowed" grass/weed field with a grass depth of 3 inches and then climb to a height of 50 feet in a distance of 200 feet. The landing gear must be configured with respect to the center of gravity such that it has no tendency to tip over during the takeoff roll. In addition, the spacing of the main and rear gear must be such that neither the tail nor the propeller strikes during the ground roll. [MI]

- **Propeller/Engine**

  The aircraft must be designed to provide at least a 3.5 inch propeller ground clearance to allow for ground roll on the aforementioned unprepared surfaces. [DI]

- **Stability and Control**

  The center of gravity must be placed such that the aircraft is statically stable. [DI] Control will be achieved through the use of no more than 4 S28 servos. [MI]

- **Performance**

  The aircraft must be capable of performing a steady, level, 60 foot radius turn at a velocity of 25 ft/s. In addition, the aircraft load factor can have a maximum value of at least 2.0 during any maneuver. [MI]

- **Loiter time and Range**

  The aircraft must be capable of servicing every airport in Aeroworld, loiter for one minute, and still be capable of reaching the closest secondary airport for each destination.[MI]

- **Altitude Restriction**

    During the indoor portion of the design validation, the altitude of the technology demonstrator must not exceed 25 feet. [MI]

- **Survivability**

    The vital components of the radio control system, propulsion system, and other flight systems should be able to withstand a crash from any flight condition.[MI]

- **Factor of safety**

    The material/construction of the aircraft will have a minimum factor of safety of 1.4. [DI]

- **Wings**

    Two separate, complete wings must be constructed - one will be used on the technology demonstrator, the second will be subjected to a load test to determine its point of failure.[MI]

- **Regulation responsibility**

    All FAA and FCC regulations for operation of remotely piloted vehicles and others imposed by the course instructor must be observed.[GI]

- **Passengers**

    The aircraft must be capable of carrying 4 passengers as well as 2 crew members requiring 8 cubic inches for each passenger and crew member as well as an additional 4 cubic inches of baggage space per person.[MI]

    - Note: This differs from the original DR&O. Originally the design team believed the requirement to be 6 passengers plus two crew members. They were later informed that the six passengers included the two crew members.

- **System Installation/Maintenance time**

    The radio control system and complete propulsion system must be removable and positioned in the airframe such that a complete system installation can be performed in 20 minutes. [MI]

- **Fuel/batteries**

    The fuel/batteries must be placed in the wing carry-through structure to simulate actual industry practice of wing fuel storage. [MI]

- **Cost**

    The raw materials used to construct the aircraft will have a maximum cost of 200 dollars. [MI]

- **Size**

    All components of the airframe and supporting structure must be designed to allow for transportation from the design lab to the validation sites. In particular, the aircraft sections must be able to pass through the openings having dimensions of 7 feet in height and 3 feet in width. [DI]

2.3 OBJECTIVES

- **Handling qualities**

    The aircraft will be designed such that it has relatively benign handling qualities to allow it to be flown by novice pilots.

- **Cruise velocity**

    As this aircraft is to fill a distinctly new mission as compared to the existing fleet of larger commercial aircraft, it will demonstrate an improved cruise speed of 60 ft/s.

- **Takeoff distance**

    The aircraft will be capable of taking off within 28 feet to allow service to all airports in Aeroworld.

- **Range**

    The aircraft will have an effective range of 30000 feet or greater allowing for the required non-stop service between all existing airports in Aeroworld as well as the required loiter time and alternate routing.

- **Wind allowance**

  Throughout all phases of flight, the aircraft will be capable of withstanding a gust of up to 10 mph.

- **Weight**

  The weight of the aircraft is not to exceed 4.5 pounds.

- **Throttle**

  The aircraft will perform at variable throttle settings allowing for controlled flight during both the indoor and outdoor phases of the validation.

- **Landing gear/Taxiing**

  The landing gear will be configured to allow for adequate ground control on both prepared and unprepared surfaces enabling the aircraft to turn in a 10 foot radius during taxi.

3.0 CONCEPT SELECTION

3.1 INTRODUCTION

The first step in devising the individual concepts was to list the major goals for the aircraft. The key factors came down to the aircraft having a high cruise velocity and a low cost. A third, yet not as important, factor in devising the individual concepts was innovation. The individual concepts presented four possibilities for the final concept: a high wing design, a low wing design, a canard design, and a pusher propeller design.

3.2 HIGH WING DESIGN

Two out of the six individual concepts featured a high wing design (Figure 3.1). This design has the advantage of being inherently stable with regard to roll. Because of the restoring moment caused by the fuselage, little or no dihedral would be needed for roll stability. The high wing design also had the advantage of a large data base of past experience.

Since (according to the design requirements) the fuel must be located in the wing carry through, access to internal components would be a problem. Adjusting the battery pack would involve removing the entire wing. This accessibility problem was the primary reason for choosing another concept.

3.3 LOW WING DESIGN

Three out of the six individual concepts were low wing planes. These designs featured the passengers seated two abreast, with two levels (illustrated in Figure 3.2). The main advantage of the design was the accessibility to the interior through the top of the plane. Another advantage was the relatively large data base. This documentation of past experience greatly aided the initial

iteration of size, weight, and performance parameters. This concept also featured ailerons coupled with dihedral for better roll control. These advantages were incorporated into *Icarus*.

The disadvantage of the individual designs was the fuselage shape. Sitting the passengers in the two abreast fashion increased the frontal area and hence increased the overall drag of the aircraft. The primary design objective for Recent Future, Inc. was to maximize cruise speed. Large drag is an obvious detriment to this objective.

3.4 CANARD DESIGN

The next individual concept entailed a canard design, shown in Figure 3.3. The canard was placed high on the fuselage, while the wing was mounted low. The remaining structure is comparable to the high and low wing designs.

There are a few advantages of the canard. One advantage is that the canard will stall before the wing during flight. This makes for a safer aircraft. Even if a small amount of lift is lost as a result of the canard surface being stalled, the larger main wing is still producing a significant amount of lift, because the main wing has not yet stalled. Another advantage of the canard design is that unlike an aft tail, the canard produces positive lift. This adds to the lift of the wing, instead of decreasing it as an aft tail does.

The main disadvantage of the canard came about due to the proposed design of a large main wing and a very short fuselage. The fuselage was kept small in order to minimize drag. Because of the short fuselage, the moment arm to the canard would be quite small, thus forcing the canard surface to be quite large to obtain the desired control. When the canard surface is made this large, the airplane obtained is in effect one with two large main wings, as opposed to one with a main wing and a smaller control surface.

3.5 PUSHER PROPELLER DESIGN

The final individual concept featured a pusher propeller configuration (illustrated in Figure 3.4). This concept included a radically shaped fuselage designed to minimize space and cross-sectional area. The motor would be attached above the main fuselage and would lock down a removable high wing.

The main advantage of this design was innovation. The radically different profile would set this plane aesthetically apart from other designs, past and present. Aerodynamically, this design optimizes the efficiency of the wing by exposing it to a clean airflow. Theoretically, the small fuselage cross section would reduce drag and minimize weight. The last advantage concerned the placement of the propeller. In this elevated position, this design could shorten the landing gear and still meet the tip clearance requirements set by the design requirements. Since the landing gear represents a significant fraction of the total drag (25-40% in past aircraft), reducing the size of the gear should increase high speed performance.

This design had disadvantages as well. The main disadvantage came from the fact that the pusher propeller configuration had not been tried before with the same class of motor. Thus with no data base, this option brought a large amount of risk. The main technical disadvantage of this design comes from the placement of many of the internal components. With the motor in the middle of the fuselage, the two heaviest pieces of equipment (motor and fuel) are located near or aft of the desired center of gravity position. This would make balancing the airplane and achieving the desired control power very difficult. Finally, while the wing efficiency would increase, the propeller efficiency would drop. This loss would come from the fact that the propeller no longer would experience clean flow.

While this design had much sentimental support and innovative appeal, its technological risks proved too great. Given the limited experience of the members of Recent Future, Inc. and the lack of a past data base, this design seemed too radical.

3.6 *ICARUS REWAXED*

The final concept chosen incorporated many of the strengths of the individual concepts, while eliminating the weaknesses. A summary of strengths and weaknesses is shown in Table 3.1. *Icarus Rewaxed* is a low wing aircraft using dihedral, rudder, and ailerons for roll control. This low wing also allows easy access to internal components. The minimal fuselage concept of the pusher propeller design was chosen to minimize frontal area, thus minimizing drag. This fuselage design involves seating the passengers in a single row.

In order to maximize cruise speed, the *Icarus* features low drag airfoil sections in the horizontal tail section. This subtle departure from many past designs provides better drag performance than the usual flat plate. The *Icarus* is also equipped with a three-bladed propeller to maximize thrust, therefore increasing the cruise velocity and decreasing the takeoff distance.

The overall design remained simple so to keep cost to a minimum. The decision was made that innovation was secondary to cost, and thus the appearance of the aircraft remained contemporary and simple to minimize the man hours necessary for construction.

Diagrams of the external and internal configurations are shown in Figures 1.1 and 1.2.

Table 3.1: Summary of Concepts

CONCEPT	STRENGTHS	WEAKNESSES
High Wing	• better roll stability • large database from past designs	• lack of accessibility to internal components
Low Wing	• accessibility • large database from past designs • ailerons/dihedral	• large frontal area
Canard	• canard free from wing interference • stalls before wing • positive lift	• large size of canard
Pusher Propeller	• innovation • wing sees clean flow • shorter landing gear - less drag • small fuselage cross section	• lack of database/ high risk • difficult to achieve stable CG location • reduced propeller efficiency
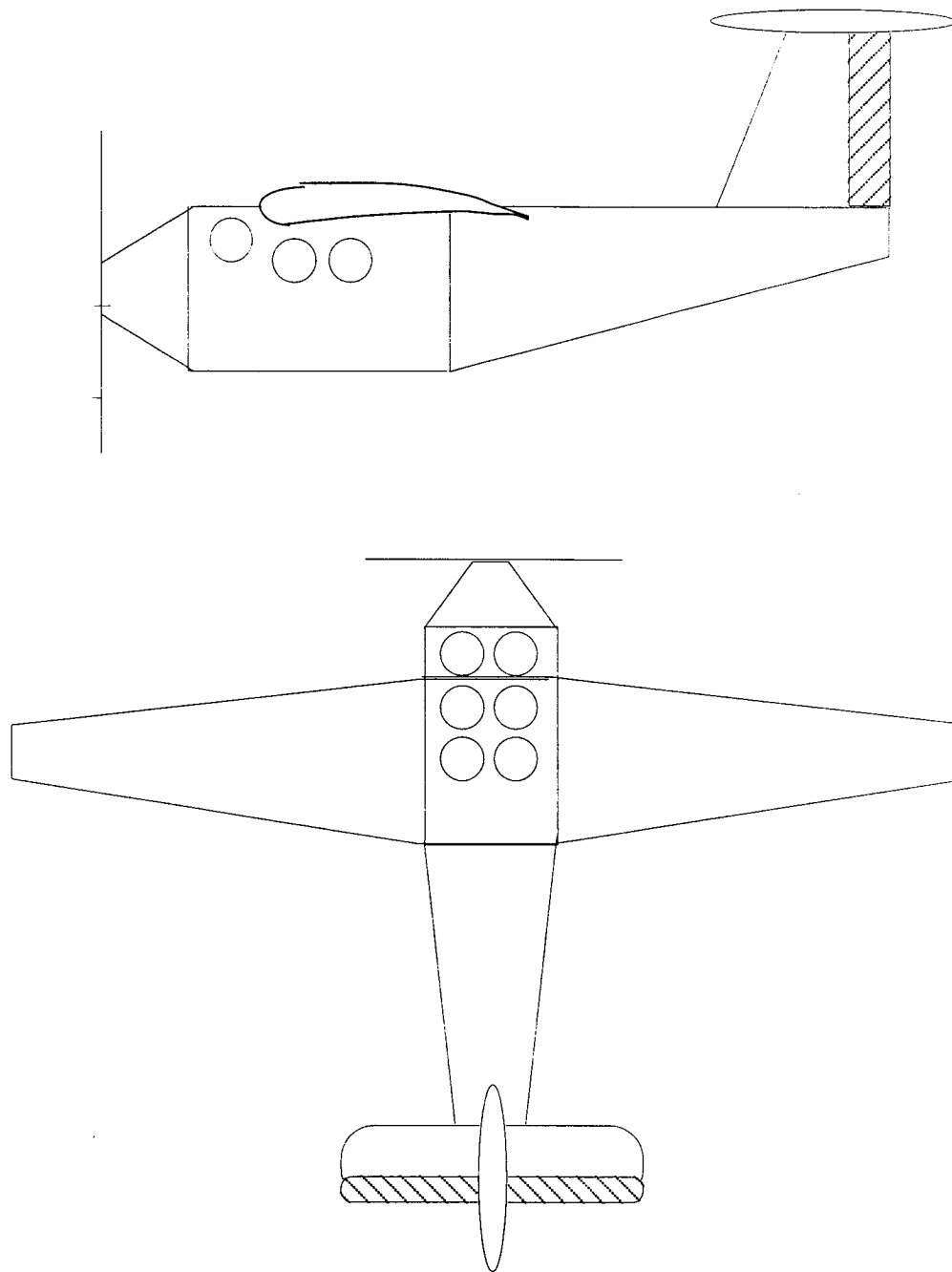
Figure 3.1: High Wing Individual Concept
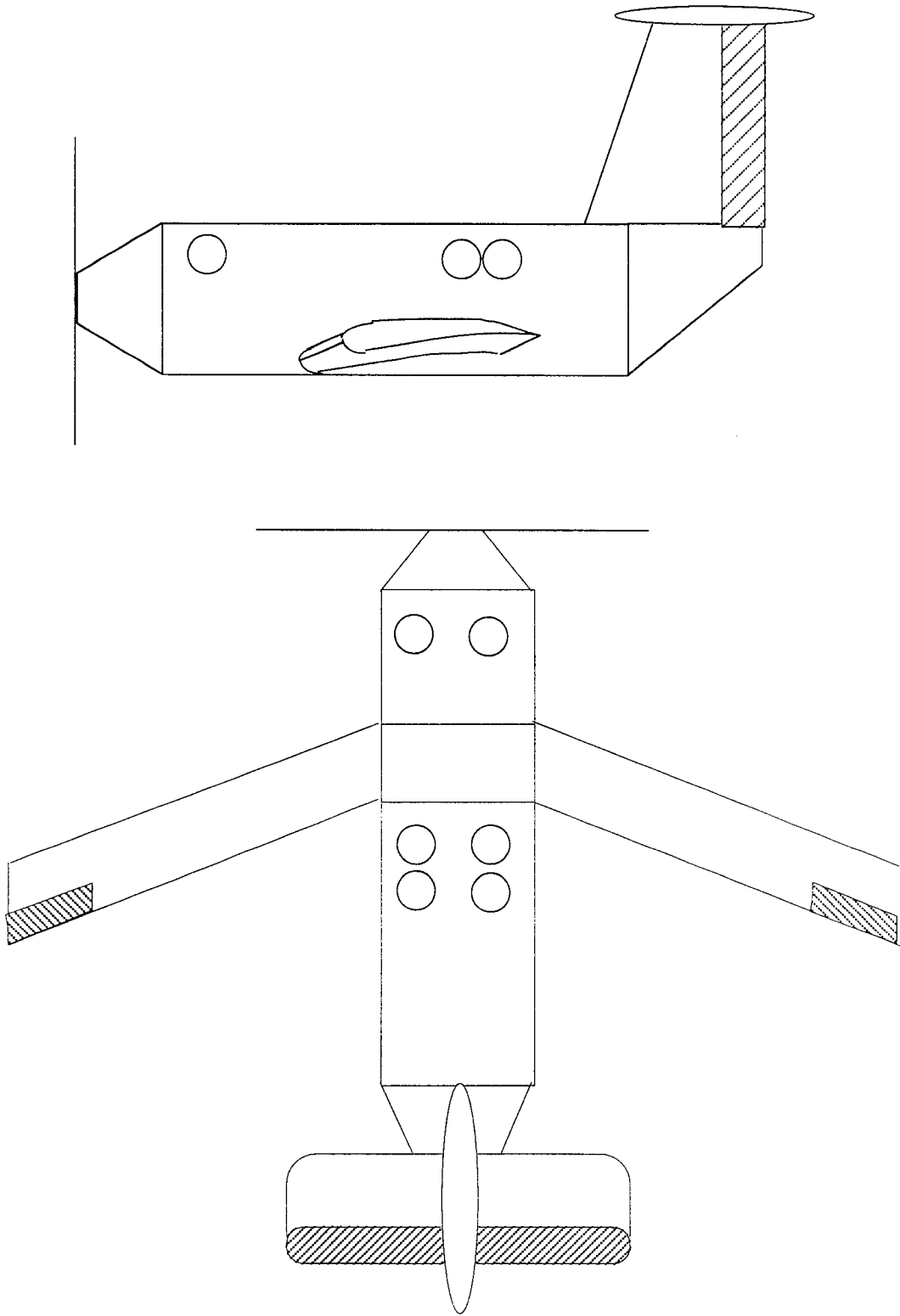
Figure 3.2: Low Wing Individual Concept
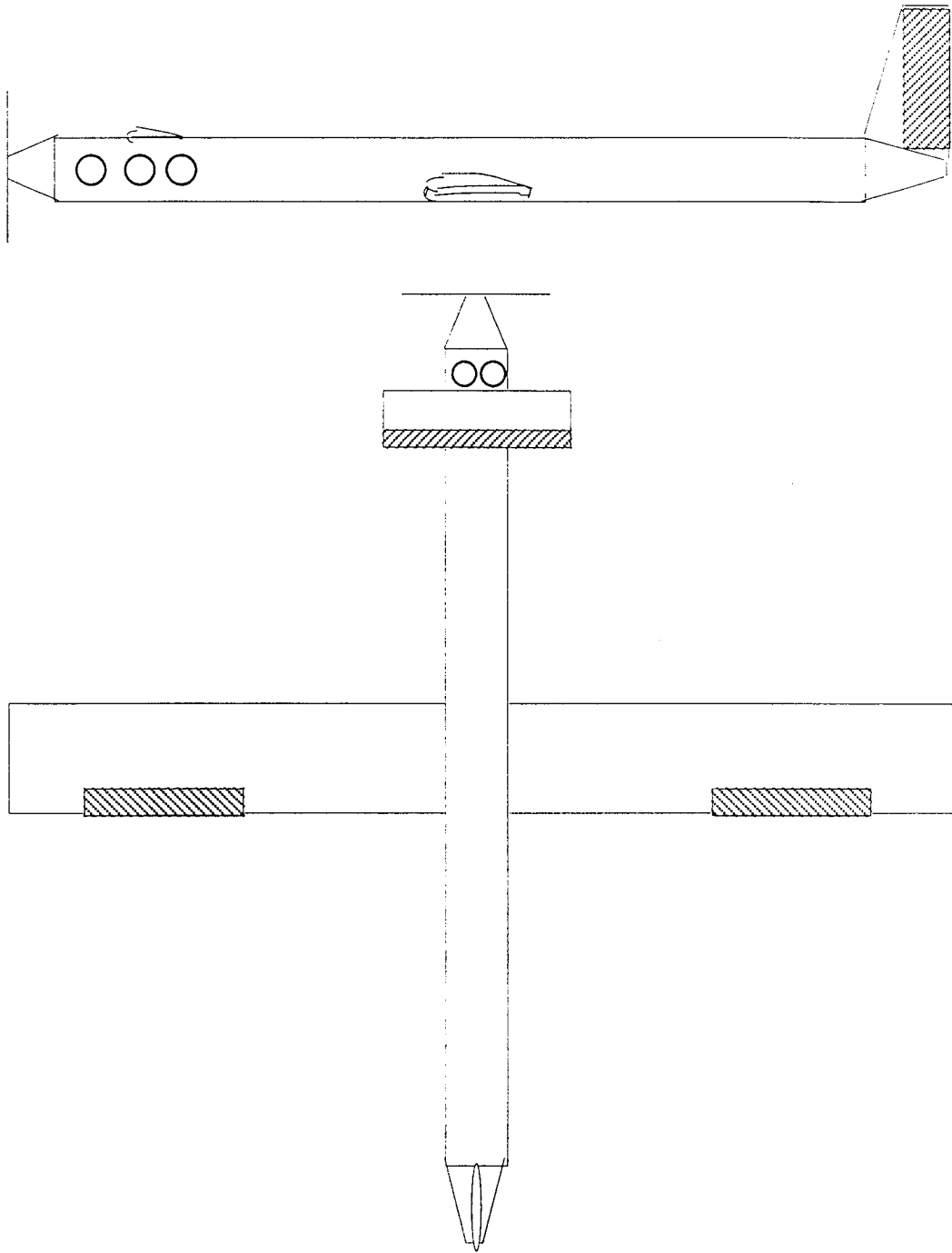
Figure 3.3: Canard - Individual Concept
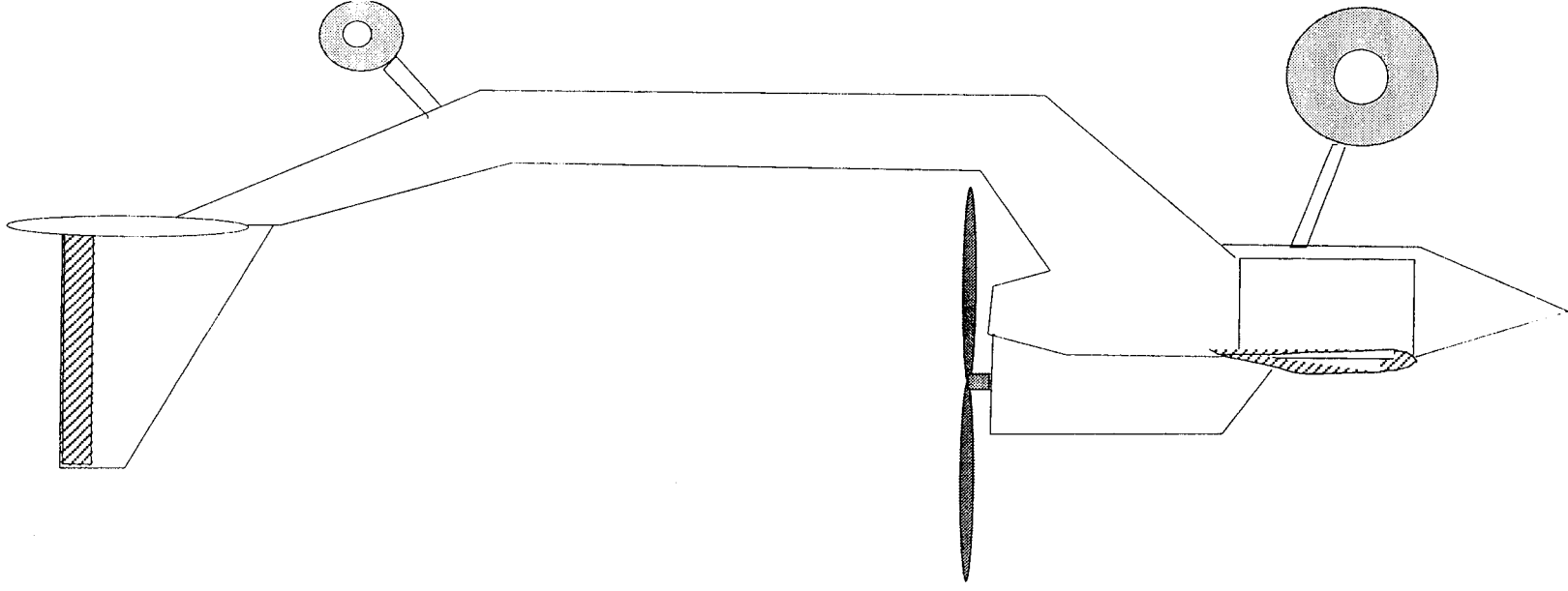
Figure 3.4: Pusher Propeller Individual Concept

3 - 9

4.0 AERODYNAMICS

4.1 INTRODUCTION

The two main design drivers for the aerodynamics group were the low-speed takeoff requirement and the high-speed cruise objective. These factors influenced every major decision made, in particular the choice of airfoil and the dimensions of the wing planform.

4.2 AIRFOIL SELECTION

Icarus will fly at Reynolds numbers ranging from 150000 to 300000. The selection of an airfoil section designed for operation at these low Reynolds numbers is an important part of the wing design. Thus, the first major responsibility of the aerodynamics group was to select an airfoil section for the wing. A trade study was performed, comparing several different airfoil sections. All airfoil data was obtained from Reference 4.7. The initial cursory screening was based on two objectives: low C_d value at the estimated values for cruise C_l and takeoff C_l for the estimated Reynolds number, and a $C_{l\,max}$ of at least 1.0. A low cruise C_d is necessary in order to achieve the goal stated in the Design Requirements and Objectives (DR&O) of a 60 feet/second cruise speed. A low takeoff C_d and a high $C_{l\,max}$ are important for meeting the DR&O objective of taking off within 28 feet to allow service to all Aeroworld airports. Nine airfoils survived this initial screening to advance for further study, namely: the DF101, E205, S2091, S3010, S4061, SD6080, SD7084, RG15, and the CLARK-Y. The primary airfoil characteristics such as: $C_{l\,max}$, cruise C_d, takeoff C_d, $C_{d\,min}$, thickness, and camber, were rated in order of importance, with $C_{l\,max}$ and minimum cruise C_d being the two most important parameters, again based on mission and DR&O requirements.

The mission of Recent Future, Inc. is to produce a <u>high-speed, low-cost</u> airplane that is manufacturable by the current work force. Because this high-speed craft will spend much of its flight time in cruise, a minimum cruise drag is essential for good fuel economy. Thus, the selection of an airfoil section with a low cruise C_d was vital.

In addition to the high-speed cruise requirement, the airplane had to meet a fairly stringent group-imposed objective of taking off in under 28 feet; hence takeoff performance could not be neglected. *Icarus* was designed to take off at a relatively low speed of 29 feet/second ($V_{TO} = 1.2*V_{stall}$), hence a large C_l was required, given this low speed. This high C_l could be accomplished two ways: by increasing the aspect ratio of the wing thus increasing the 3-D lift curve slope, and by increasing section $C_{l\ max}$. Section $C_{l\ max}$ could be controlled through choice of an appropriate airfoil. Since $L=C_l*0.5*q*S$, increasing C_l with all other things constant would obviously increase lift. Hence, Recent Future, Inc. made an effort to choose an airfoil section with a fairly high $C_{l\ max}$, in order to meet the takeoff requirement of 28 feet at the chosen low takeoff speed.

Another option for meeting the takeoff distance requirement was to use high-lift devices. Full-span high-lift flaps were considered at some length, but eventually were not incorporated into the design, primarily based on the experiences of prior Aeroworld airplanes. It seemed from past years that a simple hinged flap added extra weight, manufacturing complexity, and cost, without a radical improvement in takeoff performance. This was because the effect of the additional drag and moment created by the deflection of the flaps outweighed the small amount of additional lift created.

Although low C_d and high $C_{l\ max}$ were the two primary parameters used to guide the airfoil selection process, other factors were considered, including: stall behavior, thickness, camber, and the general shape of the airfoil. The stall

behavior was judged based on the appearance of the lift curve slope: it was desired that the region near $C_{l\ max}$ be relatively flat and that the curve not show a precipitious drop after stall, meaning that the stall would be gradual. The thickness of the airfoil was important, for integrity of the internal spar support structure. Also, because Recent Future, Inc. decided to use ailerons for roll control, the thickness and shape of the airfoil trailing edge were critically evaluated, as this is where the ailerons were cut out.

Based on all these factors, plus the advice of the authors of Reference 4.7 concerning the various airfoils in question, the DF101 was selected as the airfoil for *Icarus*. As can be seen in Table 4.1, the DF101 presents the most desirable combination of important characteristics. With a cruise C_d of approximately 0.0082, the DF101 has the second lowest cruise C_d of all nine airfoils considered. The $C_{l\ max}$ of 1.14 was adequate for meeting the 28 feet takeoff roll requirement. Also, the stall characteristics are acceptable according to the above-mentioned criteria. The thickness of 11% was deemed acceptable for production purposes by our structures experts. Finally, the overall shape of the airfoil (see Figure 4.1) seems to be conducive to ease of balsa wood/Monokote construction, because there is no complex curvature involved (such as a reflexed trailing edge) which might present construction problems, such as difficulty in maintaining the true airfoil shape along the span.

The moment coefficient for the DF101 section has a value of -0.0582, obtained from the data (Ref. 4.7). Treatment of C_{mo} appears later in Section 7, Stability and Control Systems.

<u>**Figure 4.1: DF101 profile**</u>
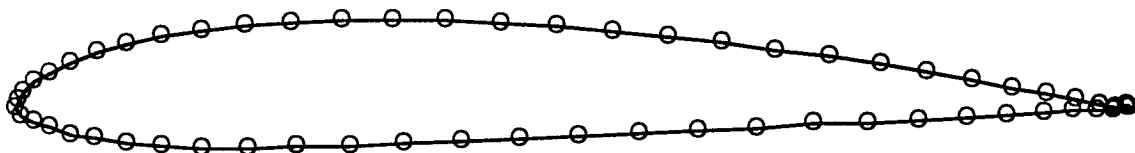
Table 4.1: Airfoil Characteristics

Airfoil	Cruise C_d	$C_{l\,max}$	Stall	Thickness
S2091	0.011	1.4	14°	10.1%
S3010	0.009	1.18	12°	10.3%
DF101	**0.0085**	**1.15**	**12°**	**11.0%**
RG15	0.0078	1.07	12°	8.9%

A similar airfoil selection process, based on similar selection criteria, was performed for the horizontal tail section. The horizontal tail was constructed as an airfoil section, as opposed to the flat plate designs of previous years. A trade study on this subject was performed, and it was found that the use of a symmetric airfoil section for the horizontal tail caused a significant savings in drag. For the same planform area, a horizontal tail constructed of airfoil sections created 50% less drag than a flat plate design. This drag savings can be accomplished with a minimum increase in design weight, as shown in Section 9.6.

The airfoil section chosen for the horizontal tail was the SD8020. In Figure 4.2, the aerodynamic benefit of using the symmetric SD8020 section as opposed to a flat plate is most clearly seen. The tail operates at a Reynolds number of approximately 150000. At this Reynolds number, the minimum C_d of 0.008 for the SD8020 is considerably lower than 0.014, the $C_{d\,min}$ for the flat plate.

Figure 4.2: Flat Plate Drag Curves as Compared to SD8020 Drag Curves
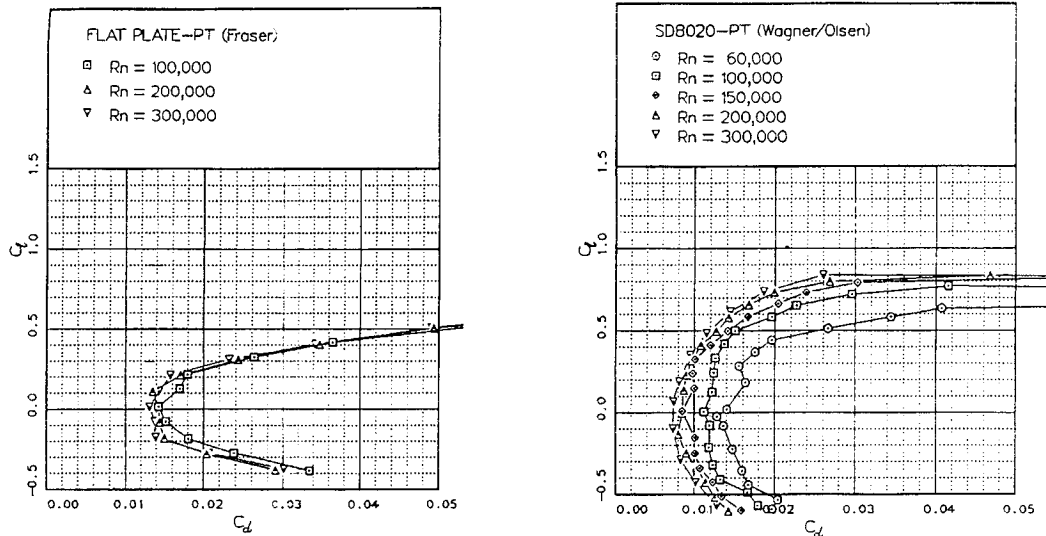
4.3 WING SIZING

The primary driver in sizing the wing was the tradeoff between low and high-speed performance. At a takeoff velocity of 29 ft/s, *Icarus* could meet the takeoff distance requirement of 28 feet. Because of the low takeoff velocity, in order to obtain a reasonable value for C_L, a large wing area was required at the takeoff condition. At cruise, however, the minimum wing area possible was desired. This area would be lower than that required for takeoff. At the desired cruise attitude, the cruise C_L was lower than the takeoff C_L. However, the design cruise speed is twice that reached during takeoff and landing. Because of the dramatic increase in speed, less wing area would be necessary to support the same weight. Less wing area results in less cruise drag, which translates into better fuel economy. Clearly, a compromise between these two conflicting factors had to be reached. The design wing area of 7.5 ft^2 represents the minimum wing area required to get off the ground in 28 feet and thus meet the takeoff requirement.

The 7.5 ft^2 of wing area was distributed as follows: span = 7.35 feet, and chord = 12.25 inches. It was desired to keep the chord over 12 inches in order to keep the lowest estimated Reynolds number (RE at takeoff) greater than 150000, because the drag polars of all the airfoils considered showed somewhat erratic and unpredictable behavior at RE < 150000. Also, due to structural considerations, a thick airfoil was desirable to allow adequate space for the main wing spar and wing box structure. Hence, a larger chord meant greater thickness (t/c=11%), thus meeting the specifications of the structures group.

The wing is of simple rectangular planform. It was decided not to incorporate taper or sweep, due to increased construction complexity and resulting cost. As pointed out in Reference 4.5, page 192, incorporating taper into a wing would increase manufacturing cost. For a tapered planform, each airfoil section would have to be cut individually, because the size of the sections would change from root to tip. It is estimated that this would take twice as long as the procedure for a rectangular planform, that of cutting all the same-size airfoils at once. Given the current tools and manufacturing techniques available, incorporating sweep into the wing would also require a more complicated manufacturing process than that of a rectangular section. Thus, because the mission statement specifically states that *Icarus* is to be a low-cost airplane, neither taper nor sweep was included in the design of the main wing.

4.4 COMPLETE CONFIGURATION AERODYNAMICS
4.4.1 LIFT CONSIDERATIONS
A modified lifting-line code (Ref. 4.3) was used to predict the wing loading as the wing approached stall. Stall prediction was accomplished by varying the angle of attack and scanning for sections along the span which exhibited predicted section lift coefficients in excess of that entered as the maximum lift coefficient of

1.14 for the DF101 airfoil. When the lift coefficient of any one section exceeded the $C_{l\,max}$ for the DF101 airfoil the entire aircraft was considered stalled. This was deemed an acceptable approach due to the fact that our wing uses a constant airfoil section along the span. Notice from Fig. 4.3 that at 12°, the stall is predicted to occur over roughly the inboard two feet of the span. The ailerons incorporated into the design, however, were placed outboard of the stalled flow region, thus controllability is maintained even at high angles of attack.

Figure 4.3: Spanwise Wing Loading at Stall Angle of 12°
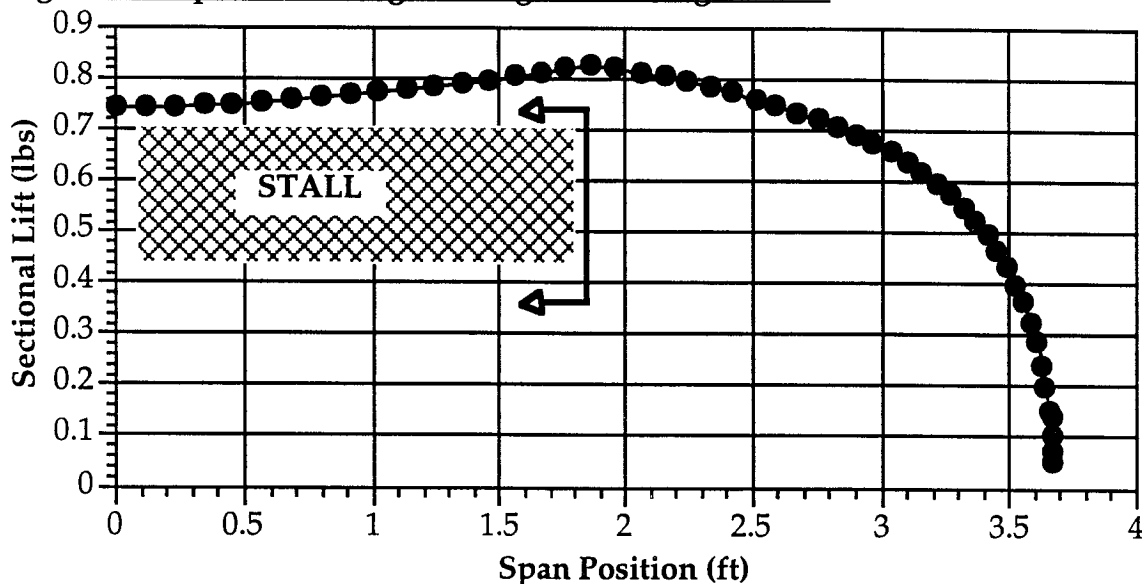
The lift curve for the complete airplane was also found from the aforementioned lifiting-line code. This was done by spanning a range of angles of attack including the predicted stall region and recording the corresponding wing lift coefficient. These wing lift coefficients were found by integrating the section lift coefficients across the half-span (due to symmetry) and then dividing by the half-span. The section lift curve slope obtained from this method was then corrected for a wing of finite aspect ratio using the formula:

$$m = \frac{m_0}{1 + m_0/\pi AR}$$

The lift curve slope was thus computed to be 4.55 / radian. The predicted lift-curve slope for the complete configuration is shown in Figure 4.4.

Figure 4.4: Lift Curve Slope for Complete Configuration Aircraft
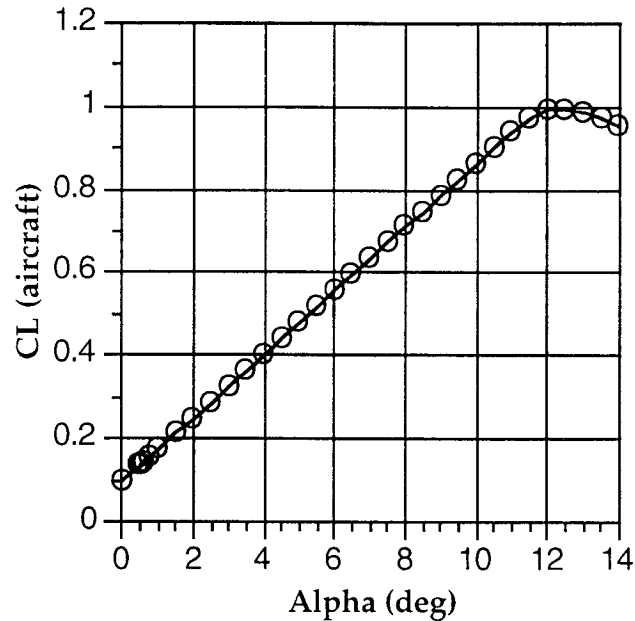
4.4.2 DRAG CONSIDERATIONS

Once the lift coefficients at various angles of attack for the complete aircraft configuration were determined, the corresponding drag polar could be found by assuming a polar of the form:

$$C_D = C_{D_0} + \frac{C_L{}^2}{\pi A \, Re}$$

where C_{D_0} and e, the efficiency factor of the airplane, were computed using the component breakdown method presented in Reference 4.6. The drag polar thus obtained for the entire aircraft is shown in Figure 4.5.

Figure 4.5

Complete Aircraft Configuration Drag Polar
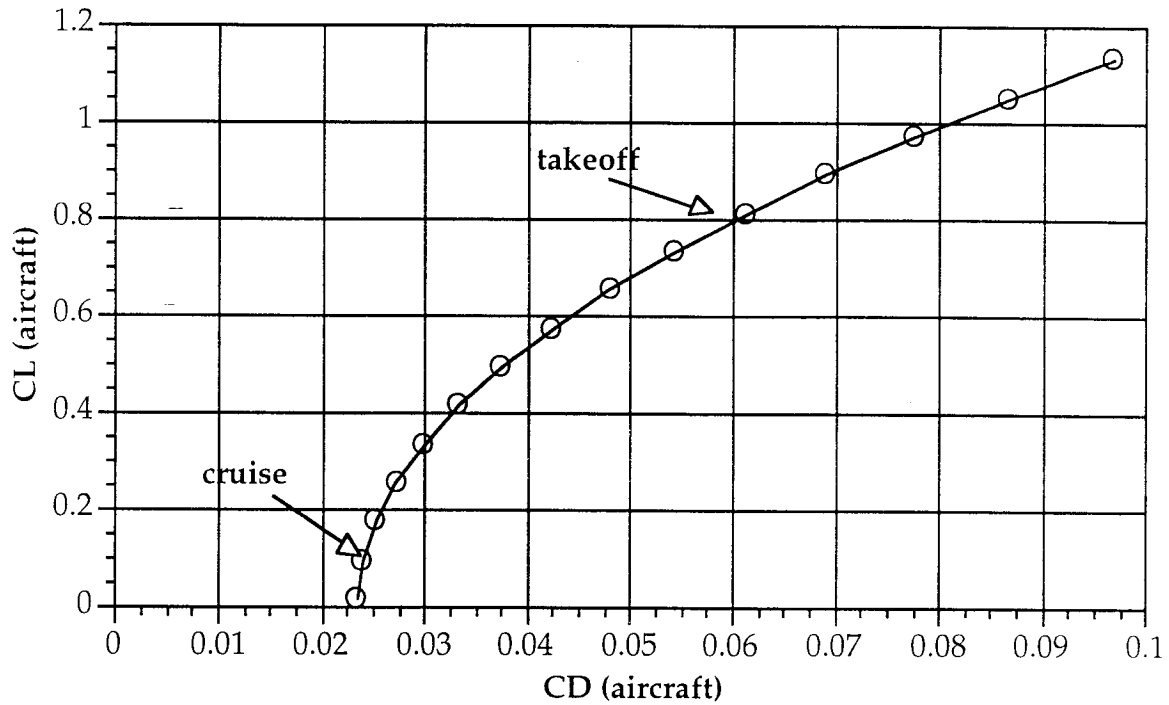
The parasite drag coefficient was computed using the formula:

$$C_{D_0} = \sum \frac{C_{D_\pi} S_\pi}{S_{ref}}$$

The present study used empirical estimates of the component drag coefficients ($C_{D\pi}$) as given in Ref. 4.6, for all components except the landing gear. A detailed estimate of landing gear drag was computed separately, based on the size and configuration of the landing gear designed specifically for *Icarus*, and modeling the struts and tires as cylinders. The $C_{D\pi}$ for a cylinder was obtained from Reference 4.5. Finally, an additional 15 percent was included to account for interference effects. Table 4.2 shows the component breakdown. The relative contribution of each component is shown graphically in Fig. 4.9.

Table 4.2: Contribution of Each Component

Component	$C_{D\pi}$	$S\pi$ (sq. in.)	Data Source
Wing	0.0070	1080.5	Reference 4.6
Fuselage	0.110	9.625	Reference 4.6
Horizontal Tail	0.0080	224.0	Reference 4.6
Vertical Tail	0.0080	71.5	Reference 4.6
Landing Gear- Tires (Main)	1.1	1.875	Reference 4.5
Landing Gear- Struts (Main)	1.1	1.125	Reference 4.5
Landing Gear- Tire (Tail)	1.1	0.9375	Reference 4.5
Landing Gear- Strut (Tail)	1.1	0.5	Reference 4.5
Interference	15%		Reference 4.6

Figure 4.9: Component Drag Breakdown
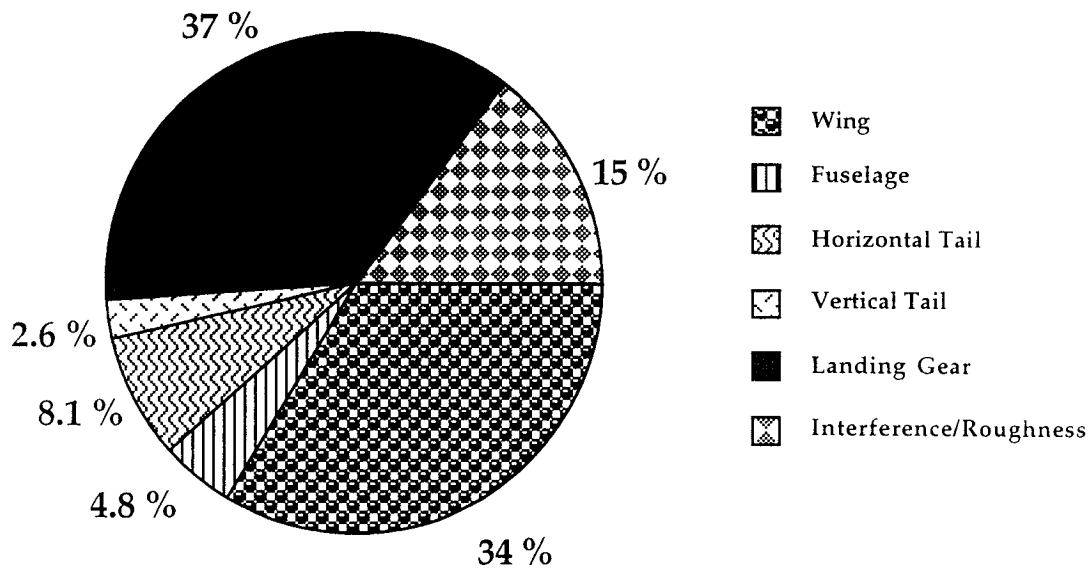
Note the large percentage of the drag which is due to the landing gear. Because of the requirement in the DR&O of 3.5 inches of tip clearance on unprepared surfaces, the size of the landing gear must be fairly large relative to the rest of the airplane, hence causing a significant portion of the total drag. Recent Future, Inc. has investigated the possibility of including fairings around the gear to reduce the drag. Several methods have been considered. The method to be used for the prototype involves attaching Monokote to the struts, in an attempt to provide the effect of a splitter plate.

4.4.3 EFFICIENCY AND COST CONSIDERATIONS

From Figure 4.7, one can see that at the design cruise velocity, L/D cruise is not equal to L/D max. This was due to the conflicting requirements of low-speed and high-speed performance. In order to cruise at L/D max, the cruise speed would have been approximately 33 ft/s, which is no improvement over

previous Aeroworld aircraft. However, it was discovered that the cost per flight actually decreases with increasing cruise velocity. (see Figure 4.8) Although the fuel cost per flight increases with higher cruise velocity, the depreciation cost drops. The depreciation cost is the cost per flight divided by the number of flights in a lifetime. A higher cruise velocity leads to a shorter design flight time, thus making it possible to increase the number of flights in a lifetime. Hence, the depreciation cost drops enough to not only offset the rise in fuel cost, but to actually cause a net decrease in total aircraft cost per flight. For example, an increase in cruise speed from 50 to 70 feet per second decreases the cost per flight by $0.80. For the computed lifetime of the aircraft of 864 flights, this translates into a savings of almost $700, just by increasing the cruise velocity by 20 feet per second. Hence, even though a high cruise speed means not flying near L/D max (and thus means less aerodynamic efficiency) the cost analysis shows that the higher cruise velocity actually is more beneficial (lower cost). Thus, it was decided to cruise at near maximum rpm, at a cruise velocity of 72 feet/second.

Figure 4.7: Comparison of High and Low Speed Cruise Efficiency
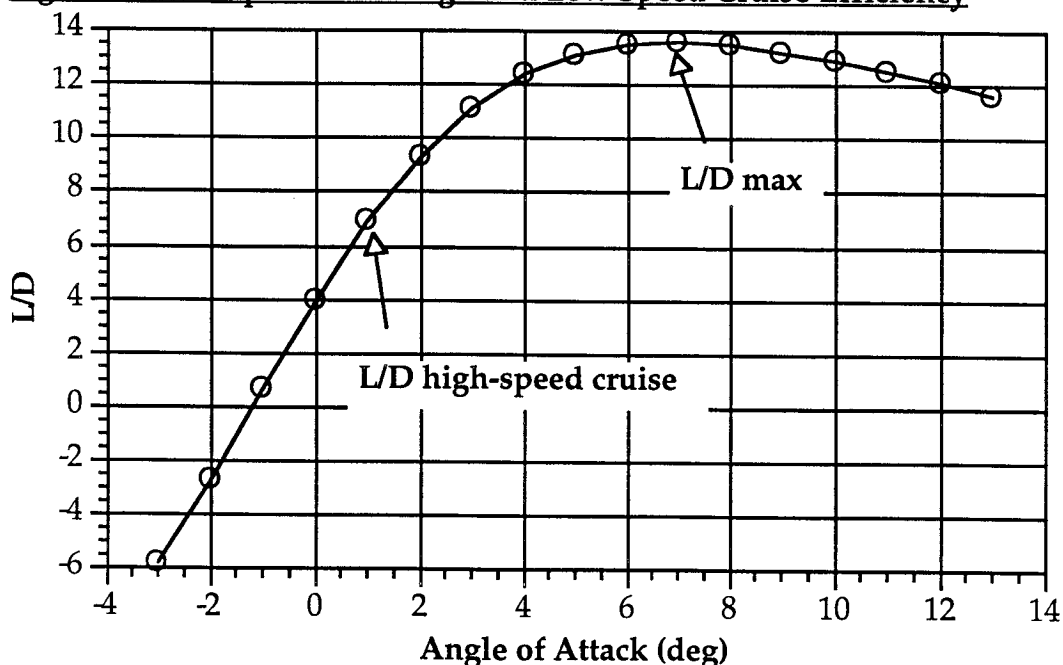
Figure 4.8: Effect of Increased Cruise Speed on Cost Per Flight
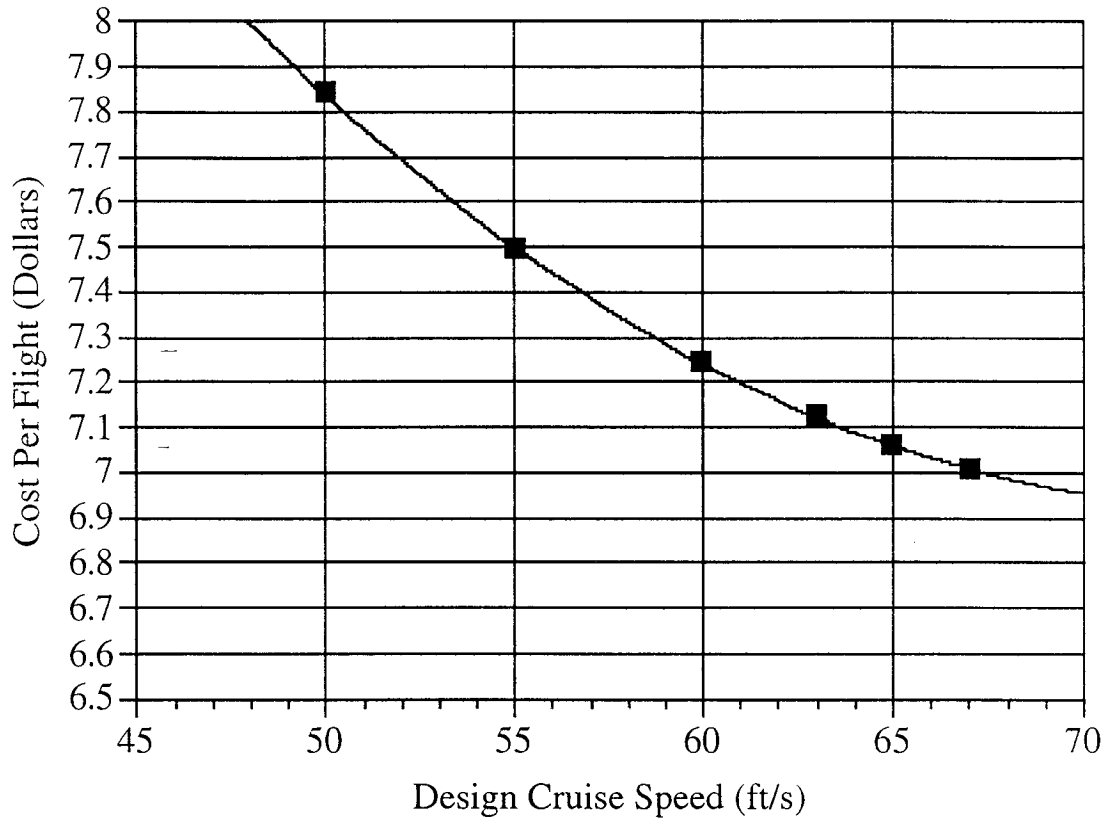
References

4.1. Anderson, John D., Jr. <u>Fundamentals of Aerodynamics</u>, 2nd edition. New York: Mc-Graw Hill, Incorporated, 1991.

4.2. Anderson, John D., Jr. <u>Introduction to Flight</u>, 3rd edition. New York: McGraw-Hill, Incorporated, 1989.

4.3 Capozzi, Brian and Fay, Jonathan. Lifting Line Code, written for AE350 Fall 1992, modified by J. Fay for AE441 Spring 1994.

4.4. Kuethe, Arnold M. and Chow, Chuen-Yen. <u>Foundations of Aerodynamics: Bases of Aerodynamic Design</u>, 4th edition. New York: John Wiley and Sons, 1986.

4.5. McCormick, Barnes W. <u>Aerodynamics, Aeronautics, and Flight Mechanics</u>. New York: John Wiley and Sons, 1979.

4.6. Nelson, Robert C. "Subsonic Drag Estimation: Component Build-up Method." Department of Aerospace and Mechanical Engineering, University of Notre Dame, 1993.

4.7. Selig, Michael S., Donovan, John F., and Fraser, David B. <u>Airfoils at Low Speeds</u>. Virginia Beach: H.A. Stokely, publisher, 1989.

5.0 PROPULSION

5.1 REQUIREMENTS AND OBJECTIVES

The key objectives which set the expectations for the propulsion system were high cruise velocity (at least 60 feet/second), a takeoff distance of less than 28 feet, and a range of at least 30,000 ft. Other contributing factors to the choice of propulsion system were weight and cost minimization, and a target time of no more than 20 minutes for motor installation and removal. The prototype must have a variable throttle control in order to fly at a maximum speed of 30 feet/second inside Loftus and reach its cruising speed of 72 ft/s outside. Since noise abatement and pollution control were of concern to Recent Future, Inc., electric propulsion was chosen to protect the immediate community and environment. Table 5.1 breaks down the propulsion system of *Icarus Rewaxed*.

Table 5.1: Summary of Propulsion System

Type of Motor	Astro 15 (Gear Ratio = 2.21)
Propeller Designation	Zingali 10-8
Number of Blades	3
Number of Batteries	13
Battery Pack Capacity	1400 milliamp hours
Battery Pack Voltage	15.6 volts

5.2 Propeller Selection

The three main criteria which drove the propeller selection were cruise velocity, propeller diameter, and takeoff distance. In order to be competitive in the six-passenger general aviation class of airplane, Recent Future, Inc. needed to design a high cruise speed aircraft (at least 60 ft/s as specified in the DR & O). To be able to reach this velocity, a propeller with high thrust coefficients and high efficiencies at advance ratios of 0.5 or greater was needed. Profile drag of the airplane was also of paramount importance. The coefficient of parasite drag was the most sensitive parameter when determining cruise speed. Since initial drag estimates pointed towards the landing gear as making up as much as 50% of the profile drag, any decrease in propeller diameter allowed for a reduction in landing gear strut length, thereby reducing the airplane's coefficient of profile drag. Lastly, the takeoff roll necessary for *Icarus Rewaxed* to rotate was of concern. The propeller had to provide sufficient thrust at low advance ratios (less than 0.3) in order to meet our design requirement takeoff distance of 28 ft. This allowed *Icarus Rewaxed* to service all airports in Aeroworld. Static thrust provided the best measuring stick for takeoff performance.

Four 2-bladed and two 3-bladed propellers were studied on the Prop 123 Fortran Program (Ref 5.1), with corrections made for tip losses, induced velocity, and low Reynold's number environment (see Appendix E for 10-8 three-bladed propeller Prop 123 printout). The outputs of the computer simulation included coefficient of thrust, coefficient of power, and efficiency at values of advance ratios ranging from 0.2 to 0.9. Figure 5.1 displays the efficiencies versus advance ratios for the 2-bladed propellers. Propellers with diameters greater than 12 inches were not modeled for fear of a sharp increase in drag due to longer landing gear struts.

As shown in Figure 5.1, the 10-7 and 11-7 propellers had the highest efficiencies at advance ratios of 0.5 and up (*Icarus Rewaxed* cruising speed advance ratios) with the 10-7 having a peak efficiency of .795 at a .650 advance ratio. Figure 5.2 illustrates the two 3-bladed propellers' efficiencies versus advance ratio. The 10-8 is more efficient than the 11-7 in all phases of the flight regime, peaking at a .840 efficiency at an advance ratio of .830. Figure 5.2 is labeled with the advance ratio and corresponding efficiency that the *Icarus Rewaxed* equipped with the 10-8 propeller cruises at. Figures 5.3 and 5.4, which depict the relationship between coefficient of thrust and advance ratio for the 2-bladed and 3-bladed propellers respectively, provided the final measure of merit for propeller selection. Both 3-bladed props had much higher thrust coefficients at low advance ratios (important for takeoff) and high advance ratios (important for cruise) than all the 2-bladed propellers. Although the 3-bladed 11-7 performed better than the 10-8 at low advance ratios, the 10-8 bested the 11-7 handily at high advance ratios in both efficiency and thrust coefficient.

The only tradeoff for using the 10-8 propeller was cost. At $15.00, it was $10.00 more expensive than any of the 2-bladed propellers. Recent Future, Inc. decided it was worth the increase in cost because its high efficiencies and thrust coefficients were needed in order for *Icarus Rewaxed* to meet its takeoff distance requirement and cruise velocity objective.

Figure 5.1: Determining the Most Efficient Two-Bladed Propeller
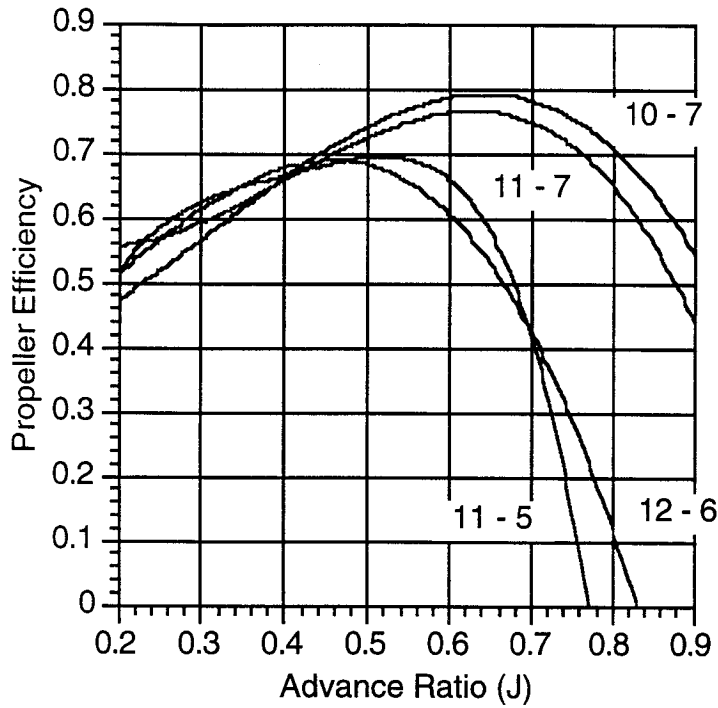
Figure 5.2: Determining the Most Efficient Three-Bladed Propeller
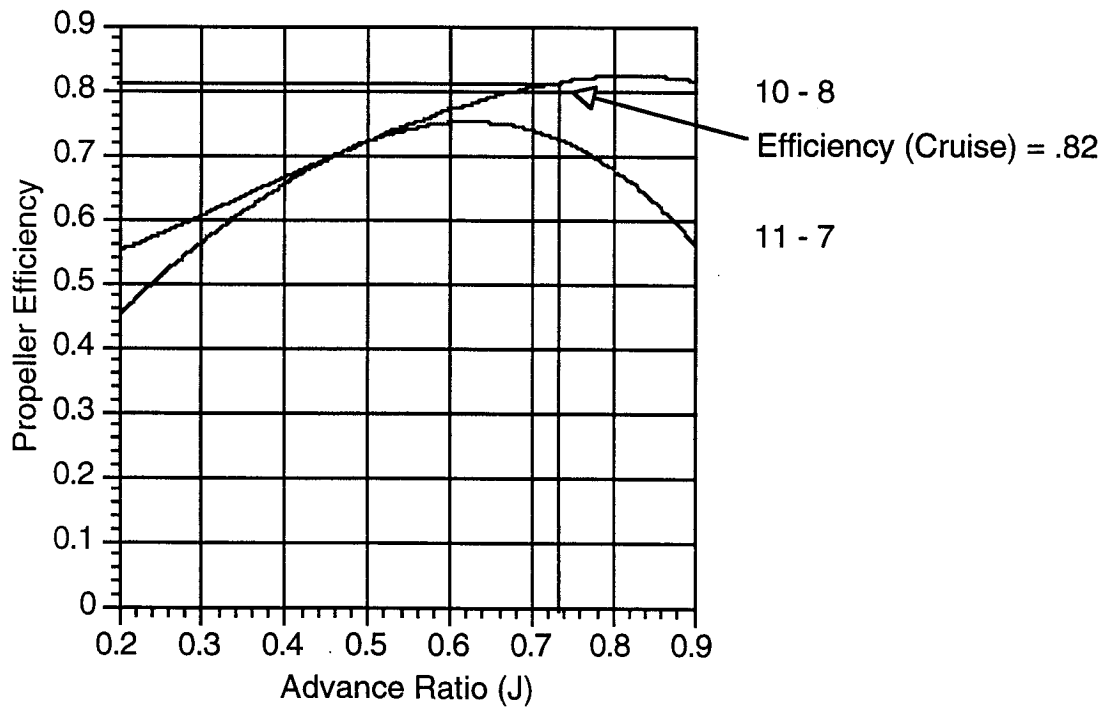
**Figure 5.3: Two-Bladed Propeller Thrust Coefficient across Flight
Advance Ratio Range**
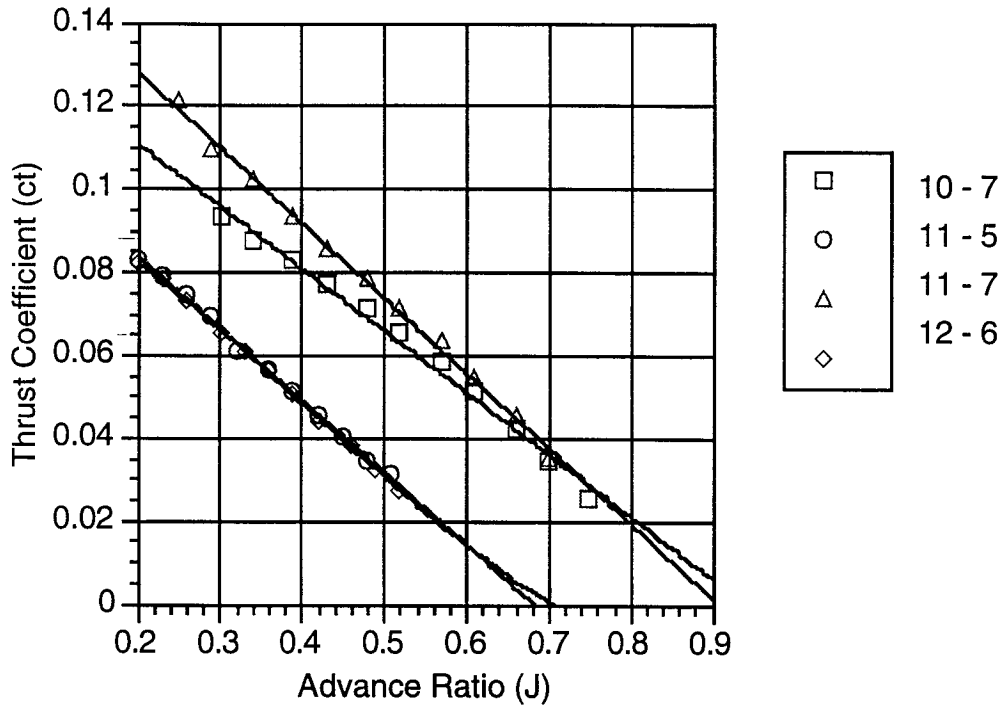
**Figure 5.4: Three-Bladed Propeller Thrust Coefficient across Flight
Advance Ratio Range**
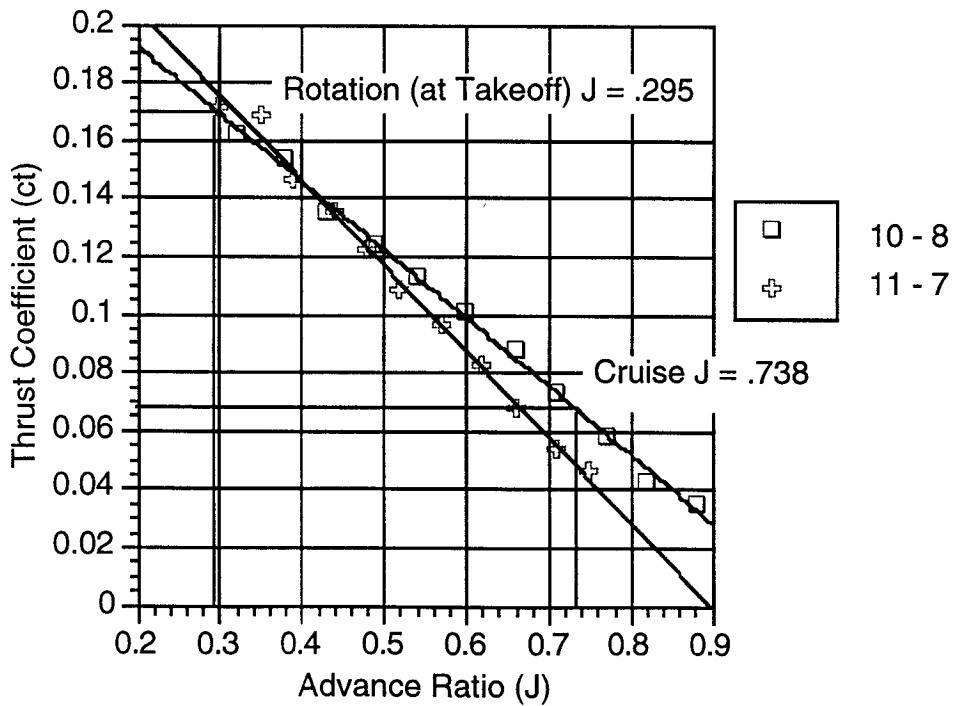
5.3 MOTOR SELECTION

The driving forces in selecting the motor were maximum Revolutions Per Minute and power output. We limited our options to the Astro 15 and the Astro 25 in that the next smallest motor could not supply enough power for our 144 Watt takeoff requirement and anything larger than the Astro 25 would result in excessive weight. High propeller RPM's were essential to reach our 60 ft/s cruise objective. The Astro 15, which has a maximum motor RPM of 16500, was able to spin the propeller much faster than the more powerful yet slower Astro 25. As it turned out, using a gear box with a 2.21 ratio of motor RPM to propeller RPM, 15500 motor RPM were needed to drive the 10-8 propeller for *Icarus Rewaxed* to cruise at 72 ft/s. In addition, the motor has to be able to supply enough torque to spin the propeller at maximum takeoff voltage. If it cannot, *Icarus Rewaxed* cannot takeoff in 28 ft. Rated at 200 Watts, the Astro 15 produces enough power to both meet our takeoff roll and our cruise speed objectives. Since the Astro 15 is $61.00 cheaper, 4.5 oz. lighter, and capable of rotating the propeller at a higher rpm than the Astro 25 (rated at 300 W) while still providing the required power, it became the obvious choice of motor for the propulsion system. Table 5.2 compares the weights (which include a gear box), costs, maximum motor power, and maximum motor RPM.

Table 5.2: Motor Characteristics

Motor	Weight (oz)	Cost	Max Motor Power	Max Motor RPM
Astro 15	25	$107.00	200 W	16500
Astro 25	38	$174.00	300 W	10000

5.4 BATTERY CHOICE

The power pack's purpose was twofold. It must supply the motor with enough voltage to produce sufficient thrust to meet the 28 ft takeoff roll

requirement and enough battery capacity to reach the design requirement range of 30000 ft at a design objective cruise speed of 60 ft/s. The 30000 ft range requirement allowed *Icarus Rewaxed* to transit non-stop between any two airports in Aeroworld, loiter for one minute at its cruise velocity and, if necessary, access a secondary airport in the case of complications with the original destination. This range took into consideration a possible diversion to an alternate airport with a subsequent two minute loiter.

Since RPM of the propeller is directly related to the voltage applied across the motor, the number of batteries needed was dictated by takeoff. Using the Takeoff Program (Ref 5.3), *Icarus Rewaxed*, equipped with a 10-8 three-bladed propeller and an Astro 15 motor, necessitated 15.6 volts to takeoff in 28 ft (see Appendix E for Takeoff Program printout). At 1.2 volts per cell, 13 batteries were linked in series to achieve 15.6 volts. The static thrust that the propulsion system produced at takeoff was 3.64 lbs. The value of the rolling friction coefficient between rubber and hard astroturf used for the study was .05. Since the motor had to sustain this high voltage, high RPM condition for a short duration during takeoff and subsequent climb to an altitude of 25 ft, only 11 mah of current was drained from the batteries. Table 5.3 gives a breakdown of the flight phases, the voltage needed to maintain the speeds, the current draw of the motor, the time of each phase, and the resultant current drain on the batteries.

Table 5.3: Current Drain of Flight Phases

	Voltage	Current	Time	Current Drain
Takeoff	15.6 V	15.0 A	1.7 s	7 mah
Climb (25 ft)	15.6 V	15.0 A	1.0 s	4 mah
Cruise (72ft/s)	14.9 V	11.8 A	417 s	1361 mah
			Total	**1372 mah**

With a maximum voltage of 15.6 volts, the maximum straight and level speed which *Icarus Rewaxed* flies at is 75 ft/s. The motor RPM at this speed is 16150 with a power draw of 115 W, still within the 16500 RPM maximum motor speed of the Astro 15 motor. The addition of another battery was not used efficiently because motor speed limitations prevented*Icarus Rewaxed* from increasing its maximum velocity. Since takeoff parameters were met with 15.6 volts, another battery would only be a cost and weight liability. The battery drain for cruise velocities ranging from the takeoff velocity of 29 ft/s to the maximum velocity of 75 ft/s were compared for a 30000 ft range using the RPV program. To take advantage of the 15.6 volts available, Recent Future, Inc. wanted to cruise at as high a velocity as was practical. Recent Future, Inc.'s initial cruise speed objective of 60 ft/s only required 1300 mah batteries. However, an increase in cruise speed was worth the cost to upgrade to 1400 mah batteries ($4.00 per cell - 1300 mah vs. $4.50 per cell - 1400 mah). With 1400 mah batteries, *Icarus Rewaxed* cruises at a speed of 72 ft/s, 12 ft/s above the 60 ft/s design objective, for the design range of 30000 ft. This required a voltage of 14.9 volts and a current draw of 11.7 amps, resulting in a battery drain of 1361 mah (see Appendix E for RPV printout at cruise speed). *Icarus Rewaxed* has 25 mah in reserve for taxi and landing.

5.5 MOTOR CONTROL AND INSTALLATION

The propulsion system allows the pilot to change the power available from the motor and hence the velocity of the aircraft by incorporating a speed control. The pilot uses 100% throttle to takeoff and climb. Once achieving altitude, the pilot then throttles back to approximately 45% throttle to maintain an indoor flight speed of 30 ft/s. When outdoors, the pilot throttles back to 95%

throttle to maintain a design cruise speed of 72 ft/s. During a turn or an increase in altitude, the pilot will slightly increase throttle.

The motor was installed in the nose of the aircraft and the batteries were housed in the wing carry-through structure. The speed controller, avionics battery pack, and receiver were fixed in the fuselage above the wing.

5.6 PROPULSION AND CONTROL SYSTEMS SUMMARY

Table 5.4 gives a breakdown of the components of the propulsion and control systems for the aircraft.

Table 5.4: Propulsion and Control System Components

Component	Type	Weight (oz)	Cost
Motor	Astro 15	7.5	$107.00
Propeller	Zingali 10-8	1.552	$15.00
Batter Pack	Panasonic 1400 (13 batteries)	1.70 oz per battery 22.1 oz in pack	$59.00
Speed Controller	Tekin	1.80	$50.00
Servos	Futuba	2.223	$105.00
Receiver	Futuba	.95	$35.00
Avionics Battery Pack	Futuba	2.0	$10.00
Transmitter	Futuba	N/A	$75.00
		Total Weight = 38.13 oz	Total Cost = $456.00

The current propulsion system provides adequate performance for *Icarus Rewaxed* to cruise at 72 ft/s for a 30000 ft range. 13 Panasonic 1400 mah batteries, at 1.2 volts per battery, provides the necessary power to takeoff in 28 ft and allows access to any airport in Aeroworld. At full throttle, *Icarus Rewaxed* can takeoff at 29 ft/s and climb at a rate of 11.7 ft/s.

References:

5 - 1. Batill, Stephen F., "Prop 123," Fortran Computer Code, Department of Aerospace and Mechanical Engineering , University of Notre Dame, 1993.

5 - 2. Dunn, Patrick F., "RPV Spreadsheet," Excel Computer Code, AE454 Propulsion, Department of Aerospace and Mechanical Engineering, University of Notre Dame, 1993.

5 - 3. Batill, Stephen M., "Takeoff Performance," Computer Code, Department of Aerospace and Mechanical Engineering , University of Notre Dame, 1993.

5 - 4. Dunn, Patrick F., "AE 454 - Lecture No. 18," Department of Aerospace and Mechanical Engineering , University of Notre Dame, 1993.

6.0 WEIGHT & BALANCE

6.1 WEIGHT ESTIMATE

The initial weight estimate as set in the DR&O was 4.5 lbs., but as the design progressed it was soon found that this was much less than could be achieved. Although the aircraft was required to carry only six passengers, as opposed to 100 in previous aircraft, the payload contributes a very small percentage of the total weight. The greatest percentage of the weight is due to the engine and batteries. Because these components are the same as those used in previous Aeroworld models, the proposed aircraft did not weight substantially less than previous models. Because this aircraft was required to take off from an unprepared surface with 3 inches of grass, larger landing gear was needed, therefore increasing the weight. Initial estimates of some components (such as servos, receiver, engine) remained constant throughout the design, since they could be measured by the design team. The structural components and propulsion system provided the greatest variation in aircraft weight. Throughout the design phase, the number and type of batteries used varied, thereby varying the weight. Initial estimates of the wing, fuselage, and empennage structure were made based on data from previous airplanes, plotting weight of component versus total weight of aircraft. As the structural design became more specific, better estimates were achieved. Many components were slightly overestimated since it was difficult to predict the weight contributed by such things as glue. It was believed that a predicted weight greater than the actual weight would be better than an underestimated weight, since an underestimated weight could jeopardize the performance of the aircraft. If the actual weight were less than the predicted weight, the airplane would perform better than predicted, having a higher maximum cruise speed, longer range, and

shorter take off distance. The most difficult components to predict were the structural components, such as the wing, empennage, and fuselage. In order to predict these components more accurately, the materials which they consisted of were first determined. Then a detailed structural analysis was performed to determine how the structure was to be constructed (ie., truss, airfoil). Once this was known, the size of the various materials was determined. Knowing the density of each material, and the volume needed, the weight was computed. Table 6.1 and Figure 6.1 show a breakdown of component weights.

Table 6.1: Detailed Weight Breakdown

Component	Weight (oz)	Location (inches from nose)
Propulsion:		
engine (incl mount & gearbox)	10.30 (known)	3.00
propeller	1.552 (known)	0.0
batteries	22.10 (known)	17.35
avionics battery pack	2.00 (known)	24.25
speed controller	1.80 (known)	12.75
Structure:		
Wing	17.02 (est.)	17.93
Fuselage sections		
engine	1.97 (est.)	4.19
front	3.95 (est.)	9.63
middle	4.24 (est.)	20.00
tail	6.67 (est.)	35.38
Vertical Tail	1.31 (est.)	39.40
Horizontal Tail	2.76 (est.)	39.40
Avionics:		
elevator servo	0.74 (known)	26.50
rudder servo	0.74 (known)	26.50
aileron servo	0.74 (known)	21.25
receiver	0.95 (known)	24.25
Landing Gear:		
Main gear tires	1.16 (est.)	15.42
Main gear struts	3.20 (est.)	16.37
Tail gear tire	0.14 (est.)	41.60
tail gear strut	0.23 (est.)	41.42

Empty Total	83.57	
Payload (passengers)	0.53 (known)	

Total	84.10	

Figure 6.1: Weight Fractions
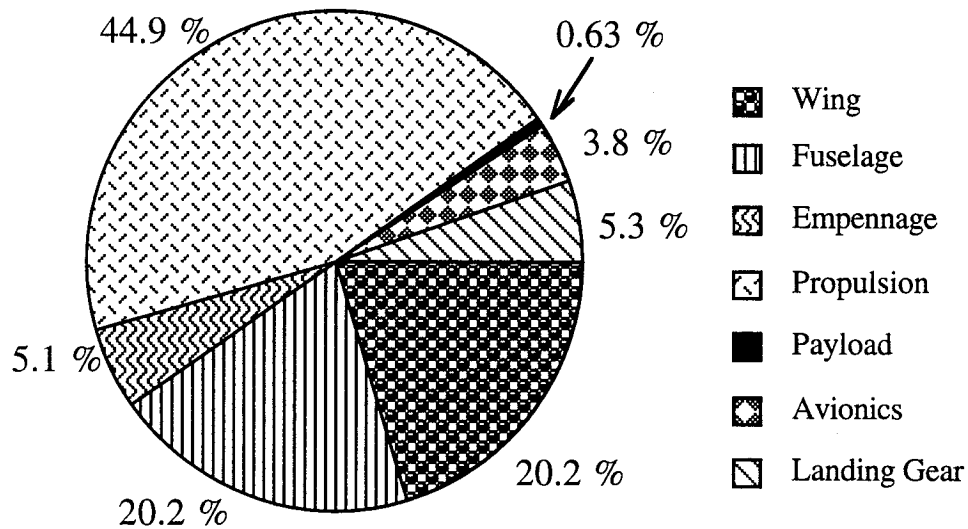
6.2 CENTER OF GRAVITY

The calculation of the center of gravity was crucial to the design because many of the stability and control calculations were based on the center of gravity location. Based on previous models in this class of airplanes, the center of gravity should be located between 25% and 30% of the mean aerodynamic chord of the wing. The final estimate of CG for this design was 29% MAC. The Y-location of the CG was 9.11 inches from the ground, located in the wing. A weight and balance diagram is shown in Figure 6.2. The CG location was greatly influenced by the internal layout. The engine and batteries had a great impact on the CG location due to their large weight fractions of 45%. The batteries were required to be placed in the wing carrythrough, and the engine was placed at the front of the aircraft. In addition, many parts come with a fixed length of wire. While additional wire could be ordered, this would increase the aircraft cost. Because the DR&O includes an objective on low cost, it was decided not to order additional wire. This caused difficulty in varying the internal configuration, so

to attain a CG location within 25-30% MAC. The center of gravity did not travel a significant amount since the only payload was the six passengers. The maximum CG travel was 0.33% MAC. This occurred when five passengers were removed. The sixth, the pilot, was assumed to remain on the aircraft at all times during flight.
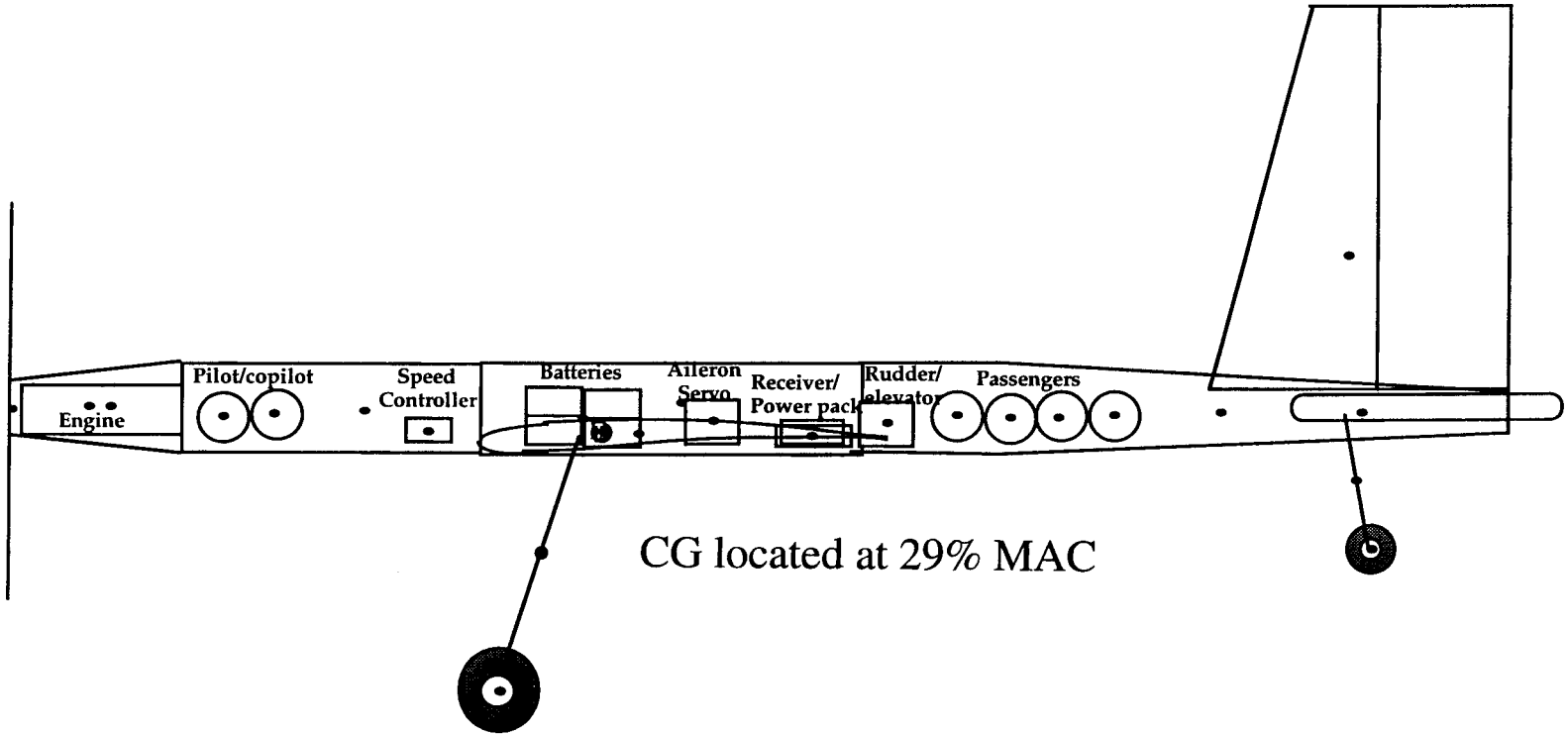
Engine

Pilot/copilot

Speed Controller

Batteries

Aileron Servo

Receiver/ Power pack

Rudder/ elevator

Passengers

CG located at 29% MAC

☐● indicates component center of gravity

(exact component locations shown in table 6.1)

Figure 6.2: Weight & Balance Diagram
(scale: 1 inch = 5.77 inches)

7.0 STABILITY AND CONTROL SYSTEM: DESIGN DETAIL

The primary objective of the stability and controls group was to perform analysis to ensure the stability of the aircraft. This analysis, coupled closely with the center of gravity position, consisted primarily of the sizing and placement of the various aerodynamic and control surfaces used to stabilize, trim, and maneuver the aircraft. The goal of the analysis was to provide an aircraft that is statically stable and exhibits benign handling qualities such that it can be flown not only by a professional, but a novice as well.

7.1 LONGITUDINAL STABILITY

The primary figure of merit for longitudinal stability was the slope and intercept of the curve depicting the linear relationship between the pitching moment about the center of gravity and angle of attack. In the case of the present study, the relevant angle of attack is that of the wing α_w, which can be defined as the sum of the angle of attack of the fuselage reference line (α_{FRL}) and the incidence angle of the wing (i_w). For the aircraft to possess longitudinal static stability, it is required that the slope of the curve (CM_α) must be negative and the intercept (CM_o) must be positive, thus allowing for the aircraft to be trimmed at positive angles of attack. The methodology used in the development and analysis of the relevant equations governing the static stability was modeled after that given in Reference 7.1. It is noted that the contribution of the fuselage to the longitudinal stability was neglected throughout the analysis as it was assumed to be small in comparison to the contributions of the wing and tail.

Inherent in the analysis was the necessity of setting the incidence angles of the main wing and horizontal tail such that the drag at the high-speed cruise configuration was minimized. This minimum drag condition was taken to occur when the angle of attack of the fuselage with respect to the relative wind was

zero. An additional constraint was imposed such that the elevator deflection necessary at high-speed cruise was essentially zero, again to minimize drag in hopes of achieving the highest possible cruise speed. The method used to obtain the necessary incidence angles is described in the Appendix.

The first stages of the analysis consisted of a trade study aimed at determining the relative sensitivity of the aircraft's longitudinal stability to variations in volume ratio by varying the moment arm to the quarter chord of the horizontal tail as well as the span and chord of the tail surface. This first analysis, done with the incidence angle of both the wing and tail set at zero degrees, showed that the longitudinal stability was affected more by variations in span than by changes in the chord length. In light of this result, a chord of 8 inches was chosen for aerodynamic reasons as it kept the Reynolds number of the horizontal tail larger than 130,000 throughout the flight envelope. In doing so, it was hoped that the rather unpredictable behavior seen at Reynolds numbers less than 130,000 (See Reference 7.2) could be avoided, alleviating potential stability and control problems during critical stages of flight such as takeoff and landing. Thus, with the chord set at 8 inches the span of the horizontal tail as well as the moment arm to the tail surface were varied to determine their relative effect on the aircraft's stability. Representative results from this study are shown below in Figure 7.1 with a moment arm of 23 inches from the aircraft center of gravity to the quarter chord of the horizontal tail.

Figure 7.1: Variation of Longitudinal Stability with Span and Tail Incidence
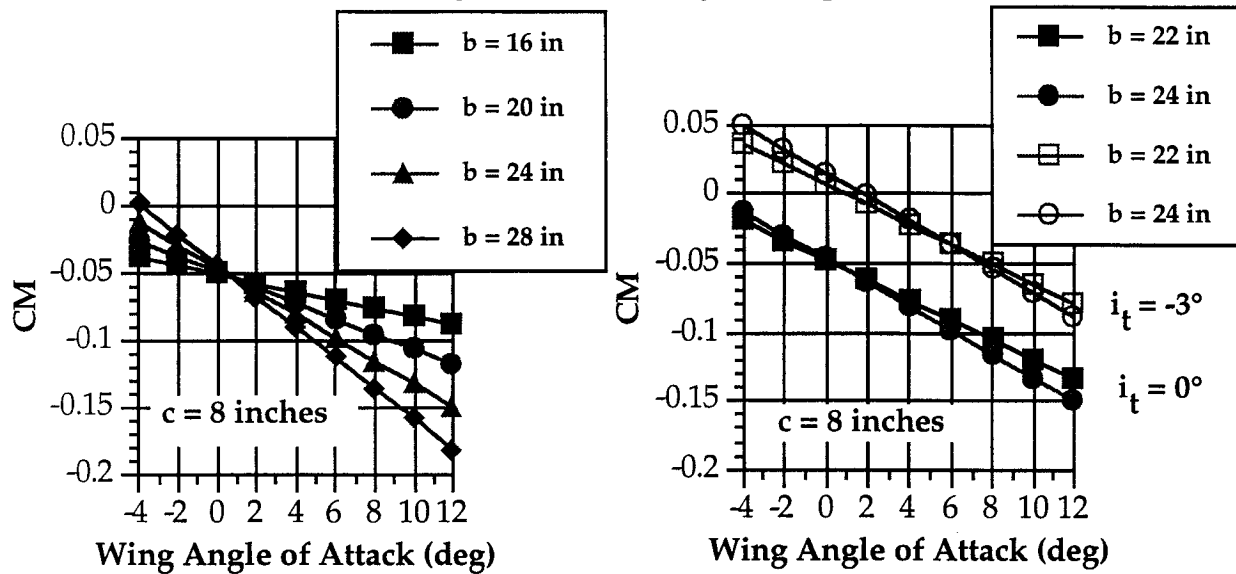
From the figure on the left, it was noted that with the chord fixed at 8 inches, the aircraft became increasingly stable as the span was lengthened. As can be seen, each curve in the figure to the left has a negative slope and thus satisfies the static stability requirements to some extent. The intercept of each of these curves, however, is negative - implying that these configurations do not allow for trimming of the aircraft at positive angles of attack. By varying the incidence angle of the wing and tail, these curves can be altered such that their intercept is changed while their slope remains the same. For the purposes of this study, the wing incidence was left at a nominal value of zero degrees with respect to the fuselage and the tail incidence was varied from zero to six degrees. It is noted that it is the relative difference between wing and tail incidence that affects the stability, not the value of each individually (i.e. a wing incidence of 1.5° and a tail incidence of -1.5° would yield the same results). Through a series of plots like those shown above, the set of possible solutions was narrowed to a region starting with a minimum chord of 8 inches and a minimum span of 22 inches. At this point, a buffer was inserted to account for the slightly destabilizing effect of

the fuselage which had previously been neglected. A parallel study was also conducted to include the effect of the variation in moment arm to the longitudinal stability. Through inspection of the results of these two studies, it was determined that, for a moment arm of 23 inches, a solution which satisfies the longitudinal stability requirements exists with a chord and span of 8 inches and 24 inches respectively for a rectangular horizontal tail. The pitching moment equation for this configuration was thus found to be CM = 0.015 - 0.01 α and the resulting curve is shown in Figure 7.2 below.

Figure 7.2: Pitching Moment Coefficient Curve for Design Condition ($\delta e = 0°$)
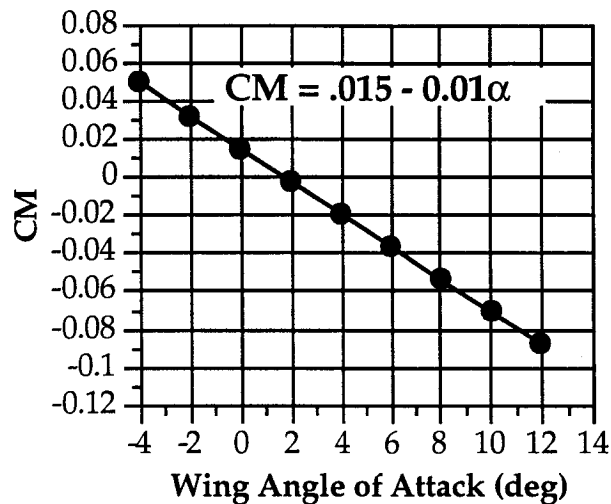
Throughout the study, the strong coupling between the weight/balance and stability of *Icarus* was readily apparent. Through several iterations, the suitable configuration above was found which yielded a static margin of approximately 14 percent and a CG position of roughly 29 percent of the mean aerodynamic chord from the leading edge of the main wing.

Having found an acceptable configuration, the design of *Icarus* seemed to ensure a certain degree of longitudinal static stability. As the stability of the aircraft depends heavily on the position of the center of gravity, however, it could be significantly affected by variations from the design point which may

occur in the actual manufacturing stage of the design. As a check on this, a sensitivity to CG placement was performed by assuming a CG travel of several inches fore and aft of the design point with all other parameters (tail area, overall length, etc.) held fixed at their design locations and sizes. The results of this study are shown below in Figure 7.3, which shows the impact of effectively lengthening or shortening the moment arm to the quarter chord of the horizontal tail surface.

Figure 7.3: Sensitivity of Longitudinal Stability to CG Position ($\delta e = 0°$)
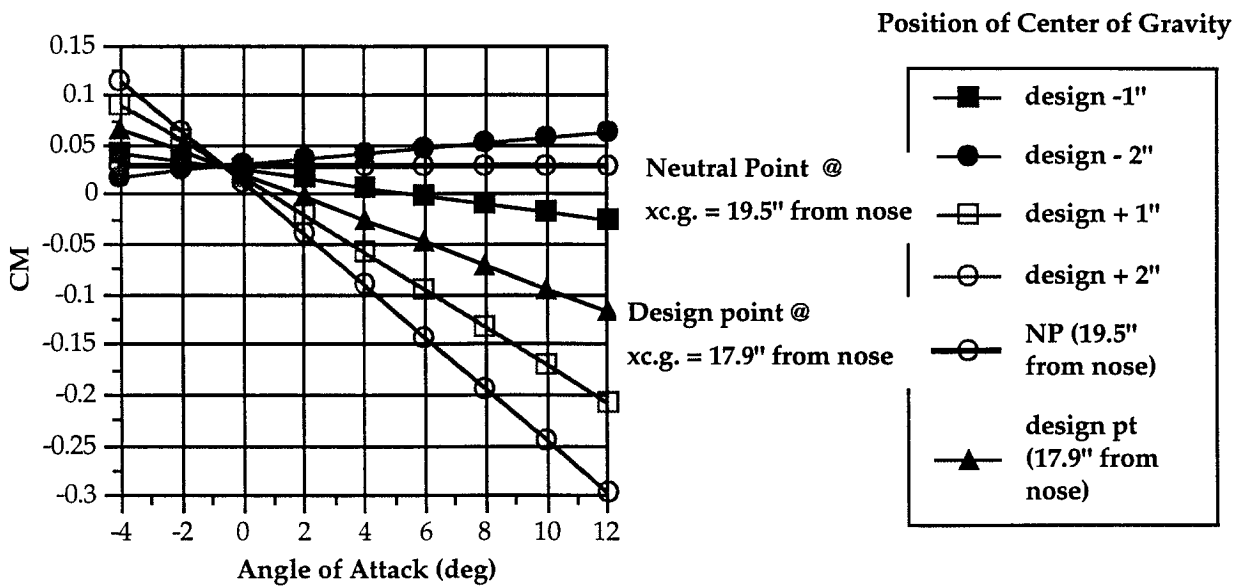
From the figure, it can be seen that the stability of the aircraft is quite sensitive to the location of the center of gravity and thus the effective length of the moment arm. As the CG moves forward of the design CG location, the slope of the curve is seen to become more negative thus making the aircraft more stable. A CG location just two inches behind the design point, however, causes the slope of the curve to be positive and causes the airplane to become statically unstable. Thus, throughout the manufacturing process, careful management of the CG location

will be necessary to ensure the longitudinal stability of the aircraft through the validation phase of *Icarus*.

7.2   LONGITUDINAL CONTROL - ELEVATOR SIZING

The elevator for *Icarus* was sized using consideration of takeoff performance as well as the ability to trim the aircraft at landing. These two requirements were weighed against one another to determine which was the more stringent and vital to the design. It is also important to be able to trim the aircraft at its cruise configurations. Since the indoor, low-speed cruise of *Icarus* is quite close to its landing speed, however, it was felt that the requirement to trim at landing would allow for trimming the aircraft at low speeds as well. The high cruise speed objective of *Icarus* did not weigh heavily on the decision making process since the incidence angles were set to alleviate the need for an elevator deflection in the high-speed configuration.

7.2.1 TAKEOFF CONSIDERATIONS

The first consideration in sizing the elevator surface was the takeoff performance of the aircraft. Since *Icarus'* configuration was that of a tail-dragger, prior to taxiing, the fuselage (and thus, the wing) was at an angle of attack relative to the ground. For the purposes of this study, the fuselage angle was set such that the wing would be at an angle to allow it to provide sufficient lift to meet the takeoff requirements imposed by the group.

It was proposed that as the aircraft began its takeoff roll, a force produced by an elevator deflection would cause the aircraft to rotate about the contact point of the main gear. As this occurs, the rear wheel rises off the ground and the fuselage becomes parallel to the ground; this is done so as to accelerate down the runway in a minimum drag or "cruise-like" configuration. It was believed that

this would allow *Icarus* to be able to takeoff within the ground roll requirement of 28 feet as set by the group in the DR&O.

To determine the elevator size for this rotation to a level attitude, a free-body diagram of the aircraft in a taxiing configuration was drawn. Through consideration of the moments acting about the contact point of the main gear, it was possible to determine the size of the elevator as well as the amount of deflection required to accomplish the rotation. Once at the minimum drag configuration, it was assumed that the elevator control power was adequate to rotate the aircraft to the necessary takeoff orientation at the appropriate distance down the runway. To assess how the velocity changes with distance along the runway, data was taken from takeoff.f (Reference 7.3). By curve-fitting the output of this code as shown in Figure 7.3, an empirical relationship between velocity and distance was found. This relationship was used to model the aircraft's velocity during the first 6 feet of ground roll (a distance arbitrarily set at which the aircraft should be level, approximately 1/4 of the distance covered prior to rotation and lift off). In doing so, the moment coefficient required to rotate the aircraft to its minimum drag configuration was found to be 0.402. By varying the size and deflection angle of the elevator, the control power was adjusted such that it was able to overcome this moment. The design configuration, consisting of a span of 26 inches and a chord of 1 inch, provided a moment coefficient of 0.428, sufficient to achieve the rotation through an elevator deflection of 20°.

Figure 7.3: Velocity of _Icarus_ During Ground Roll (Data from Ref. 7.2)
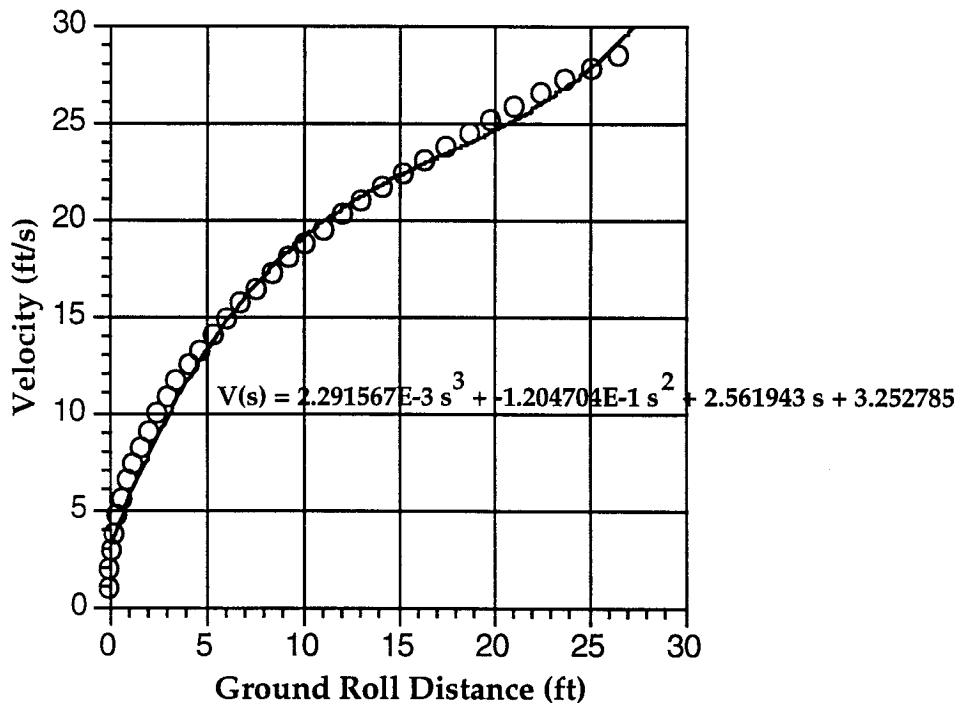
Due to the relatively short time frame in which this proposed takeoff scheme is to occur, it is possible that the pilot may not be able to react quickly enough to execute the desired maneuvers. In order to account for this possibility, the angle of attack of the wing through the ground roll is set such that, even without rotation to the minimum drag configuration, the aircraft will still be able to lift off within the 28 feet specified in the DR&O.

7.2.2 TRIM CONSIDERATIONS AT LANDING

For landing, the aircraft must be capable of being trimmed at an angle of attack near CLmax, or in this case 12°. By referring to the data from the aforementioned longitudinal stability study, it was found that for the selected tail size and moment arm, the moment coefficient required by the elevator deflection is .0911 at a wing angle of attack of 12°. This is relatively small compared to that required to rotate the aircraft at the relatively slow velocities experienced at

takeoff - thus it appeared that the rotation requirement has more bearing on the ultimate sizing of the elevator. Taking the design area and moment arm to be fixed by static stability considerations, the parameters to be varied were thus the ratio of the elevator chord to the chord of the horizontal tail (implicitly, τ, the flap effectiveness) and the maximum deflection of the aileron.

For the purposes of this design, τ was taken to be determined by the ratio of chords through reference to Figure 3.32 of McCormick (Reference 7.4) which is based on results of thin-airfoil theory. Thus, for a given deflection, the chord of the elevator was varied until the moment created by the down force on the tail was sufficient to trim *Icarus* at its landing configuration. A combination of parameters that satisfied this requirement was found with a maximum deflection angle of $\pm 20°$ (as set by the rotation requirements at takeoff) and an elevator chord to 1 inch which corresponds to a flap effectiveness on the order of 45%. The effect of the selected elevator configuration on the pitching moment curve, shown below in Figure 7.4, verifies the ability of the elevator to trim the aircraft at landing.

Figure 7.4: Variation of Trim Condition with Elevator Deflection

Figure 7.4: Variation of Trim Condition with Elevator Deflection
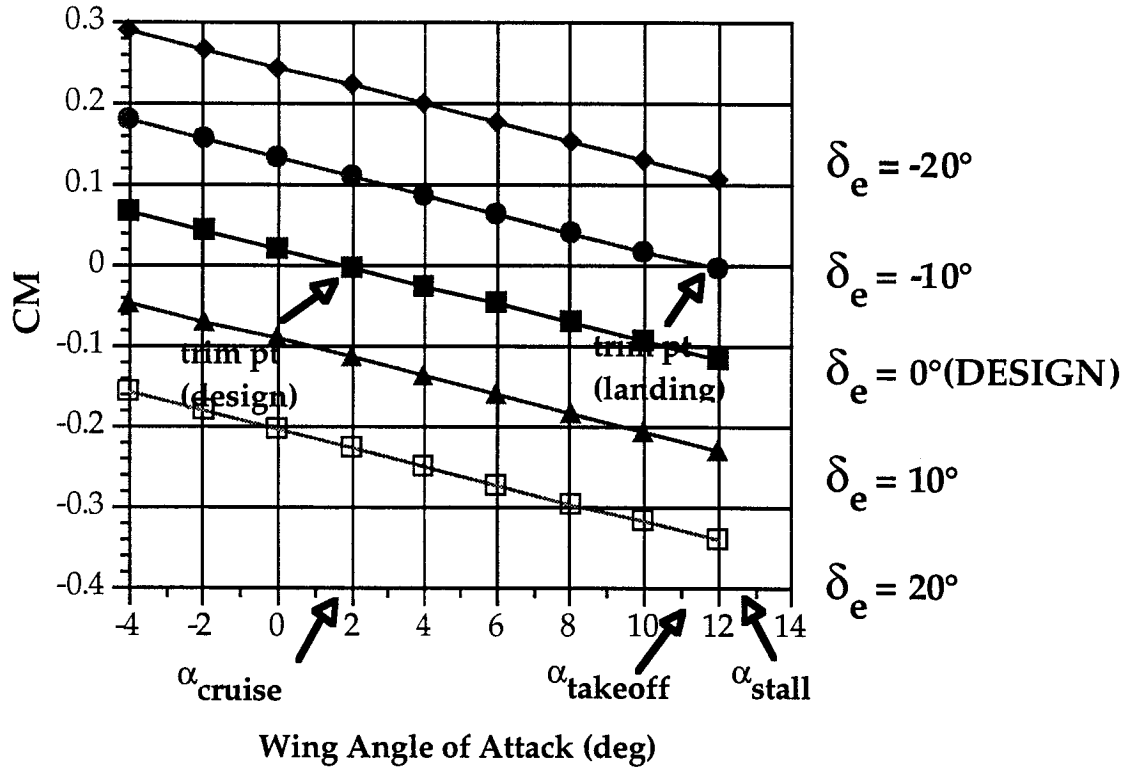
Table 7.1 Summary of Longitudinal Stability and Control

TAIL AREA (in^2)	MOMENT ARM (in)	ELEVATOR AREA (in^2)
224.0	23.0	26.0

CMO	CMα (rad^{-1})	CMδe (rad^{-1})	δe @ CRUISE (deg)	MAX δe (deg)
0.021	-0.659	-0.644	0°	±20

7.3   LATERAL STABILITY

The primary objective of the consideration of lateral stability was the sizing of the vertical tail surface. The lateral stability for *Icarus* was determined through the requirement that for directional or weathercock stability, $C_{n\beta}$ for the aircraft must be greater than zero. This implies that for a given sideslip angle, the net force created is such that the airplane becomes aligned with the direction

of relative wind. As this requirement sets the sign on the coefficient rather than a distinct value, the desired magnitude is unknown. This deficiency was reconciled through the compilation of a secondary data base of vertical volume ratios for past RPV's. The vertical volume ratio is defined as $V_v = \dfrac{S_v l_v}{S_w b}$ where S_v is the area of the vertical tail surface, and b is the span of the wing. From this data base, an average Vv was found to be in the range of 0.015 to 0.03. Thus, the root and tip chords as well as the height were chosen such that the vertical volume ratio fell within this range. At the same time, with this set of parameters, the sign on $C_{n\beta}$ was verified to be greater than zero, having a value of 0.0474.

7.4 LATERAL CONTROL

The sizing of the rudder was accomplished through the consideration of a possible landing in a cross wind (perpendicular to the intended flight path) of 10 ft/s or approximately 7 miles/hour in magnitude. A crosswind of this magnitude would induce an effective sideslip angle of roughly 20° which corresponds to a yaw moment coefficient, Cn, of 0.0163. This calculation yielded precisely the yaw moment needed to be created through a rudder deflection. Thus, in a fashion similar to that used for sizing the elevator, the chord and deflection angle of the rudder were varied to find a suitable combination which could counteract the aircraft's tendency to yaw, allowing *Icarus* to land at a given sideslip angle. The rudder chosen for this design was of rectangular planform having a chord of 4 inches and a span of 10.5 inches. Through inspection of past generations of Aeroworld planes, it was noted that our rudder size, in particular the chord, is somewhat larger than past designs. The rather large rudder chord was justified through consideration of the dual mission (high and low-speed cruise) of *Icarus*. Since the incidence angles of the

wing and tail are set for minimum drag at cruise, *Icarus* will be forced to land at a considerably higher angle of attack than past generations of Aeroworld planes which set their incidence angles for low-speed cruise. At this larger angle of attack, it is possible, due to the relative position of the vertical tail with respect to the main wing, that the effectiveness of the rudder be washed out by the wake off the wing - a problem hoped to be prevented through our rudder sizing.

7.5 ROLL STABILITY

According to the objectives set forth by Recent Future, Inc., *Icarus* is to have relatively benign handling characteristics. Inherent in this is that the aircraft exhibit a certain degree of roll stability when subjected to gusts or other forces causing the wings to be disturbed from a wings-level attitude. For the aircraft to be stable in roll, the coefficient Cl_β (not to be confused with the lift-curve slope) which is commonly denoted as the "dihedral effect," must be less than zero. As the destabilizing effect of the fuselage to roll stability is difficult to quantify, a dihedral angle of 5° was chosen for the main wing which led to a Cl_β of -.099/radian. It was hoped that this was of sufficient magnitude to counter the effect of the fuselage.

7.6 ROLL CONTROL

7.6.1 GENERAL CONSIDERATIONS: CONTROL SELECTION

The roll characteristics of *Icarus* were governed by two issues. First, it was desired for the aircraft to be able to perform a coordinated turn, eliminating the tendency seen in observation of previous designs to slide through turns. Second, since Icarus is to have relatively benign handling characteristics, the roll rate as well as the angle of attack necessary to complete the turn must be controlled such

that even inexperienced pilots can perform rolling maneuvers. To this end, a decision was made to fit *Icarus* with aileron control surfaces rather than relying on the coupled rudder-dihedral turning philosophy implemented on past designs. In reaching this decision, consideration was given to the course that must be flown during the indoor portion of the prototype validation. As mentioned in section 7.3, due to the relative position of the vertical tail with respect to the main wing and the angle of attack necessary for low-speed flight, it was thought that the effectiveness of the rudder would be washed out by the wake shed from the main wing. If this were to occur, *Icarus'* turning performance would be seriously degraded if it relied on rudder-dihedral to turn. With aileron control, however, the turn performance should not be affected by the relatively high angle of attack required for turning as well as level flight at the low speed cruise configuration.

7.6.2 Sizing and Placement of Ailerons

Sizing of the ailerons was accomplished assuming both steady roll rates and turns through a trade study aimed at determining the sensitivity of the roll/turn performance to the sizing and placement of the ailerons. A limitation of the method used for estimating the effectiveness of the ailerons was the assumption that a strip theory analysis is valid and that the lift distribution across the aileron is uniform where in fact it is not. Despite these limitations, however, the relative roll control for various aileron configurations was assessed by varying the relative positions of the inboard and outboard edges of the aileron surfaces as well as the ratio of aileron to wing chord and observing the corresponding steady roll rates. The results of this study are shown in Figure 7.5 below.

Figure 7.5: Variation of Roll Rate with Aileron Sizing and Placement

Aileron Width, W (inches)

—■—	W = 5 in
—●—	W = 7.5 in
—▲—	W = 10 in
—◆—	W = 12.5 in
—□—	W = 15 in
—○—	W = 17.5 in
—△—	W = 20 in

Distance to Inboard Edge of Aileron From Centerline (in)
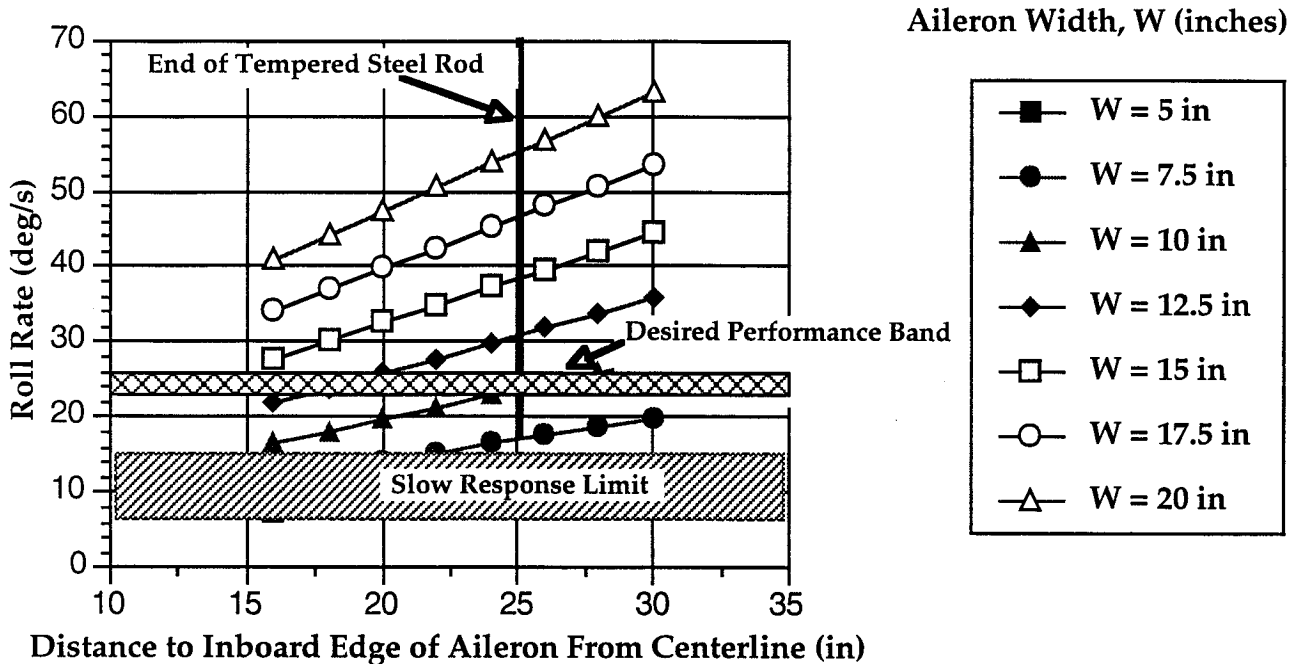
As specified in the DR&O, *Icarus* must be able to complete a 60 foot radius turn at a speed of 25 feet per second. In doing so, *Icarus* must obtain a bank angle of roughly 20 degrees. It was reasoned through consideration of the relative size of *Icarus* and the speeds at which it will fly that the aircraft should be able to obtain this required bank angle for a steady turn in approximately one second. This was done mainly by deciding that a time of two seconds or more represented a slow response, whereas a time less than one second seemed rather abrupt and was assumed to cause aerodynamic loads higher than those allowable to be experienced by the structure. The results of the sensitivity studies on roll rate alone thus showed many acceptable sizing and placement combinations.

Further considerations however, led to the closer examination of the bank angle required for the completion of a turn of a given radius. This bank angle

was computed through consideration of the forces acting on the airplane during a steady turn leading to the two equations:

$$\sum F_x = L \sin \phi = \frac{WV^2}{gR}$$

$$\sum F_y = L \cos \phi = W$$

which can be solve simultaneously to yield the bank angle, ϕ, for a given turn radius, R (which was varied from 50-60 ft in increments of 5 feet). The corresponding angle of attack required through the turn was also an important constraint on the design as the lift must be greater than the weight due to the rotation of the lift vector through the angle ϕ. Thus, a second study was performed to assess the variation in the corresponding required angle of attack with bank angle. The results of this study are shown in Figure 7.6.

Figure 7.6: Constraints on Bank Angle and Angle of Attack: Stall/Speed Limits
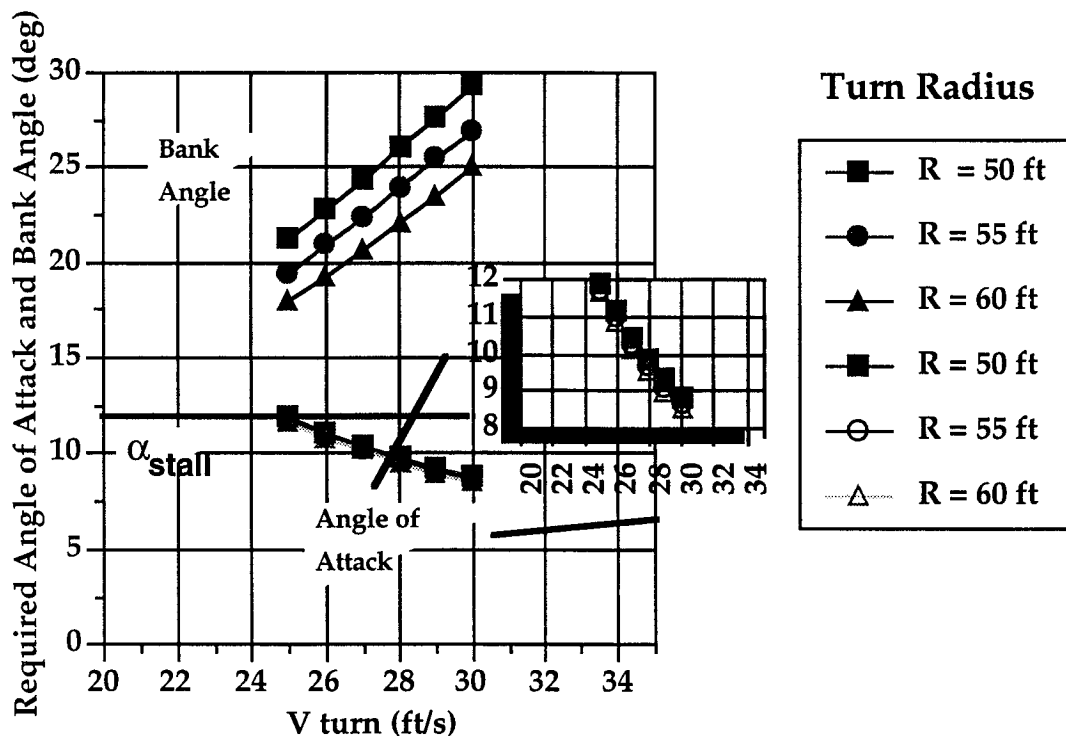
As required in the DR&O, the airplane must fly a 60 foot radius turn at a speed of 25 feet/second. From the plot, it is seen that this places the aircraft quite close to

its stall angle. In order to avoid this, it was decided that the airplane will turn in the range of 26-28 feet per second. In doing so, *Icarus* will obtain a bank angle between 19 and 25 degrees depending on the radius of the turn. Coupling these two analyses, an acceptable aileron configuration was chosen such that the desired bank angle was reached within approximately one second and the required angle of attack through the turn was not in excess of the stall angle of the wing at approximately 12.5°.

Table 7.2: Summary of Lateral/Roll Stability and Control

MOMENT ARM (in)	VERTICAL TAIL AREA (in^2)	RUDDER AREA (in^2)	MAX δr (deg)
22.0	71.5	42.0	± 30
AILERON INBOARD EDGE (in)	AILERON OUTBOARD EDGE (in)	AILERON CHORD (in)	MAX δa (deg)
24.0	36.0	1.0	± 15

7.7 CONTROL MECHANISMS

Having sized and placed the various control surfaces of the aircraft, it was necessary to determine the mechanisms by which they would be controlled during flight. Using various combinations of servos, control rods, and control horns, a scheme was proposed to actuate the various surfaces, as shown schematically below.

Figure 7.7: Schematic of Elevator/Rudder Control Mechanisms
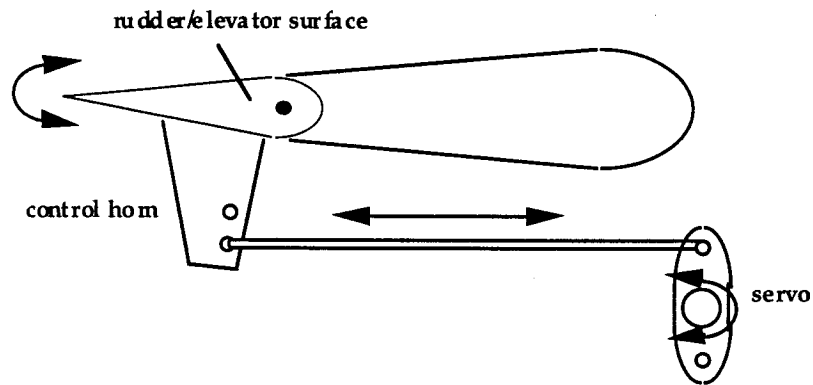
In the design of *Icarus*, it was necessary to use three servos for the actuation of the control surfaces. One servo was tied to the elevator, rudder/tail wheel, and ailerons independently. As shown in Figure 7.7 above, the elevator and rudder/tail wheel were controlled by simple pushrods activated by servo rotation. To allow for ground control during taxi maneuvers, the control system for the rudder surface was coupled with the tail wheel in such a way that a rudder deflection results in a subsequent rotation of the wheel as shown in Figure 7.8 below.

Figure 7.8: Schematic of Rudder/Tail Wheel Linkage and Control

to rudder

to servo
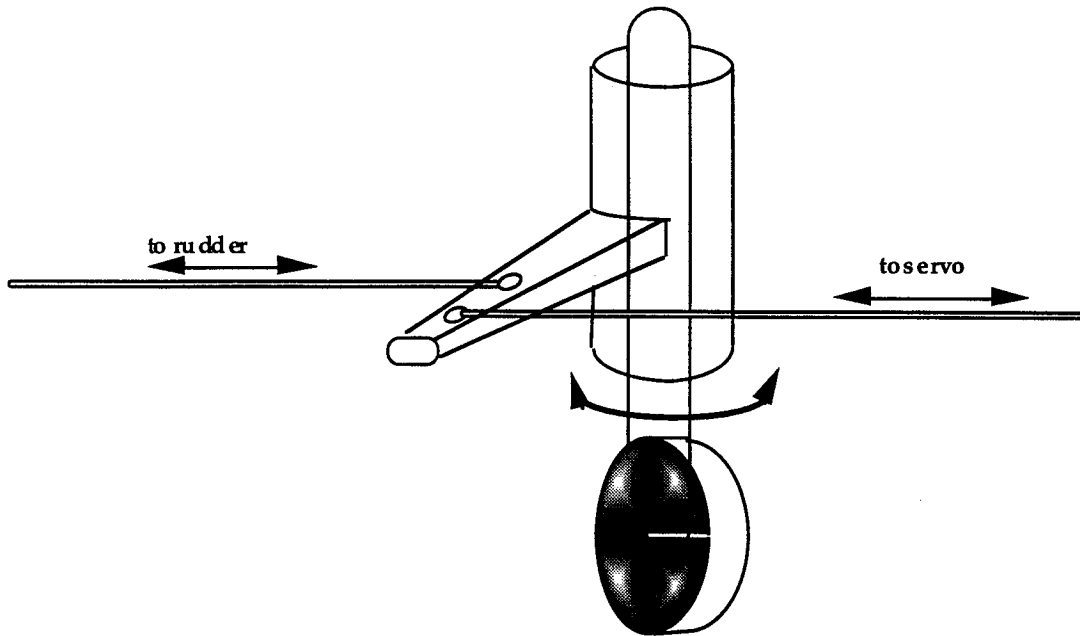
Thus, during the ground roll, an input from the pilot to the rudder servo would be coupled through the linkage to the wheel and result in a turn in the direction specified. The ailerons, however, were controlled in a different manner. Rather than through the direct pushing or pulling of a control horn, the control of the ailerons was accomplished through the use of a z-bend wire, the mechanism of which is shown below in Figure 4.9.

Figure 7.9: Schematic of Aileron Control Mechanism
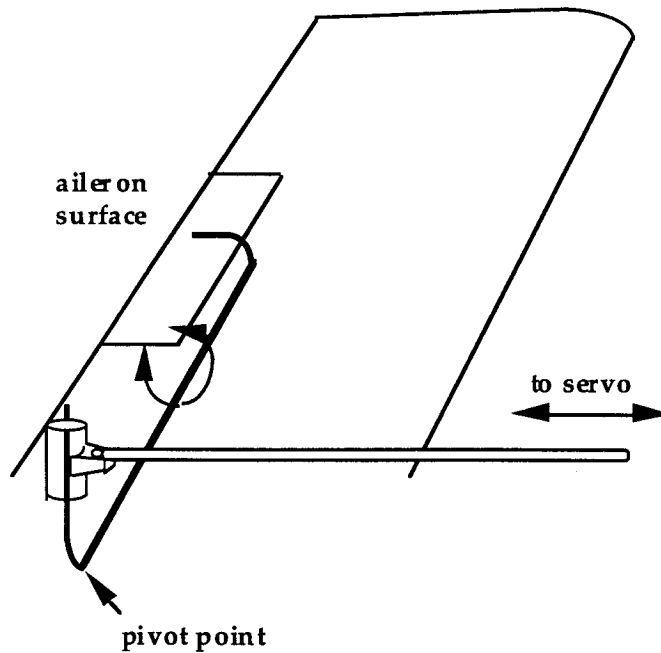
The aileron surface used in this design is composed of a solid balsa trailing edge piece which is roughly triangular in cross-section. By boring out a hole in the aileron, it was possible to embed the z-bend wire directly in the aileron surface. Epoxyed within the aileron, the wire was bent to run along the trailing edge spar of the wing (not shown) and then, once within the wing carry-through, the wire was subsequently bent upwards where, through a connection, it was tied to a control rod. This control rod is linked to a servo placed slightly forward within the fuselage. In this manner, motion of the control rod results in a rotation of the wire about its pivot point and thus in a deflection of the aileron.

References:

7.1. Nelson, Robert C. Flight Stability and Automatic Control. New York: Mc-Graw-Hill, Incorporated, 1989.

7.2. Selig, Michael S., Donovan, John F., and Fraser, David B. Airfoils at Low Speeds. Virginia Beach: H.A. Stokely, publisher, 1989.

7.3. Takeoff Performance Code: **takeoff.f**. Coded by Dr. Stephen Batill and Supplied for Use by AE441 Design Class.

7.4. McCormick, Barnes W. Aerodynamics, Aeronautics, and Flight Mechanics. New York: John Wiley and Sons, 1979.

8.0 PERFORMANCE

8.1 REQUIREMENTS AND OBJECTIVES

Once the aerodynamic forces were calculated and the propulsion system selected, performance estimates for the aircraft were made. The key sources for these estimates were the computer programs PROP123, Takeoff Performance, and Electric Performance (Ref. 8.1, 8.2, and 8.3). The objectives had for the performance results were a high cruise speed, a takeoff distance of no greater than 28 feet, and a range of at least 30000 feet so that every airport in Aeroworld can be reached non-stop. Table 8.1 gives a listing of the performance characteristics of *Icarus Rewaxed* .

Table 8.1 Performance Characteristics

Takeoff Distance	25.4 ft
Takeoff Thrust	2.734 lb
Battery Drain @ Takeoff	6.27 mahr
Takeoff Velocity	28.85 ft/s
Cruise Velocity	72.0 ft/s
Minimum Velocity	10.0 ft/s
Maximum Velocity	75.0 ft/s
Stall Speed	24.0 ft/s
Maximum Range	38300 ft
Endurance @ Max Range	890 s
Maximum Endurance	1130 s
Range @ Max Endurance	31700 ft
Maximum Rate of Climb	13.048 ft/s
Maximum (L/D)	13.94
Cruise (L/D)	7.02
Cruise Range	30870
Cruise Endurance	428.76 s
Minimum Glide Angle	4.10 degrees
Minimum Radius of Turn	55.0 ft @ bank angle = 18 deg

8.2 CRUISE VELOCITY

The key part of performance from the design requirements and objectives was the cruise velocity. The objective was to reach a cruise velocity of 60 ft/s for a 30,000 ft minimum range. When it was discovered that the cruise velocity could be surpassed while still decreasing the cost per flight, it was decided that *Icarus Rewaxed* would fly at a higher throttle setting than that necessary to fly at 60 ft/s, with the number of batteries necessary for takeoff. This resulted in a cruise velocity of 72 ft/s, which was the velocity from the throttle setting that would not use up the battery capacity and still leave battery charge for takeoff and turns. The addition of a fourteenth battery would have only pushed the motor past its maximum rpm (our current cruise velocity rotates the motor at 15516 rpm, the maximum listed rpm is 16500).

8.3 TAKEOFF ESTIMATES

Takeoff distance was a key objective for this design. Since it was desired to access every airport in Aeroworld, a 28 foot takeoff distance was required. In order to takeoff in 28 feet, the number of batteries was determined in combination with wing area and propeller. Since it was already determined that the Zingali 10-8 propeller was the most efficient and put out the most thrust, it was necessary to vary the wing planform area and number of batteries to find which combination would be the most desirable while still allowing the aircraft to takeoff in 28 feet. Using a conservative estimate for the friction coefficient (0.15), it was found that with 13 batteries and a wing planform area of 7.5 ft^2 *Icarus Rewaxed* could takeoff in 27.99 feet. The same combination with a less safe, yet more realistic, friction coefficient (0.05) allowed for takeoff in 25.39 ft.

The takeoff battery drain had little effect on battery capacity since only 0.5% of our battery pack current (7.09 mahr out of 1400 mahr) was depleted.

In order to compute the performance characteristics during takeoff, a program entitled Takeoff Performance (Ref 8.2) was used. Appendix E shows the input and output for the program.

8.4 RATE OF CLIMB

Figure 8-1 shows the power available and power required as a function of velocity for a range of power settings. From this graph it can be seen that using the full voltage of the thirteen batteries (15.6 V), a maximum velocity of 75 ft/s can be obtained. The minimum speed at this voltage is 10 ft/s. Figure 8-2 shows the relationship between the maximum rate of climb and the cruise velocity. The maximum rate of climb (13.048 ft/s) occurs at a velocity of 41 ft/s.

Figure 8.1 Power Required and Power Available Curves With Respect toVelocity
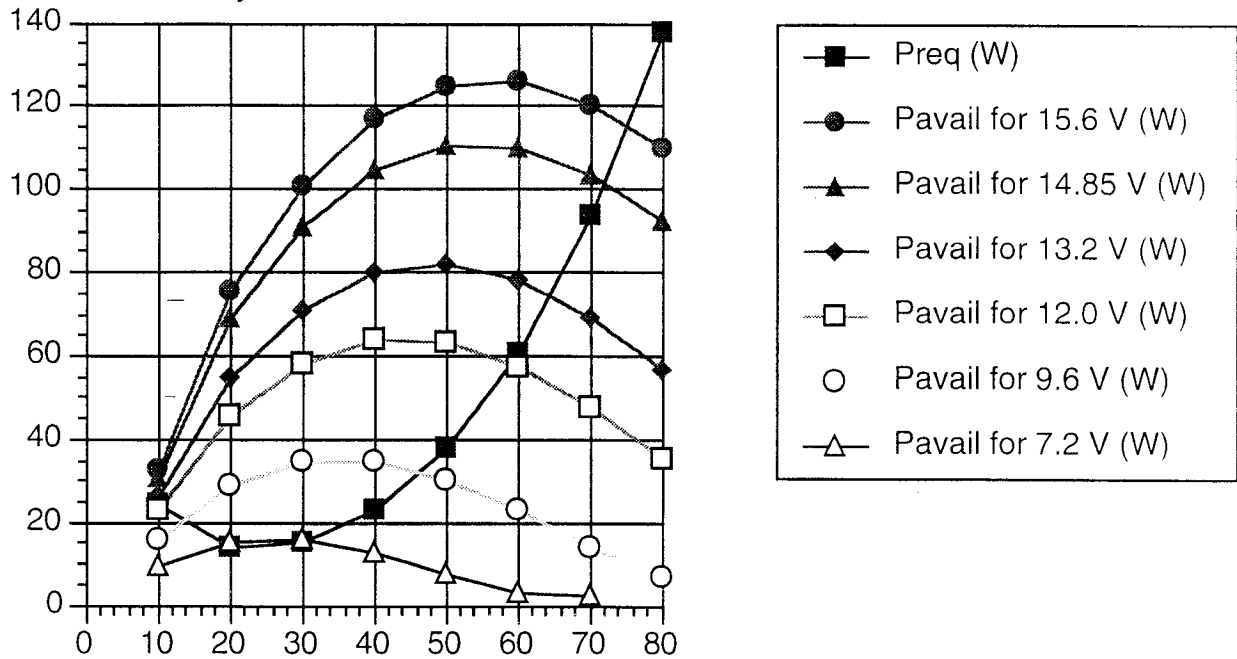
Figure 8.2 Determination of Speed Resulting in Maximum Rate of Climb
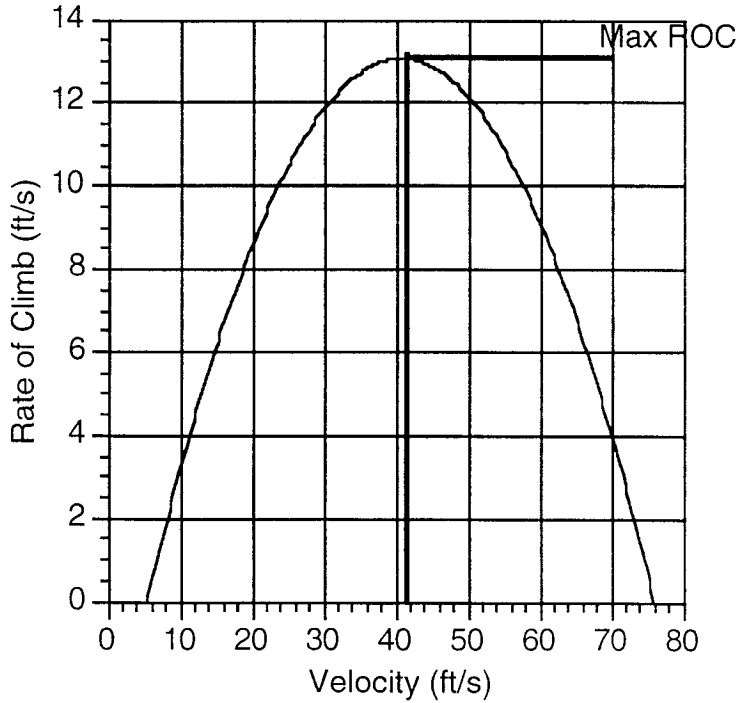
8.5 LEVEL TURN PERFORMANCE

The key to level turn performance is listed in the requirements, where it is stated that the aircraft must be capable of performing a steady, level, 60 foot radius turn at a velocity of 25 ft/s. The DR&O initially stated that our load factor will not exceed 2. Examining the relation between the bank angle and the load factor:

$$n = 1 / \cos (\phi)$$

it could be seen that a bank angle greater than 60 degrees was not desirable. To find the turn radius relationship:

$$R = V^2 / g * \tan (\phi)$$

was used. In this relationship R and V were known, thus the required bank angle was 18 degrees which corresponds to a load factor of 1.05, well below the maximum load factor of 2.0. Substituting the stall speed of 24 ft/s for the aircraft into this equation it was found that the minimum turn radius was 55 ft.

8.6 RANGE AND ENDURANCE

The range and endurance for the *Icarus Rewaxed* were compared against velocity as shown in Figures 8-3 and 8-4. It is important to note that the values for both endurance and range do not include the two minute allowance for loitering. From these figures it can be seen that the maximum range of the aircraft is 38,266.5 ft and occurs at a cruise velocity of 43 ft/s. The endurance for this maximum range then is 889.92 s. The maximum endurance is 1132.06 s and occurs at a cruise velocity of 28 ft/s. The range for the maximum endurance is 31697.02 ft. The values for the range and endurance came from an RPV program in Excel which was modified to include the range and endurance (Ref. 8.3).

Figure 8.3: Comparison of Maximum Range to Range at Cruise Speed

Max Range = 38266 ft

Cruise Range = 30870 ft
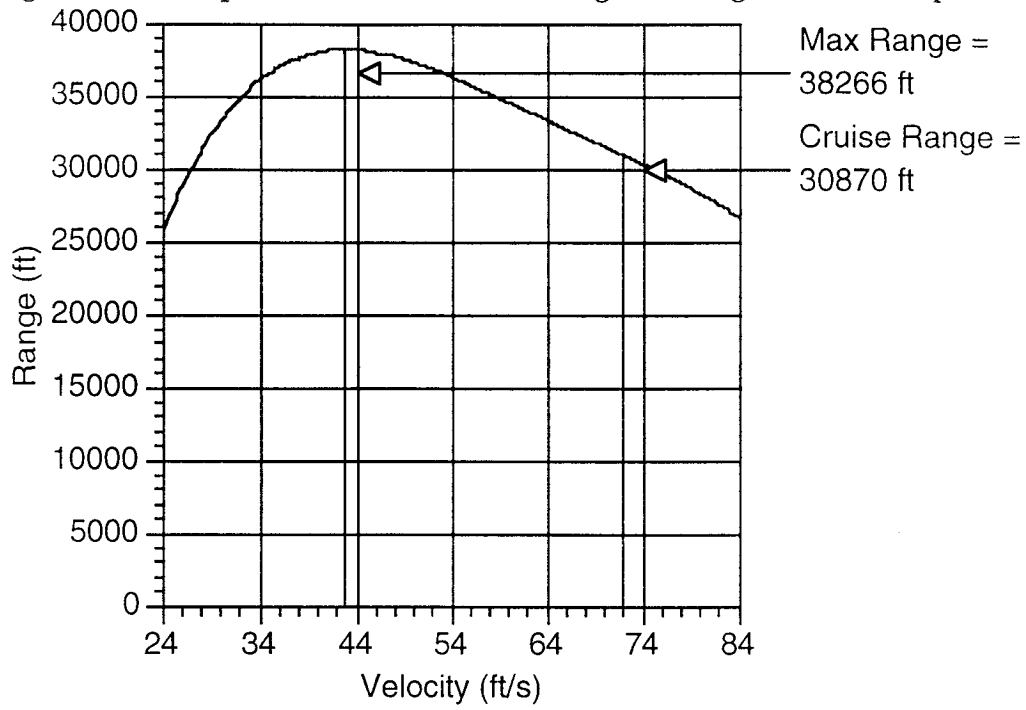
Figure 8.4: Comparison of Maximum Endurance to Endurance at Cruise Speed
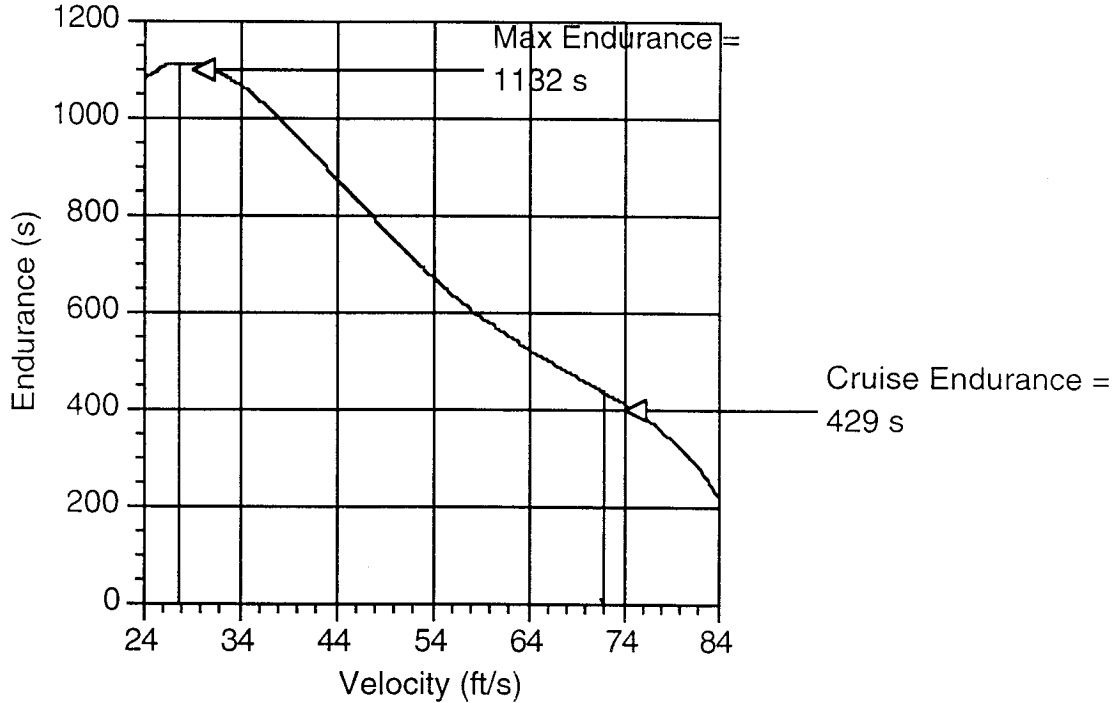
8.7 RANGE VS. PAYLOAD

The range of the aircraft increases with decreasing payload as depicted in Figure 8-5. The points on the plot were taken at the cruise speed of 72 ft/s. It can be seen from the graph that the loss of passengers has very little effect on the range of the aircraft (from 30912 to 30891) since they only make up 0.9% of the total weight.

Figure 8.5: Effects of Payload on Range
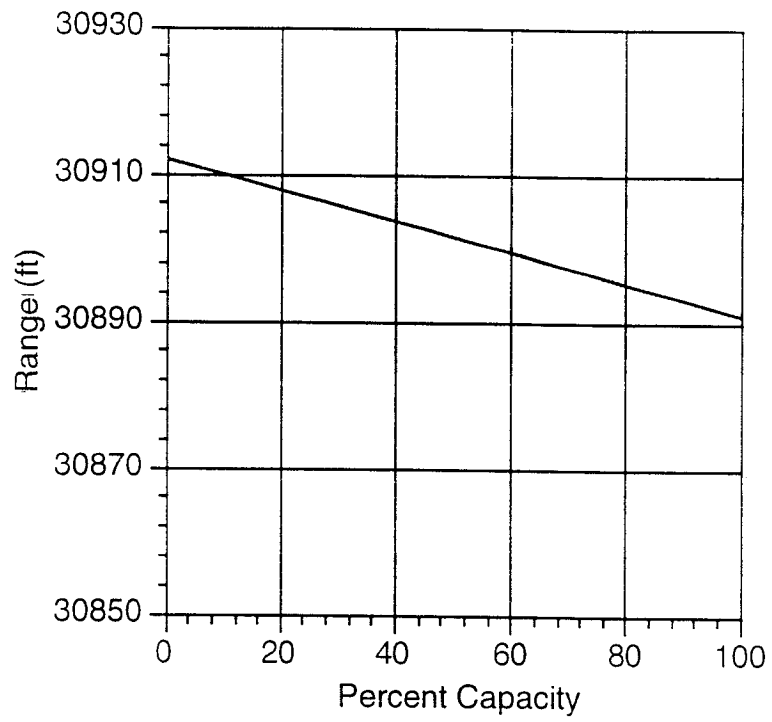
References

8.1 Batill, S., "PROP123", Fortran computer Program, University of Notre Dame

8.2 Batill, S., "Takeoff Performance", Fortran computer program, University of Notre Dame

8.3 Dunn, P., "RPV Performance" Excel computer program, AE 454 Propulsion class, University of Notre Dame

8.4 Dunn, P.,"Ae 454-Lecture No. 18", Department of Aerospace and Mechanical Engineering, University of Notre Dame, 1993

9.0 STRUCTURES AND WEIGHTS

The goal of the structures department was find a design that can safely withstand the expected loading conditions, survive extreme flight conditions, and accomplish the mission with a minimum weight. To meet this goal, the following objectives were formulated in accordance with the Design Requirements and Objectives (DR&O) established by Recent Future, Inc.:

Structures Group Objectives:
- Design the structure to maintain integrity under normal flight regimes. This flight envelope is defined to include takeoff and landing impact loads, and flight load factor limits of 2.75 and -1.5 .
- Provide adequate strength to withstand extreme loading conditions without catastrophic failure. This includes loads caused by a sharp-edged gust of 10 feet/second at cruise velocity (increasing the load factor to 4.5).
- Provide a factor of safety of at least 1.4 on all load bearing structures.
- Provide the necessary space for four passengers and two crew members.
- Position the fuel/batteries in the wing carry through structure.
- Allow easy removal of the wing component
- Minimize the weight by not over-designing the aircraft. The measure of this objective will be to have a margin of safety approaching zero at the extreme recommended load condition (n = 2.75).
- Provide at least 3.5 inches of propeller clearance in the landing gear design.
- Explore the use of new, advanced materials in the wing design.

9.1   MATERIALS SELECTION

Recent Future, Inc. studied many types of prospective materials for the . With the goals of light weight and high strength, wood was the material of choice for most of the aircraft. Wood is readily available, inexpensive, lightweight, and easy to tool. Three types of wood were considered: balsa, spruce, and birch plywood. Other types of wood were not considered because of a lack of experience in past designs. Balsa has a very low density and thus will be used

whenever possible. It is also the least expensive. However, balsa has a limited strength and was not used in areas where the shear flows or bending moments became significant. Spruce is very strong in compression and relatively strong in tension (see Table 9.1). These characteristics made spruce a natural choice for the fuselage longerons which have to support the bending moment in the airplane. Spruce was also used as a leading edge spar for the wing to give it extra support and to protect the shape integrity of the Monokote. Birch plywood has the advantage of being able to support load in more than one direction. It is relatively strong in all directions, but also very heavy. This material was used at the engine attachment and at the floor attachment for the wing.

Two other "advanced" materials were considered: Steel and Graphite. These materials have the advantage of providing a very large amount of stiffness and strength for a very low weight. We purchased a steel shaft and obtained a test section of graphite to validate our predictions. As expected, the advanced graphite gave very good stiffness and strength/weight characteristics, but the cost of $65.00 per shaft put too much of a strain on our budget. The steel shaft, detailed above in the Section 9-1b, gave almost the same performance as the graphite with a cost of $15.00 per shaft.

The final material used in the aircraft is the Monokote skin covering. This material not only provides the desired aerodynamic shape, it also contributes to the overall strength and stiffness of the structure.

Table 9.1: Material Properties[1]

Material	Density(oz/in^3)	σ_{com} (psi)	σ_{ten} (psi)	τ_{xy} (psi)
Balsa	0.0928	600	400	200
Spruce	0.256	9000	6200	750

[1] The properties of the steel shaft were determined by testing. Other materials properties were from Ref. 2, and the past data base.

Birch Plywood	0.370	2500	2500	2500
Monokote	.000125(lb/in^2)	N.A.	25	25

Table 9.1b (cont.)

Steel Shaft: Weight: 4.27 oz   Length: 47 inches   Thickness: 0.4 mm

Eavg: 20×10^6 psi

9.2 LOAD CONDITIONS

The effect of velocity on load factor for the recommended flight regime is shown in Figure 9.1 . With the V-N diagram, an estimation can be made of the maximum loads that the airplane can experience, and hence guide the design process. The maximum lift-coefficient of *Icarus* was estimated to be 1.03. This information, along with the airplane geometry and sea level atmospheric conditions, was then used to plot the stall limits shown in Figure 9.1 .

The gust lines were calculated using the method outlined in Reference 9.1, p. 467 for a gust of 10 ft/s.[2] The gust lines show a vital design consideration: at the higher speeds, a sharp gust will take the airplane beyond the recommended load envelope. The recommended maximum load factor(n) for maneuvers is 2.75 (-1.5 for negative loads), but with a 10 ft/s gust at cruise, n approaches 4.75 . This relatively violent flight extreme is an important consideration in the wing structural design, in line with the requirements listed above.

The recommended load limit of 2.75 was calculated based on margins of safety of the fuselage components (explained in section 9.3 -- see Table 9.1). This limit sets some basic restrictions on the pilot. Because of the potential for large loads caused by gusts, Recent Future, Inc. recommends that on windy days (where a gust of 10 ft/s is expected), the pilot not exceed a velocity of 45 ft/s.

---

[2] A detailed derivation of these curves is shown in Appendix C.2.

Figure 9.1: V-N Diagram
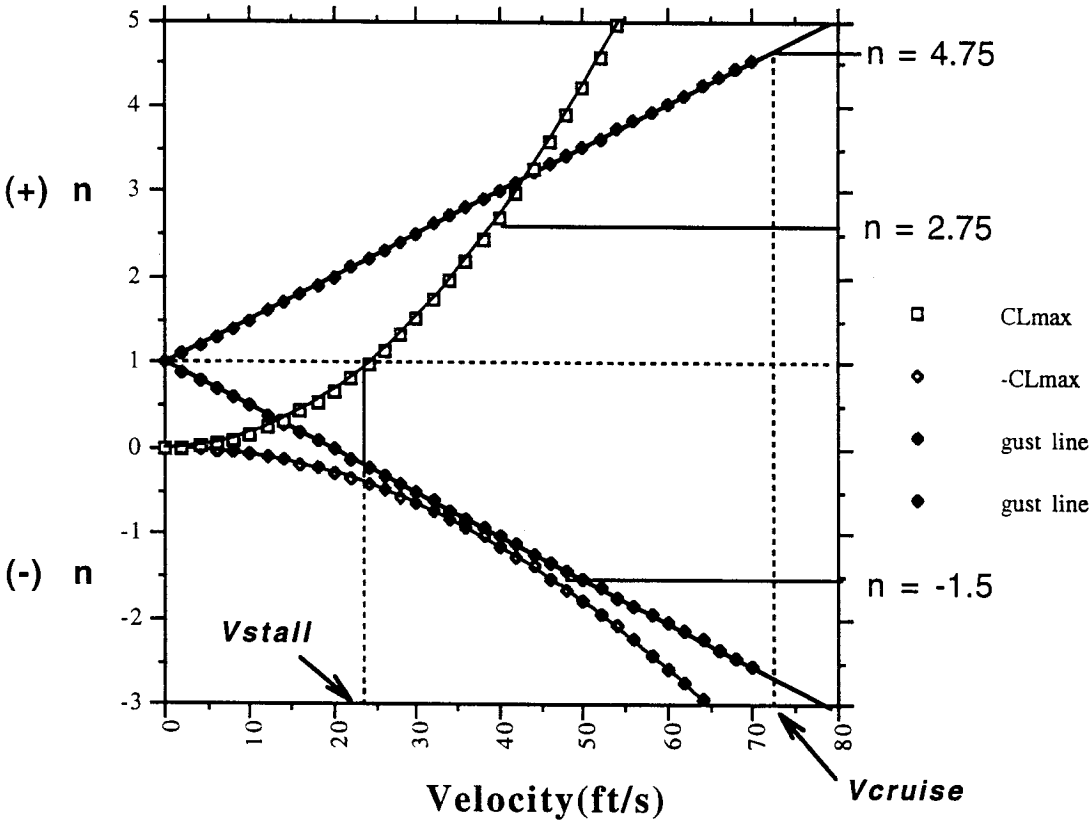
Figure 9.2: Weight Distribution Nose to Tail
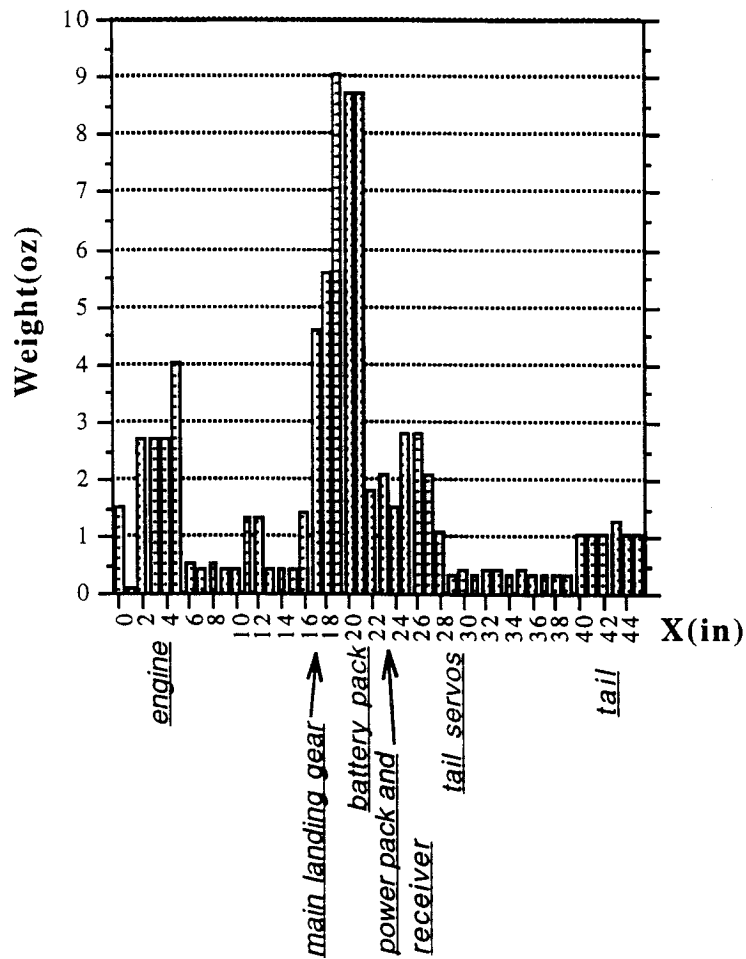
9.3   FLIGHT AND GROUND LOADS

The weight distribution of the airplane is shown in Figure 9.2. The

component loads in this graph were analyzed as distributed forces over their

respective lengths. These loads determined the shear and bending moment

diagram for the airplane as shown in Figures 9.3a and 9.3b. Figures 9.3a and 9.3b

were found by applying resultant point loads at the landing gear positions. This

modified weight distribution was then integrated from x=0 at the nose to x =45

at the end of the tail. The bending moment diagram (Fig. 9.3b) was found by

integrating the shear diagram from nose to tail. Figures 9.4a and 9.4b show the

shear and bending moment diagrams for the airplane in a steady, level flight

condition.

Figure 9.3: Shear and Bending Moment Graphs for Ground Loads (n = 1)

a)

b).
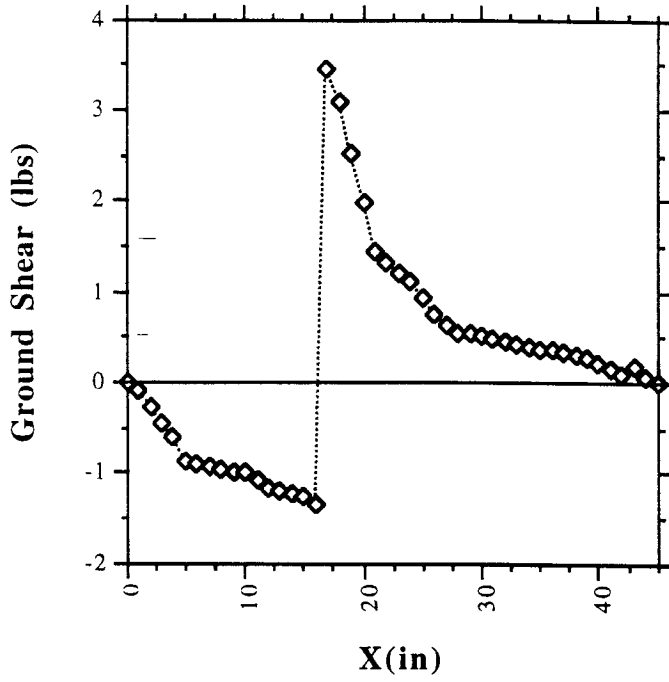
Sign Convention
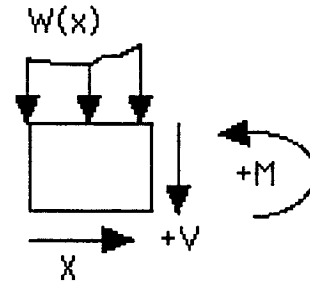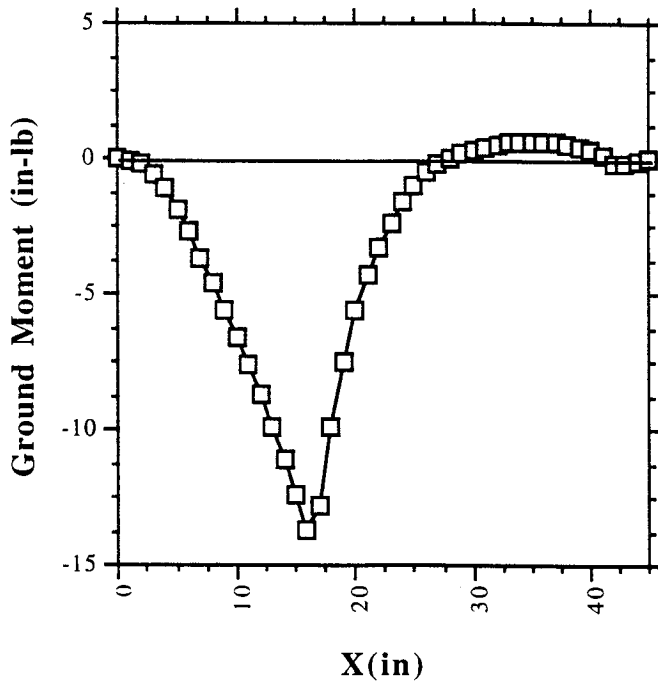
Figure 9.4: Shear and Bending Moment Diagrams for Steady, Level Flight

a).

b).

Sign Convention

9 - 7
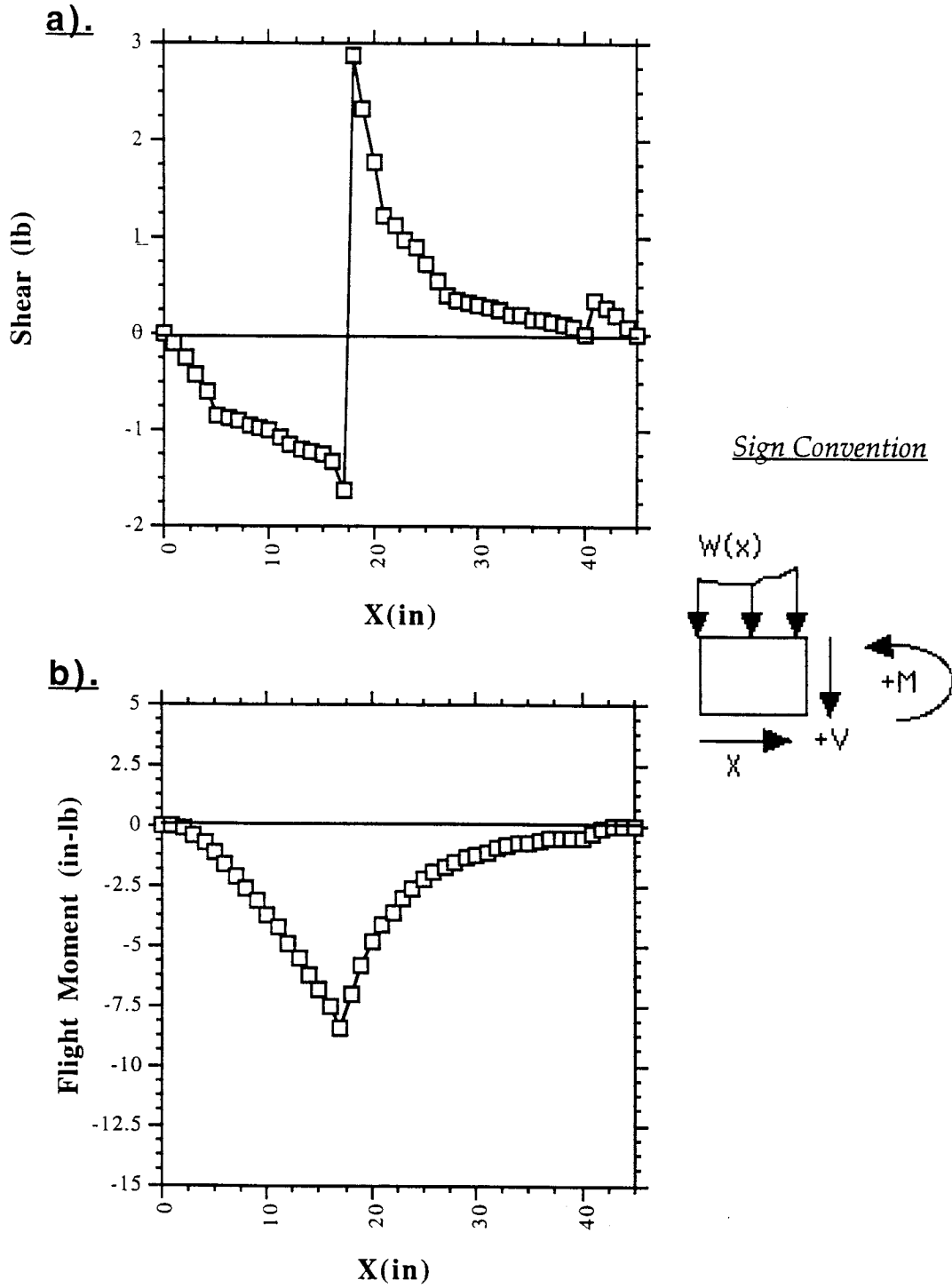
9.4   FUSELAGE

The fuselage was designed to minimize weight yet still supply adequate support. The structural performance of the fuselage was determined in a large part by the bending and shear results shown in Figures 9.3 and 9.4. Since the fuselage experiences varying degrees of shear forces and bending moments, the design breaks the fuselage structure in four sections (see Figure 9.5). Each of the four sections has the same cross-sectional area: Width = 3.5 in; Height = 2.75 inches.

Figure 9.5: Airplane Fuselage Sections
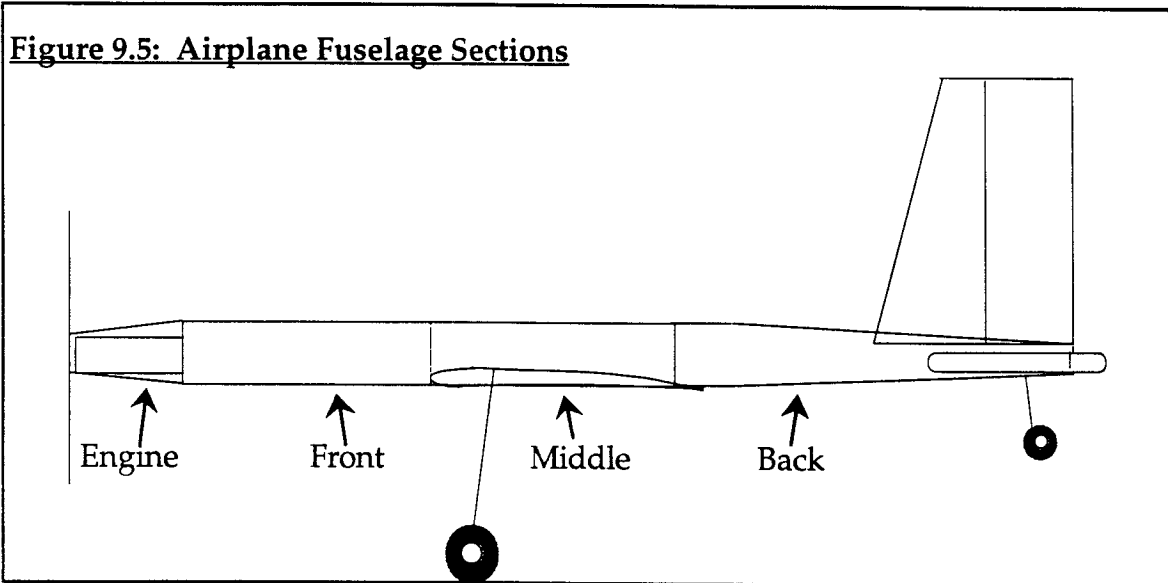
The first section acts basically as an aerodynamic cover for the motor. This 5 inch section was composed primarily of a balsa wood truss covered in Monokote. This truss does not support any loads other than its own weight. Included in this section is a plywood board that serves as the point of attachment for the motor.

The second section was 11 inches long and composed of a wooden truss. Due to the relatively large bending moments in this section caused by the weight of the motor, spruce was used for the main longerons. Spruce provided the highest tensile and compressive strength of the wooden materials considered (see

Section 9.1: Materials Selection) and thus was the material of choice for the longerons. In order to minimize weight, the rest of the truss was made of balsa. This structure houses the pilot, co-pilot and the speed controller.

The third section, 11.5 inches long, experienced the highest shear forces and bending moments. For this reason, this section must be the most structurally sound. All the forces from the landing gear and wing flow to this section first. For this reason, single sheets were used for the walls in lieu of a truss design. These boards were made of balsa. The resulting increase in thickness in the vertical direction dramatically increases I in the formula:

$$\sigma_{max} = \frac{M\,y}{I}$$

because I is proportional to height cubed in this direction. Rearranging this equation shows that a much larger moment can be supported using this design over a truss. The obvious penalty for this design came in weight. However, using balsa as the main material, and with a fuselage that has a fairly small cross-section, the total weight of these boards was 2.4 ounces (see Table 9.3). The batteries, aileron servo, receiver, and power pack were all located in this section.

The back section was 17.5 inches long and composed of a balsa wood truss supported by spruce longerons. This design provided adequate structural integrity by allowing the spruce to support the main load, while using the lighter balsa whenever possible. This section housed the remaining four passengers and connected the tail and rear landing gear to the rest of the structure.

The front and back sections of the fuselage will provide room for six passengers. In these areas, a thin balsa sheet will provide the floor necessary to support these passengers.

Table 9.2 shows the factors of safety for each fuselage load bearing component on the ground and in a steady, level flight condition. It also shows conservative estimates of the margins of safety for the fuselage under a 2.75g

load condition. The margins of safety here are very close to zero. This leads to the decision that the airplane should be flown within an n=2.75 envelope. These margins of safety were calculated using a factor of safety of 1.4 (as outlined in the DR&O) and they do not take the Monokote or other small load bearing devices into account. But since there was also a chance of flaws in the material that could lead to early failure, a limit of 2.75g flight conditions is recommended.

The individual components and weight estimations of each section is shown in Table 9.3 .

Table 9.2: Fuselage Structural Safety Margins

Ground Condition:

Section:	Load Bearing Component	Max Stress (psi)	Factor of Safety
Front	Spruce Longerons	3840	1.6
Middle	Balsa Boards	104	3.8
Back	Spruce Longerons	1920	3.12

Steady Level Flight Condition:

Section:	Load Bearing Component	Max Stress (psi)	Factor of Safety
Front	Spruce Longerons	1920	3.12
Middle	Balsa Boards	70	5.7
Back	Spruce Longerons	1920	3.12

Load Factor (n) = 2.75

Section:	Load Bearing Component	Ultimate Load (lbs)	Margin of Safety
Front	Spruce Longerons	396	0.023
Middle	Balsa Boards	324	0.043
Back	Spruce Longerons	396	0.023

Table 9.3: Fuselage Component Design

Section:	Component:	Material:	Weight(oz):
Engine Housing:	Hardwood block	Plywood	1.34
	Spars	Balsa	0.52
	Monokote:		0.11
Front Truss:	Monokote:		0.25
	4xlongerons	spruce	0.70
	Truss:	balsa	3.30
	floor:	balsa	0.45
Middle:	Monokote:		0.26
	2xmain spar:	balsa	2.40
	Plywood floor:	Plywood	1.11
	floor:	balsa	0.47
Back:	Monokote:		0.39
	4xmain spar:	spruce	1.68
	Truss:	balsa	2.46
	2xControl Rods:		0.54
	floor:	balsa	0.71
Total:			**16.7**

9.5 WING

The wing was designed to withstand the expected load conditions, survive extreme load conditions, and be easily attached and removed. The wing was manufactured as a separate entity to facilitate the component validation test[3]. A detailed drawing of the complete wing-fuselage connection is included at the end of this section.

The recommended n = 2.75 was derived from structural considerations about the wing spar and from the margins of safety in the fuselage showing in Table 9.1. The pilot can exceed this load factor without structurally damaging the airplane, but this recommendation ensures safety and structural integrity.

---

[3] This test involves loading the wing to structural failure.

The wing spar design is shown in Figure 9.6. This design used a steel rod as the main load bearing component. This rod had a very high strength to weight ratio.

Figure 9.6: Wing Spar Design

balsa airfoil sections

Main Wing
(steel) spar

Trailing Edge
(balsa) spar
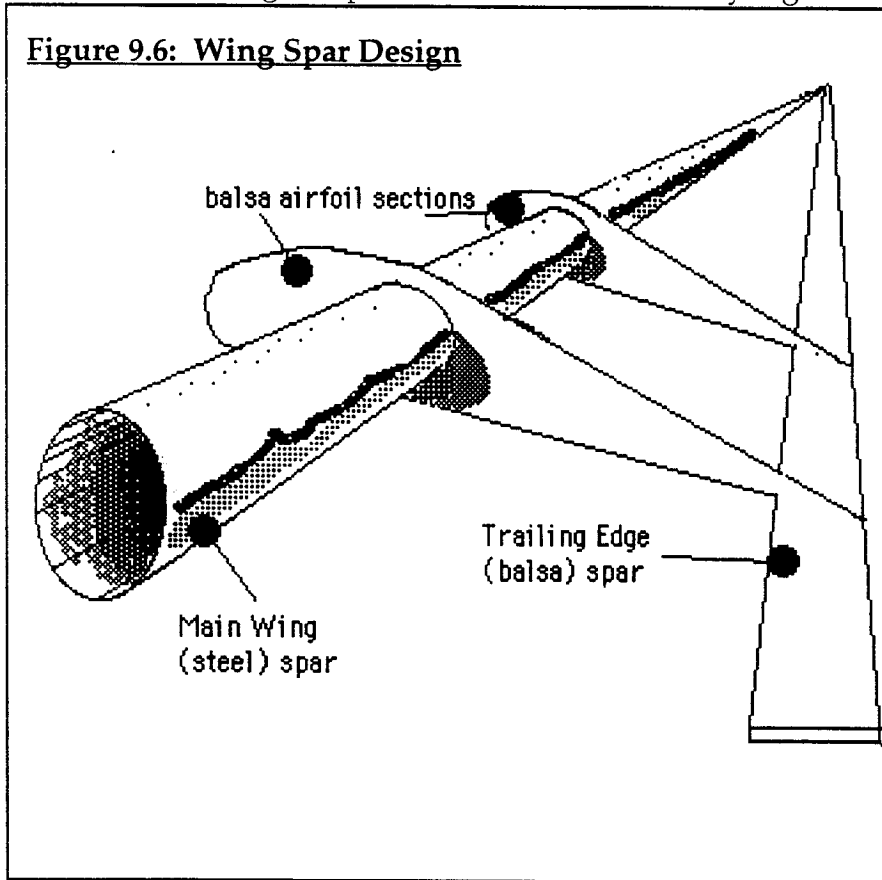
It also had stiffness characteristics that were comparable to past wood designs. The use of the rod was justified by the fact that it can support a much higher load (then wood) without approaching its maximum allowable stress. This minimizes the chance of component failure. A test component was purchased from a subcontractor[4] to validate theoretical results. The tests involved clamping the rod at one end and applying a point loads at a fixed moment arm of 1 ft. We were able to sustain a force of 25 lbs at this distance without any residual plastic deformation.

The wing spar was then analyzed under a 3g load condition. This load condition corresponds to a turn radius of 60 ft at cruise. This loading is extreme yet conceivable with emergency or acrobatic maneuvers or strong gusts. The spanwise lift distribution and subsequent shear and bending moment diagrams

---

[4] *The Club Doctor* in Mishawaka, IN.

are shown in Figure 9.8[5] . These graphs represent the wing cantilevered at its midpoint. The sign convention for these graphs is as follows:
- *X = spanwise position with 0 at the root, 46 at the wing tip*
- *Shear (V) is taken as positive upwards*
- *Bending Moment is taken as positive in the counter-clockwise direction*

Notice that with this load condition, the maximum bending moment about the root is 125 in-lb. Our test, with the 25 lb load applied 12 inches away from the root put a moment of 300 in-lb about the root without permanent deformation.

The stiffness characteristics of the steel beam are also comparable to the previous wooden designs. Figure 9.7 shows the expected tip deflection for the 3g loading condition. It must be stated that this figure represents only the wing spar. The actual wing has a leading edge spar (to maintain leading edge integrity), a trailing edge spar (to facilitate the ailerons), and is covered in Monokote. These three extra factors increased

Figure 9.7: Wing Tip Deflection for n=3
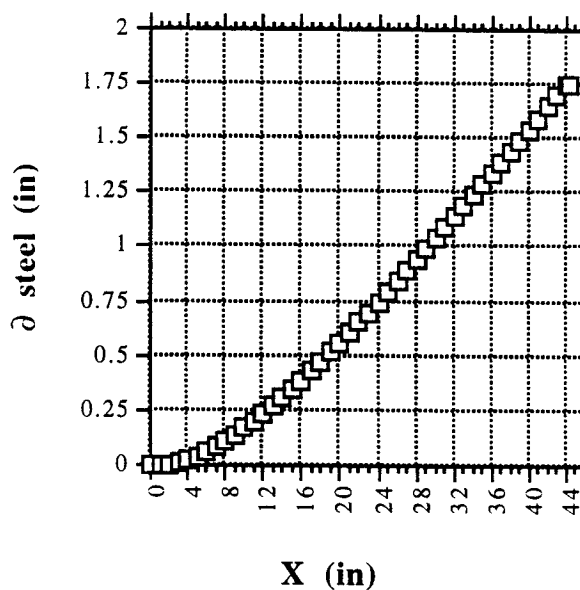
the stiffness and overall strength of the wing. In effect, our analysis is a very conservative estimate of the wing structural performance.

The extreme load condition of a vertical sharp-edged gust at cruise speed (corresponding to n ≈ 4.75 from Figure 9.1) gave a moment about the root of approximately 450 in-lb. Even with the considerations of the Monokote and extra spars, Recent Future, Inc. recommends that the pilot avoid this loading

---

[5] A detailed description of the theory behind plots 9.7 and 9.8 is shown in Appendix C.1 .

Figure 9.8: Spanwise Lift, Shear, and Bending Moment Distribution on Wing
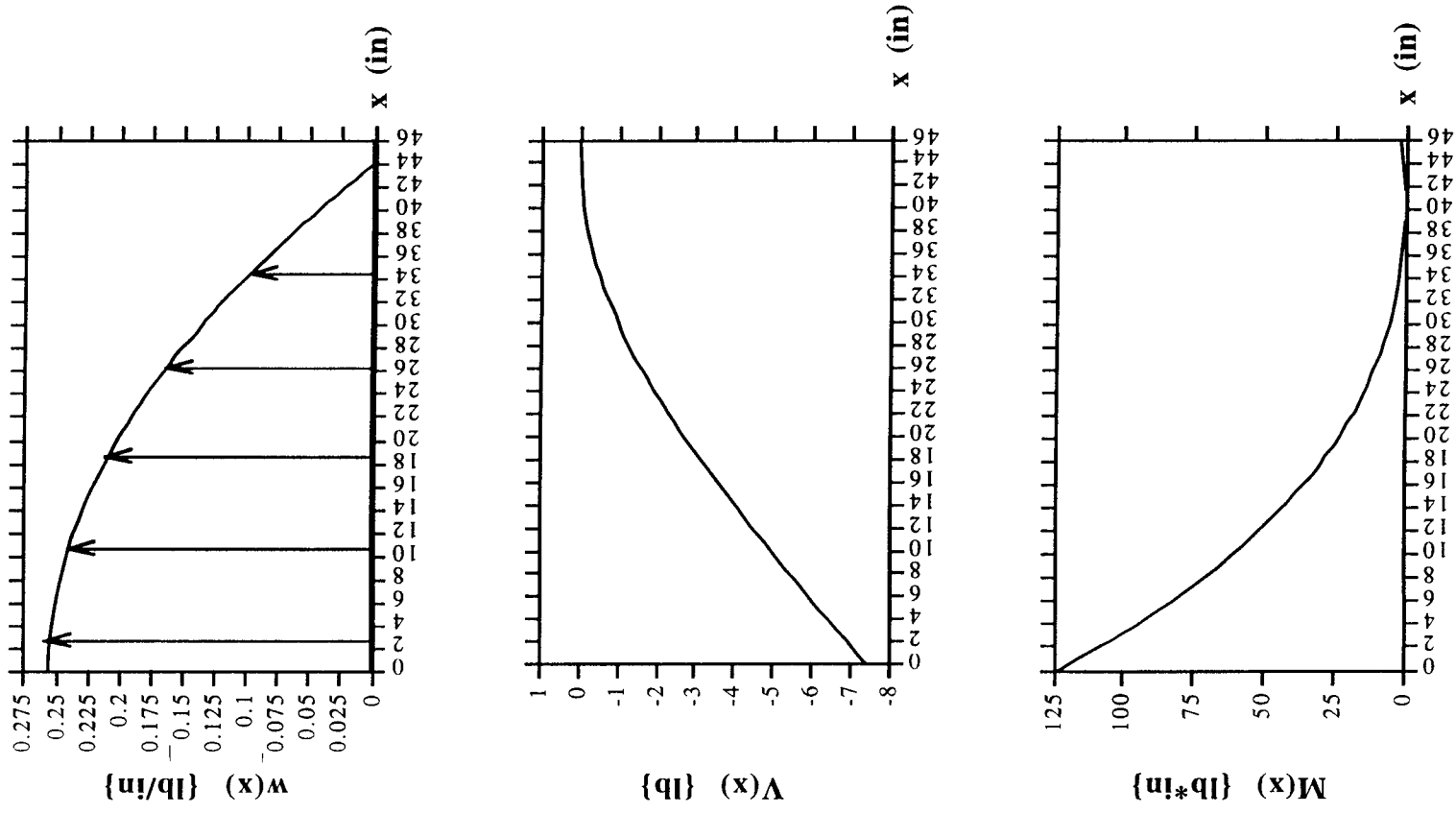
condition to protect the fuselage integrity. Therefore, on a particularly windy day, the pilot should not exceed a speed of 55 ft/s.

The one potential drawback of the steel shaft was a weight penalty. However, the weight of the steel shaft was competitive with previous wooden designs. Figure 9.9 shows the weights of two wooden designs (I-Beam and single Beam) compared to the weight of the steel shaft. As the thickness of the beams increases, the steel shaft actually

Figure 9.9: Steel Shaft Weight vs. Standard Wooden Spar Weights
Beam and I-Beam indicate past wing spar designs. Thickness refers to the cross-section of Beam and the flanges of the I-Beam.
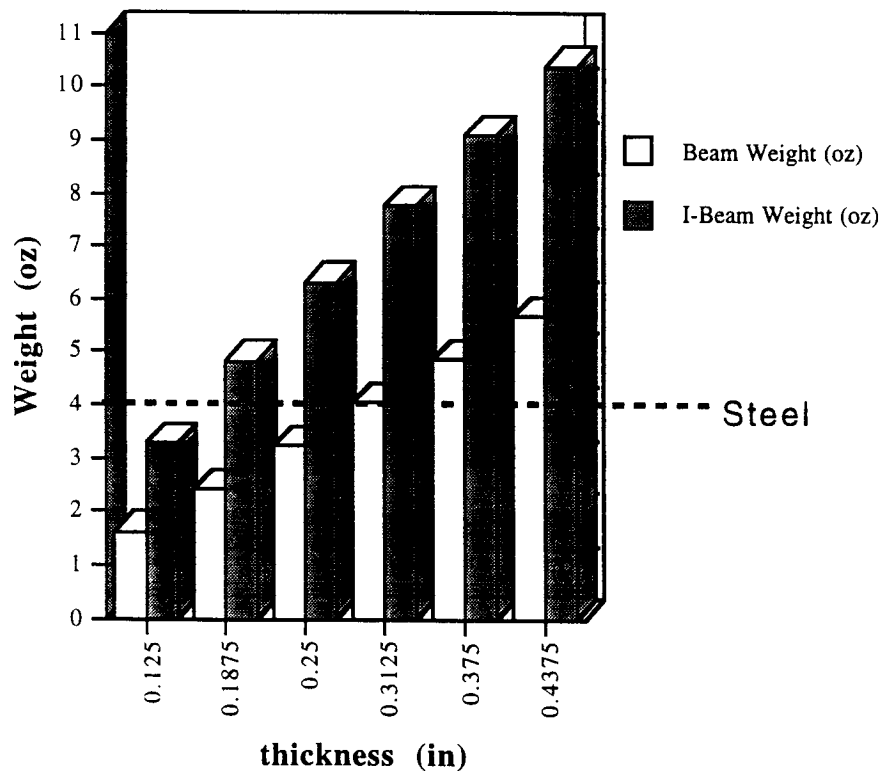
provided a weight advantage. The total estimate of the wing weight, including all other components, was 1.1 lbs, a figure that is very similar to the weights of past wings in our data base.

There are other drawbacks to using the steel shaft. The first drawback occurs in the challenge of affixing the wood to the steel itself. The subcontractor assured us that a strong epoxy will more than do the job. Because extremely heavy wooden pieces are successfully attached to similar shafts in the design of golf clubs, he thought gluing balsa airfoil sections would not be a problem. The second drawback was caused by the fact that the steel shaft does not traverse the entire span of the wing. Wooden spars were called upon to support the wing for 18 inches at each wing tip. Since the resultant wing loading in flight occurs approximately at 17 inches from the midpoint (well within the steel rod's boundaries), these wooden spars do not have to support a significant amount of weight. The last drawback occurs because the shaft is tapered at one end. While this did not significantly affect the structural characteristics, it did shift the center of gravity of the wing slightly off-center (0.62 inches). This was easily counterbalanced by shifting the battery packs.

Balsa airfoil shapes were glued directly to the main shaft at intervals of 4 inches. These provided the framework for the Monokote, which gives the wing its aerodynamic shape. The Monokote was also used to create hinges connecting ailerons. The trailing edge spar shown in Figure 9.6 was used to support the wing and provide the area for the ailerons. The ailerons were nothing more than cut-out sections of this spar attached to rotating control rods. A single aileron servo provided the necessary motion.

The wing was attached to the underside of the fuselage. Two plywood "floor" sections provided support for screws affixing the wing to the fuselage. Rubber bands also gave added support. With this design, the wing can be easily removed and reattached. A detailed drawing of the wing/fuselage connection is shown in Figure 9.17, included at the end of this section.

9.6   TAIL SECTIONS

In many past designs in Aeroworld, the horizontal tail was composed of flat plates. However, the *Icarus* uses airfoils to make the horizontal tail more like a wing. This decision was made for three reasons: 1.) The aerodynamic characteristics of an airfoil as opposed to a flat plate were much better; 2.) The beams supporting the airfoils sections allowed greater loading than flat plate designs; and 3.) The flat plate did not save the airplane a significant amount of weight.

Past designs cited weight savings as a motivation for using flat plates. However, our analysis of the tail section showed that a flat plate gave minimal --

Figure 9.10: Tail Section Weight Analysis
Note: "I-Beam" and "Single Beam" indicate designs that can support airfoil ribs. The total weight of the horizontal tail is shown in this graph.
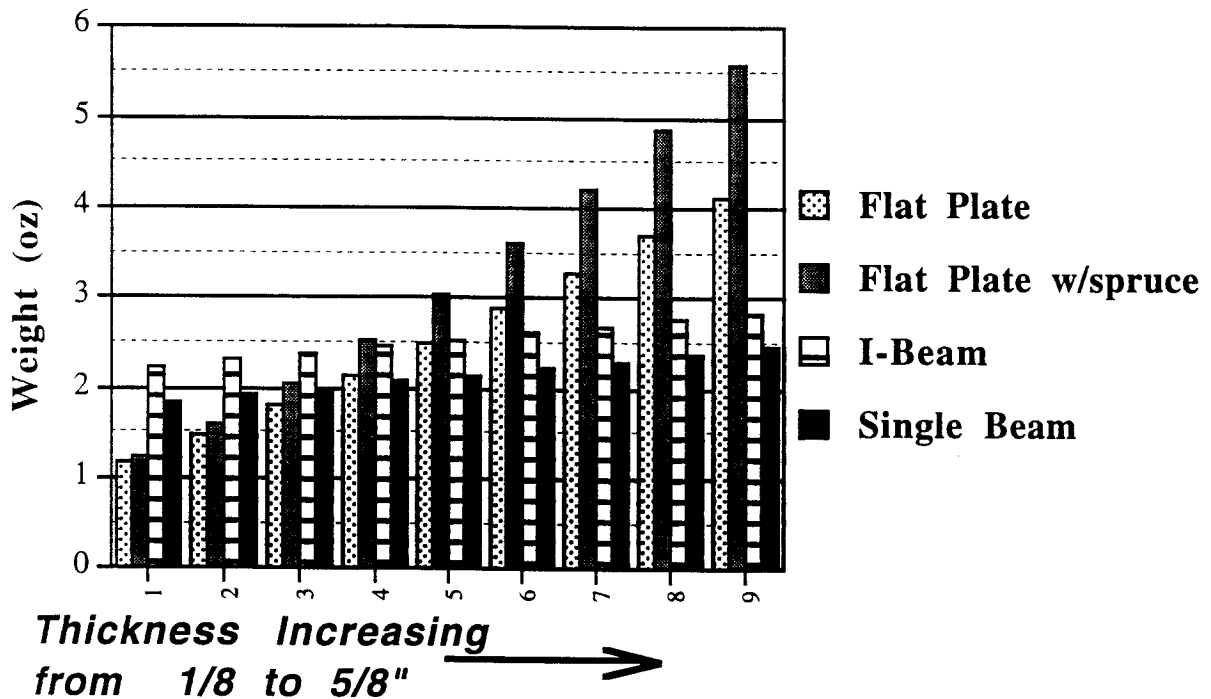
if any -- weight savings. This is shown in Figure 9.10. In this figure, the I-Beam

and Single Beam are the two designs considered to support the airfoils. Figure 9.10 shows the total weight of the horizontal tail for each design. The graph shows that as the thickness of the flat plate spars increase, the weight becomes comparable to the airfoil design. Even at the very lowest thickness (a very flimsy and structurally unsound design) the weight savings is on the order of only one ounce.

An I-Beam was selected as the main spar based on the results shown in Figure 9.11. This graph shows the predicted stresses in the tail components for the maximum flight load conditions. There is a definite structural advantage in using either of the beam designs (and hence airfoils). The greater thickness in the beams reduced the stress caused by a given moment, thus allowing greater loads.

Figure 9.11: Stresses in Horizontal Tail Section

Thickness Increasing ⟶
from   1/8 to 5/8"
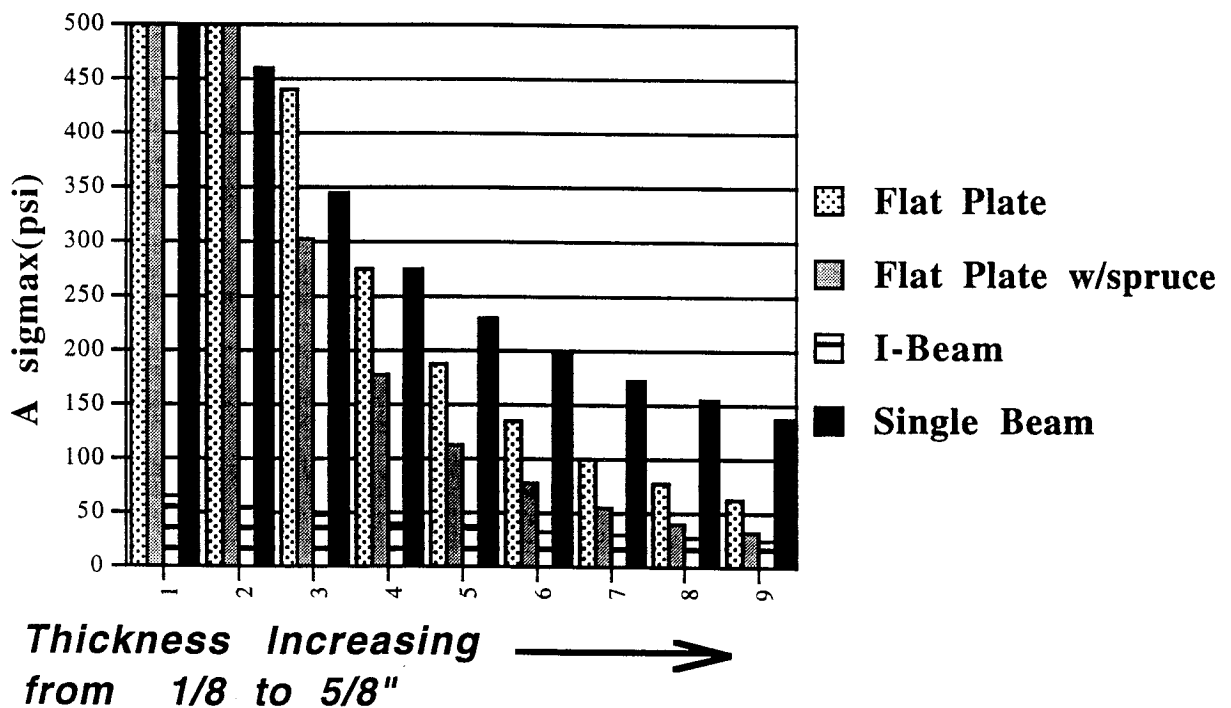
The aerodynamic benefit of using airfoils instead of a flat plate came in the drag breakdown. This topic is discussed more thoroughly in the Aerodynamics section of this proposal. The thicker yet more aerodynamic shape of the airfoil design gave more structural integrity and a better drag profile with only a modest penalty in weight.

The vertical tail was swept and made from a balsa wood truss section. Since the height of the vertical tail was less than half of the span of the horizontal tail, the drag penalty for this flat plate was minimal compared to the rest of the plane. The manufacturing time savings from a flat plat plate design[6] and the inherent cost benefits outweighed the marginal performance benefit of using airfoils.

9.7   LANDING GEAR

According to the DR&O, *Icarus Rewaxed* must be able to takeoff from unprepared ground in 3.5 inches of grass. In order to give the propeller adequate clearance for this condition, our landing gear struts were longer than those used in past designs. This longer gear must be able to adequately support the stresses involved in landing. The desired characteristics of the landing gear are that it provided shock absorbance (through deflection) and did not allow either the nose, tail, or wing tip to hit the ground. To design the main gear, a "worst case scenario" of a 3g load placed on only one tire at landing (i.e., the airplane is banked) was used. In order to determine the length of struts needed for the main gear, the clearance requirement based on the DR&O was first calculated. This is 7.125 inches from the ground as shown in Figure 9.12.

---

[6] With a swept design, each airfoil section would have to be individually cut. This process would significantly increase manufacturing time.

Figure 9.12: Main Landing Gear Geometry
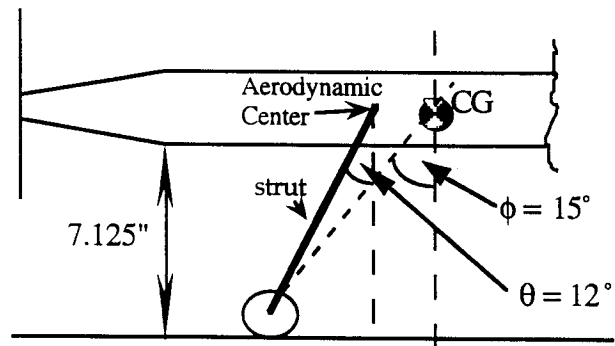
Foam tires with a diameter of 2.5 inches were used. The foam had adequate strength and provided a weight advantage over rubber tires. The main gear was attached to the steel shaft at the wing quarter-chord. From the analysis of the strength of the steel rod, it was determined that the landing gear load would not cause significant stress in the shaft. Therefore, the main gear struts were treated as cantilever beams.

First an analysis of available diameters of steel was performed by finding the maximum load a given diameter can withstand at various angles, θ, (where θ is defined as in Figure 9.12). This was done using the relationship

$$\sigma = \frac{My}{I}(FS)$$

The properties of steel were found using Reference 9.2. From this analysis it was determined that the minimum diameter of steel which can be used is 0.125 inches. In order to meet the design objectives of high speed, efficient flight, drag minimization of this component was vitally important, since the landing gear contributed approximately 37% of the total drag of the airplane. Next, the angle θ was determined. Figure 9.13 shows a plot of θ and maximum force allowed versus strut lengths. Since the design is for a 3g load ($\approx$15 lbs. for this aircraft), anything below 15 lbs. was unacceptable. Therefore, the only adequate angle was 5°. However, Recent Future, Inc. felt that 5° is too small of an angle. With

such a small angle, the airplane could easily tip over. In Reference 9.3, a "rule of thumb" for the angle φ is given as being between 13°-20° in order to prevent the plane from tipping nose down upon landing. With θ being only 5°, φ is only 8°. Assuming both tires hit the ground, a greater angle can be used. Based on this relaxed requirement, φ was chosen to be 15°. This causes θ to be 12°.

To determine the length of the struts it was necessary to examine the deflection at landing. Some deflection is desired in order to provide shock absorbance, but the deflection could not be so great that the propeller hit the ground. Due to the clearance requirement and the angles chosen, the minimum length of the strut that can be used is approximately 9.4 inches. This allowed a perpendicular distance of 8 inches. The 8 inch distance allowed tip clearance, including some deflection.

Figure 9.13: Maximum Landing Force on Strut vs. Length of Strut
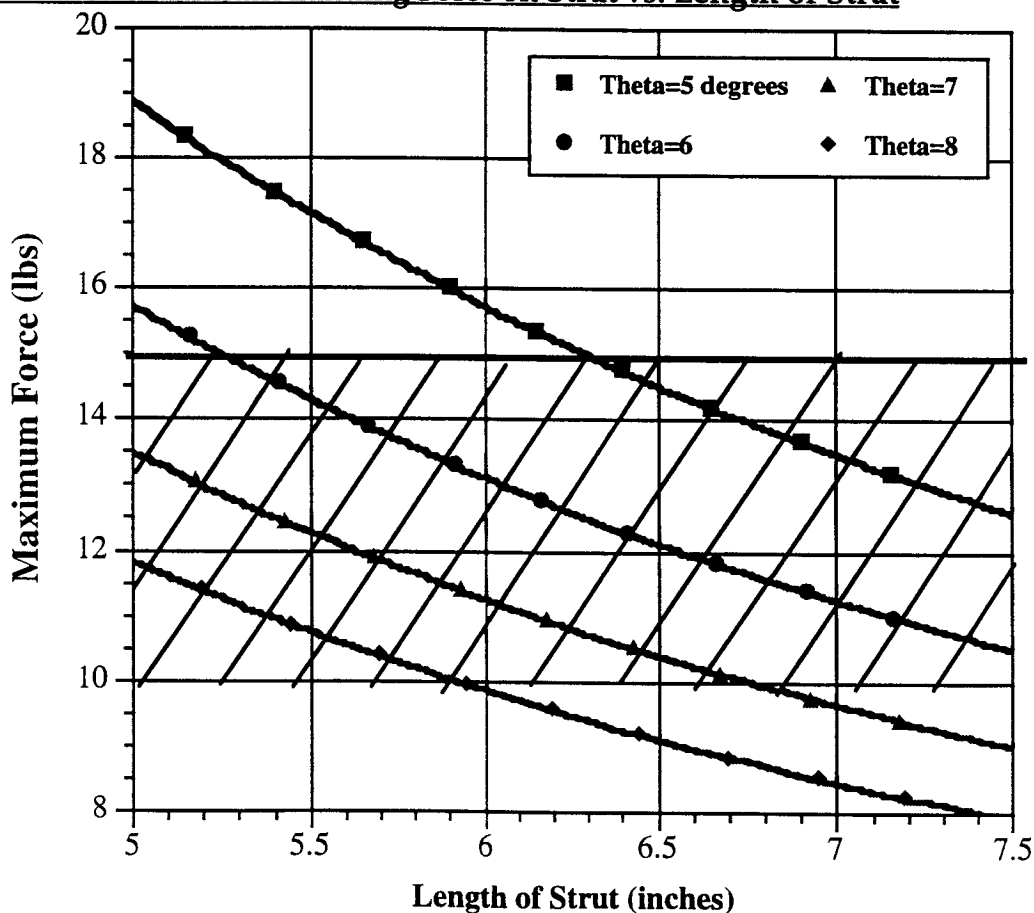
For the tail gear, a foam tire of 1.5 inch diameter was chosen, and a strut length of 4 inches was needed so that the horizontal tail remains 3.5 inches above the ground in accordance with the DR&O.

The exact placing of all gear was determined based on a maximum turnover angle of 60° (Ref. 9.3). This was determined using the geometry of Figure 9.14 . From this, the tail wheel was positioned 41 inches from the nose. The main wheels were placed 16 inches from the nose, at a distance of 24 inches apart. This geometry gave a turnover angle of 43°. Another "rule of thumb" in Reference 9.3 is that the distance between the tires should be about 1/4-1/3 the wing span. This geometry meets that criterion. The final design is shown in Figures 9.12 and 9.15.

Figure 9.14: Schematic to determine turnover geometry
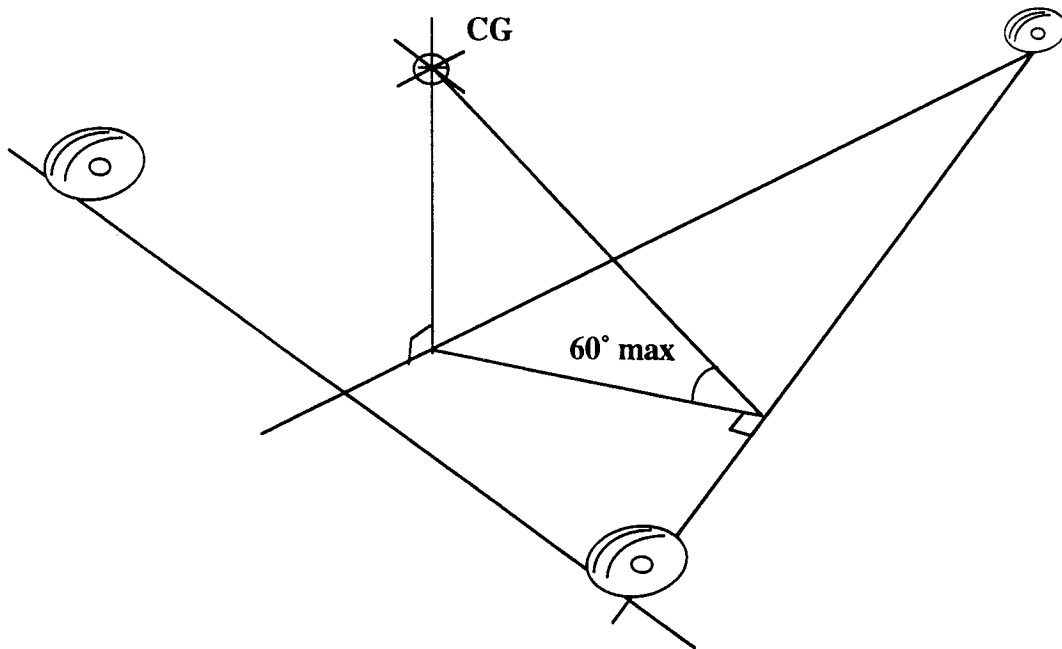
Figure 9.15: Landing Gear Geometry

L=9.4

5°

13°

W=24"
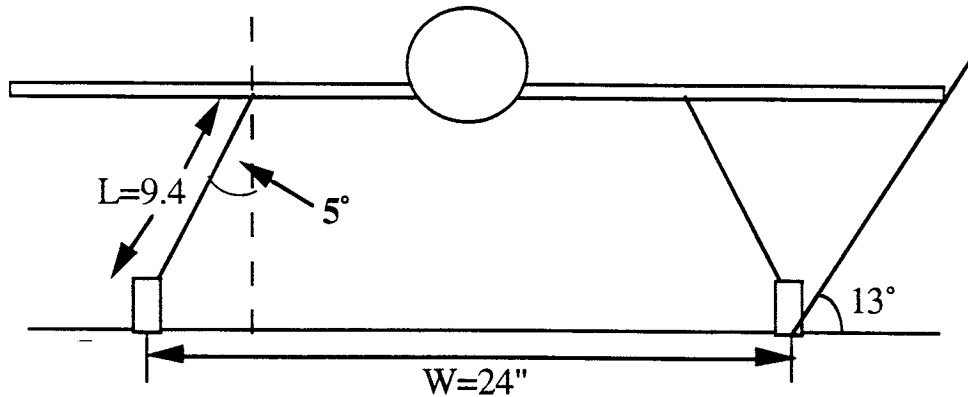
The last important aspect of the landing gear design was the attachment it to the fuselage. The method chosen is shown in Figure 9.16. The strut followed the main wingspar for added support. It was attached to the wing carry-through 4 inches behind the main wing spar. This gave enough of a moment arm to dissipate the forces of landing without damaging the fuselage or wing carry-through.

Figure 9.16: Landing Gear Attachment to Fuselage

Side view   Top view

main wing spar

main strut

attachment of strut to wing carry-through

strut braced along main wing spar(steel shaft)

point where strut slopes down toward ground
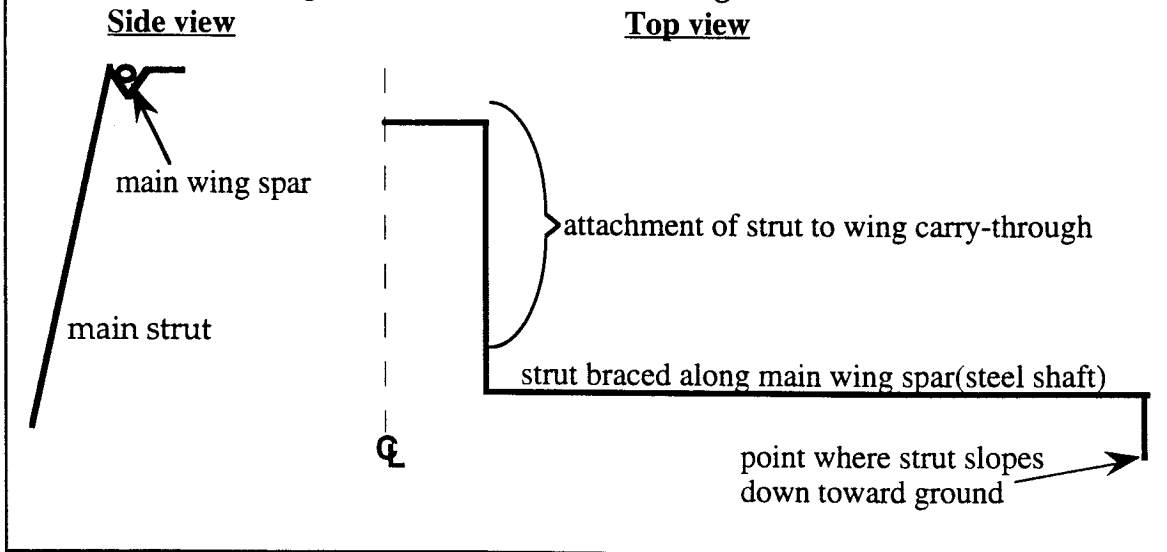
Figure 9.17: Wing Attachment to Fuselage

TO SCALE:
(1 box = ½ ")

$\frac{1}{4}$ "

FUSELAGE SHAFTS

WING SHAFT   I - ½ "

← DOTTED PART IS PART OF
WING STRUCTURE. TWO SCREWS
ATTACH IT TO FUSELAGE FLOOR.

2½ "

BATTERIES

15 "   5

NOTE: AILERON SERVO +
BATTERIES WILL REST ON
TOP OF FUSELAGE FLOOR.
REMOVING THE WING DOES NOT
REMOVE THESE COMPONENTS

AILERON SERVO

AILERON CONTROL RODS

TRAILING EDGE (WOOD) SHAFT
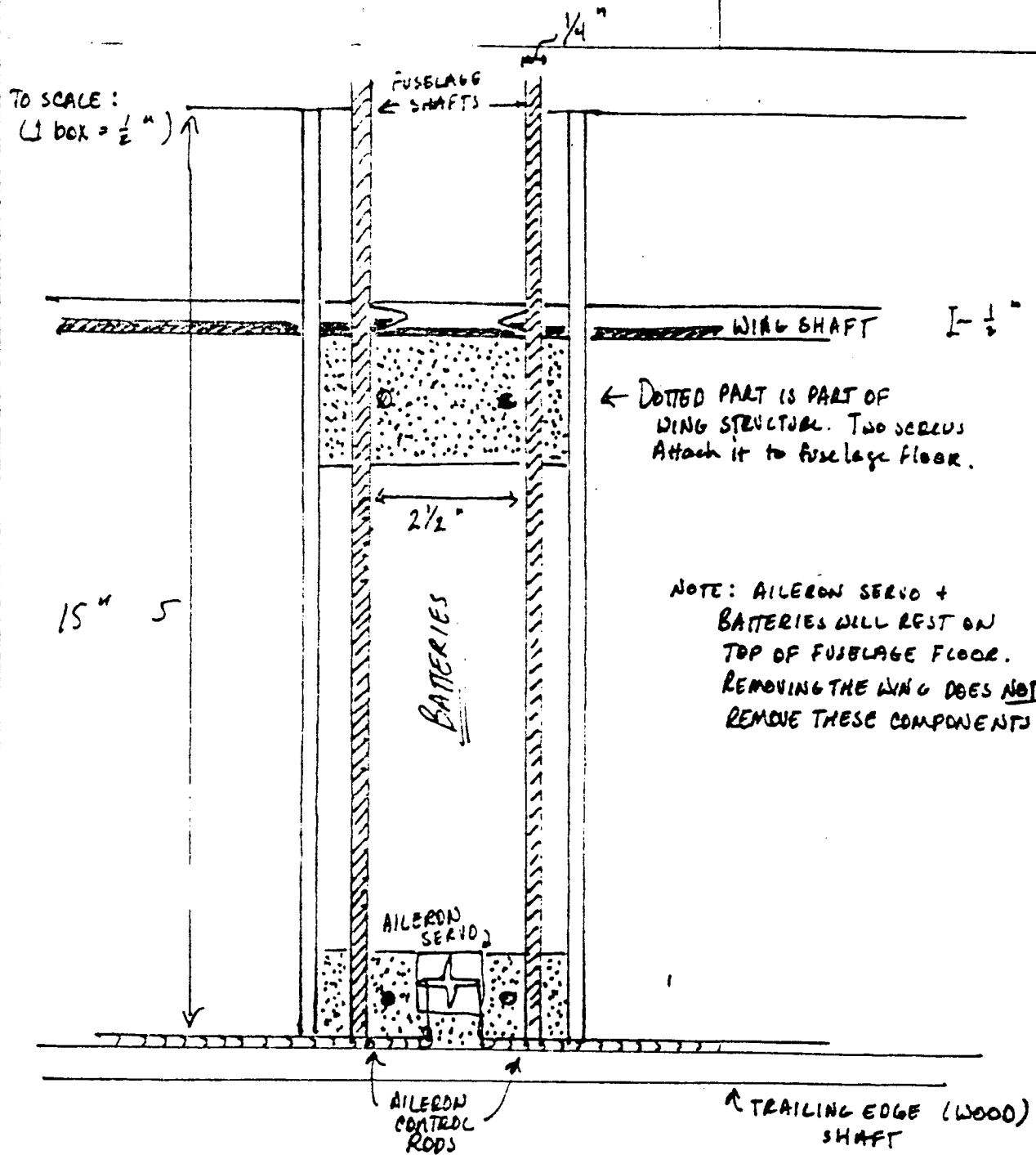
References:

1.) McCormick, Barnes W. Aerodynamics, Aeronautics, and Flight Mechanics.
New York: John Wiley & Sons, 1979.

2.) Beer, Ferdinand P. and E. Russell Johnston, Jr. Mechanics of Materials. New
York: McGraw-Hill Book Company, 1981.

3.) Stinton, Darrol. The Design of the Airplane. New York: Van Nostrand
Reinhold, 1983.

10.0 ECONOMICS

10.1 ECONOMIC GOALS

Second only to cruise velocity, cost was the most important driving force for *Icarus Rewaxed*. In a depressed market that is trying to make a comeback in Aeroworld, it was essential for Recent Future, Inc. to design and produce a high-speed, highly maneuverable general aviation airplane that is competitive yet affordable. The goal of Recent Future, Inc. was to make its cost per flight as small as possible. Areas of concern during the manufacturing stage were:

- increased efficiency during construction thus reducing man-hours, the largest percentage of the overall cost.
- careful manufacturing planning ensuring near perfect ordering of raw materials. This reduced excess material and the fee to dispose of it.

In order to enhance performance and durability, Recent Future, Inc. incorporated ailerons, a steel shaft reinforced wing main spar, and airfoil section horizontal tail. Major precautions were made to keep the cost of labor and tooling in check.

10.2 COST ESTIMATES

The total cost of *Icarus Rewaxed* represents the sum of the costs of the fixed subsystems, raw materials, and manufacturing. A detailed breakdown of the costs is presented in Table 10-1. The fixed subsystem subtotal is $463. Aside from the cost of the Astro 15 motor, major contributors to the fixed subsystem subtotal are the three-bladed Zingali propeller, the 13 cell battery pack ($4.50 per

Table 10.1: Cost Estimation

I. Fixed Subsystem		
Propulsion		
motor		$107
motor speed control		$50
batteries		$59
propeller		$15
Controls		
radio receiver		$35
radio transmitter		$75
avionics battery pack		$10
switch harness		$5
miniature servo (3)		$105
wiring		$2
	Subtotal	**$463**
II. Raw Materials		
balsa		$50
spruce		$20
plywood		$5
steel shaft		$15
monokote		$40
glue		$15
miscellaneous		$10
landing gear struts		$3
main wheels		$6
tail wheel		$4
	Subtotal	**$168**
III. Manufacturing		
labor costs		$1400
(140 man-hours at $10/hr)		
tooling costs		$100
	Subtotal	**$1500**
IV. Waste Disposal		
$10/oz.		**$100**
Total		$2231
(overhead & profit)	+	$1267
Total Cost Per Aircraft		**$3498**

battery), and a third servo used for ailerons. The raw materials cost at $168 was a small contribution to the overall airplane cost. The cost of manufacturing by far made up the largest percentage of the total cost. Figure 10.1 graphically depicts the major cost brackets of *Icarus Rewaxed* production. A waste disposal and removal of hazardous material cost was added because Recent Future, Inc. is a very environmentally conscious organization. The estimates sum to a total cost of $2231. The cost of overhead, $892, was 40% the total cost of the airplane. The profit margin was 12% the cost of *Icarus Rewaxed* adjusted for overhead which yielded a total cost of $3498.

Figure 10.1: Cost Breakdown of *Icarus Rewaxed*

Fixed Subsystem

21%

Manufacturing

Raw Materials 8%

4%

Waste Disposal

67%
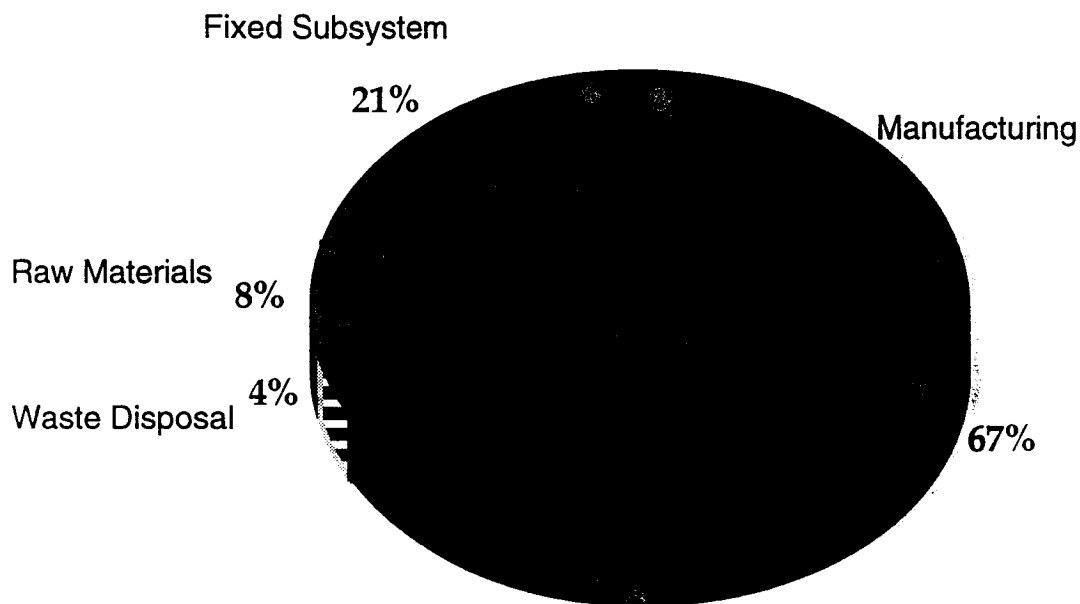
10.3 DIRECT OPERATING COSTS

The cost per flight of *Icarus Rewaxed* was based on the depreciation costs, the maintenance-insurance costs, and the fuel costs per flight. Figure 10.2 illustrates both the cost per flight and the fuel cost per flight for the entire cruise velocity range of *Icarus Rewaxed*. Recent Future, Inc. demanded that the range of

Figure 10.2: Cost Per Flight and Fuel Cost Per Flight vs. Cruise Velocity
Range = 30000 ft
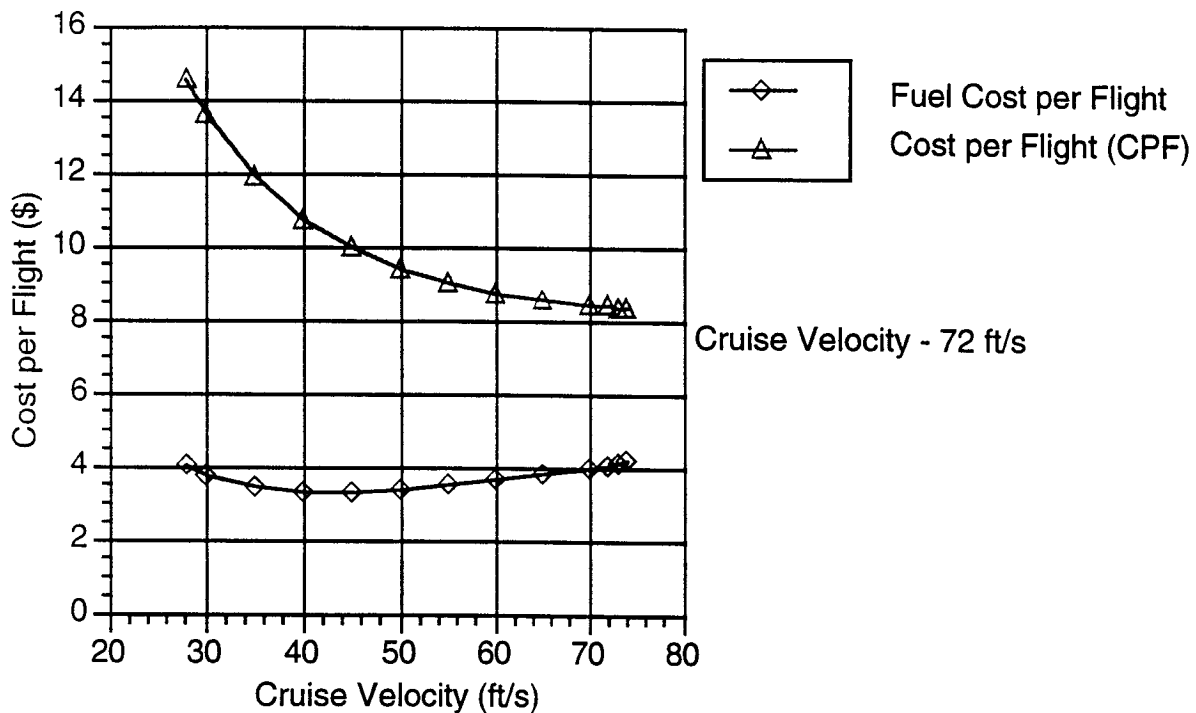
30000 ft per non-stop flight be met and accomplished at the fastest, most efficient

cruise speed. The DR&O specified this range so that *Icarus Rewaxed* can transit

between any two airports without refueling. In addition, the DR&O established

a goal cruise speed of 60 ft/s to get its customers to where they are going as

expediently as possible. The cruise velocities of 28 ft/s and 74 ft/s were the

minimum and maximum cruise speeds that met the 1400 mah current drain limit

of the battery pack over the 30000 ft range. While the lowest cost per flight

occurred at 74 ft/s as visible in Figure 10.2, a cruise speed of 72 ft/s was chosen

because its cruise current drain of 1361 mah left sufficient fuel for the rigors of

taxi, take-off and climb, and landing. The lowest fuel consumption, and

therefore the least fuel cost per flight, occurred at a cruise speed of 42 ft/s. Only

1100 mah were spent at this speed across the design range. Figure 10.2

demonstrates that although fuel cost increases with cruise velocity after 42 ft/s,

cost per flight costs decrease with increasing velocity because of the marked decrease in depreciation costs per flight. Since *Icarus Rewaxed* still had 300 mah storage remaining in the batteries and the overall cost per flight dropped as cruise speed increased, a cruise speed of 72 ft/s was settled upon. A fuel cost of $3.00/amphour was used in the calculations because *Icarus Rewaxed's* batteries were more expensive than those of the competition. Also, better grade fuel promotes more responsive performance and increases the longevity of the airplane. Since no cost penalty is incurred by flying at 72 ft/s, 12 ft/s faster than our 60 ft/s design objective, in fact it actually saves the customer time and money, *Icarus Rewaxed* uses up its fuel supply, 1400 mah of current drain, and cruise at 72 ft/s.

Table 10.2: Cost Per Flight Summary

Cruise Velocity:	72 ft/s	
Range:	30000 ft	
Flight Time:	417 s (6.95 min)	
I. Total Cost Per Aircraft		$3498.00
# Flights in Lifetime		864
Depreciation Cost Per Flight		**$4.05**
II. Operation Costs Per Flight:		
Maintenance-Insurance Costs		$0.27
Fuel ($1.50 - $3.00/amphour)		$2.04 - $4.08
Operation Subtotal		**$2.31 - $4.35**
III. **Cost Per Flight**		**$6.36 - $8.40**
IV. Cost Per 1000 ft		$0.21 - $0.28

The depreciation cost was added to the cost per flight of *Icarus Rewaxed* because of the finite lifetime of the aircraft. With a design range of 30000 ft (which allows for ample fuel to land at the nearest alternate airport with a two-minute loiter capability) and a cruise velocity of 72 ft/s, the cruise flight time is

417 s. Assuming a 100 hour lifetime, each *Icarus Rewaxed* airplane can make 864 flights. The depreciation cost of $4.05 was found by dividing the total cost of the airplane ($3498 after overhead and profit are tacked on) by the number of flights. The operation cost per flight of *Icarus Rewaxed* added the maintenance-insurance cost to the fuel cost. Although the maintenance-insurance cost increased with increasing cruise design flight speed, the $0.27 levy hardly dented the direct operating cost. The fuel cost was determined by multiplying the cruise current drain in amphours by the fuel cost of $3/amphour for a total of $4.08. This yielded a cost per flight of $8.40. If the economy grade fuel is used, the fuel cost is chopped to $2.04, resulting in a mere $6.36 cost per flight. The cost per 1000 feet ranged from $0.21 - $0.28.

References:

10 - 1. Batill, Stephen M., "Cost and Economic Analysis," AE 441 Handout, Department of Aerospace and Mechanical Engineering, University of Notre Dame, 1994.

10 - 2. Batill, Stephen M., "Manufacturing Plan and Costing Details," AE 441 Handout, Department of Aerospace and Mechanical Engineering, University of Notre Dame, 1994.

APPENDIX A

CRITICAL DATA SUMMARY

Parameter	
DESIGN GOALS:	
V cruise	60 ft/s
No. of passengers/crew	4/2
Max Range at Wmax	30,000 ft
Max Take-off distance	28 ft
Altitude cruise	25 ft (indoors)
Minimum turn radius	60 ft
Max Range at Wmin	30,000
Maximum TO Weight-WMTO	4.5
Minimum TO Weight - Wmin	4.45
Max cost raw materials	$ 200

BASIC CONFIG.	
Wing Area	7.5 ft^2
Maximum TO Weight - WMTO	5.3 lbs
Empty Flight Weight	5.24 lbs
Wing loading(WMTO)	11 oz/ft^2
max length	45 inches
max span	7.35 ft
max height	22 inches
Total Wetted Area	23 ft^2

WING	
Aspect Ratio	7.2 ft
Span	7.35 ft
Area	7.5 ft^2
Root Chord	12.25 inches
Tip Chord	12.25 inches
taper Ratio	1.0
C mac - MAC	-0.0582
leading edge Sweep	0
1/4 chord Sweep *	0
Dihedral	5°
Twist (washout)	0
Airfoil section	DF101
Design Reynolds number	375000
t/c	11%
Incidence angle (root)	0.7°
Hor. pos of 1/4 MAC	17.9 inches
Ver. pos of 1/4 MAC	9.11 inches
e- Oswald efficiency	0.83
CDo -wing	0.007
CLo - wing	0.159
CLalpha -wing	4.55

FUSELAGE	
Length	45 inches
Cross section shape	rectangle
Nominal Cross Section Area	4 in^2
Finess ratio	12
Payload volume	140in^3
Planform area	157.5 in^2
Frontal area	9.625 in^2
CDo - fuselage	0.00098

EMPENNAGE	
Horizontal tail	
Area	224 in^2
span	28 inches
aspect ratio	3.5
root chord	8 inches
tip chord	8 inches
average chord	8 inches
taper ratio	1
l.e. sweep	0
1/4 chord sweep	0
incidence angle	-2.0°
hor. pos. of 1/4 MAC	40.5 inches
ver. pos. of 1/4 MAC	9.5 inches
Airfoil section	SD8020
e - Oswald efficiency (LLC)	0.974
CDo -horizontal	0.00166
CLo-horizontal	0.0
CLalpha - horizontal	3.754
CLde - horizontal	0.343
CM mac - horizontal	0

Vertical Tail	
Area	71.5 in^2
Aspect Ratio	1.05
root chord	9 inches
tip chord	5 inches
average chord	6.5 inches
taper ratio	0.625
l.e. sweep	15°
1/4 chord sweep	11.6°
hor. pos. of 1/4 MAC	40 inches
vert. pos. of 1/4 MAC	14.2 inches
Airfoil section	flat plate

SUMMARY AERODYNAMICS	
Cl max (airfoil)	1.141
Cmo (airfoil)	-0.0582
CL max (aircraft)	1.03
lift curve slope (aircraft)	4.55/rad
CDo (aircraft)	0.0235
efficiency - e (aircraft)	0.768
Alpha stall (aircraft)	12 degrees
Alpha zero lift (aircraft)	-2°
L/D max (aircraft)	13.94
Alpha L/D max (aircraft)	8.2

WEIGHTS	
Weight total (empty)	5.22 lbs
C.G. most forward-x&y	17.78 inches, 9.06 inches
C.G. most aft- x&y	17.83 inches, 9.11 inches
Avionics	3.173 ounces
Payload-Pass.&lugg.-max	0.529 ounces
Engine & Engine Controls	14.1
Propeller	1.552 ounces
Fuel (battery)	22.1 ounces
Structure	
Wing	17 ounces
Fuselage/emp.	20.9 ounces
Landing gear	4.73 ounces

PROPULSION

Type of engines	Astro 15
number	1
placement	tractot
Pavil max at cruise	101.6 Watts
Preq cruise	101.6 Watts
max. current draw at TO	34.51 amps
cruise current draw	11.755 amps
Propeller type	Zingali 10-8
Propeller diameter	10 inches
Propeller pitch	8
Number of blades	3
max. prop. rpm	7466
cruise prop. rpm	7021.22
max. thrust	3.637 lbs
cruise thrust	1.4118 lbs
battery type	P-140SCR
number	13
individual capacity	1400 mAh
individual voltage	1.2
pack capacity	1400 mAh
pack voltage	15.6

STABILITY AND CONTROL

Neutral point	
Static margin %MAC	13.6%
Hor. tail volume ratio	0.4
Vert. tail volume ratio	0.0173
Elevator area	56 in^2
Elevator max deflection	$\pm20°$
Rudder Area	42 in^2
Rudder max deflection	$\pm30°$
Aileron Area	12 in^2
Aileron max deflection	$+20°/-15°$
Cm alpha	-0.659
Cn beta	0.0474
Cl alpha tail	3.754
Cl delta e tail	0.343

PERFORMANCE

Vmin at WMTO	10 ft/s
Vmax at WMTO	75 ft/s
Vstall at WMTO	24 ft/s
Range max at WMTO	38266.5 ft @43ft/s
Endurance @ Rmax	889.92 s
Endurance Max at WMTO	1132.06 s @28ft/s
Range at @Emax	31692.02 ft
Range max at Wmin	38266.5 ft
ROC max at WMTO	13.048 ft/s
Min Glide angle	4.2°
T/O distance at WMTO	25.4 ft

SYSTEMS

Landing gear type	tail dragger
Main gear position	14.5 inches
Main gear length	9.5 inches
Main gear tire size	2.5 X 0.75
nose/tail gear position	41 inches
n/t gear length	4 inches
n/t gear tire size	1.75 X 0.5
engine speed control	Tekin
Control surfaces	aileron, elevator, rudder

TECH DEMO - Final

Max Take-Off Weight
Empty Operating Weight
Wing Area
Hor. Tail Area
Vert Tail Area
C.G. position at WMTO
1/4 MAC position
Static margin %MAC
V takeoff
Range max
Airframe struct. weight
Propulsion sys. weight
Avionics weight
Landing gear weight

ECONOMICS:

raw materials cost	$ 168
propulsion system cost	$ 234
avionics system cost	$ 232
production manhours	140 hours
profit	$ 374.80
tooling costs	$ 100
total cost per aircraft	$ 3498

APPENDIX B

DATABASE

DATABASE

	Weight (lbs)	Area S (ft^2)	Span (ft)	Chord (in)	Aspect Ratio	Range (ft)	Hor Tail Area (ft^2)	Elevator Area (ft^2)	Vert Tail Area (ft^2)	Rudder Area (ft^2)
Penguin 90	3.513	4.67	7	8	10.5	2609	1.04	0.917	0.37	0.361
Scream-J4D 90	3	5.46	8	8.2	11.7	5500	0.63	0.21	0.38	0.21
Drag-n-Fly 90	2.73	6	8.5	8.5	12	4831	1.05		0.5	
FX-90 90	2.75	4.38	5.84	9	7.8	12210	0.48	0.04	0.35	0.21
Stealth Biplane 90	2.6	2.2	4	6.6	7.3	3000	0.688		0.375	
Hot Box 91	4.288	7.33	8	11	8.7	17000	1.01	0.1	0.42	0.29
Arrow 227 92	6	9.5	10	11.4	10.5	19966	1.57		0.72	
El Toro 91	5	6.94	8.33	10	10	33000	1.25	0.563	0.493	0.321
Pale Horse 91	4.98	7	8	10.5	9.1	20000	0.97		0.46	
RTL-46 93	5.16	9.93	9.17	13	8.5	13000	1.92		0.73	
Bunny 93	5.3	10	9.22	11.94	8.5	14355	2.98		1.18	
Gold Rush 93	5.321	10.94	8.75	15	7	16600	1.6	0.8	1	0 5
Blue Emu 93	4.79	10	10	12	10	23170	1.61	0.32	0.68	0.37
Nood Rider 90	4.94	5.83	7	9.996	8.4	8104	0.859	0.335	0.135	0.108

	Wing Area (ft^2)	Wing Weight (oz)	Wing Weight/Wing Area (oz/ft^2)
Plane 1	7.92	13.9	1.76
Plane 2	5.11	7.9	1.55
Plane 3	7.08	24.3	3.43
Plane 4	5.83	20.3	3.48
Plane 5	8.26	31.1	3.77
Plane 6	10	30.5	3.05
Plane 7	7.07	31.6	4.47
Plane 8	6.67	27.9	4.18
Plane 9	4.64	13.3	2.87

Weights and Sizes of various Hardware (From DataBook)

PART	WEIGHT(oz)	SIZE(inches)
Astro 15	7.5	Diameter=1.5, length(with gear box)=5.0
Engine mount	1.2	
gearbox	1.6	
Receiver	0.95	1.31x1.87x0.81
Power pack	2	2.18x1.18x0.56
Servo	0.6	1.0x0.75x1.5
Speed Controller	1.8	0.875x1.125x1.375
Monokote	1.8oz/1000in^2	
Astro 25	11	Diameter=1.62
Batteries: 1200mAh	1.7	Diameter=0.75, Length=1.5
1300mAh	1.7	Diameter=0.89, Length=1.67
1400mAh	1.7	Diameter=0.89, Length=1.67
900 mAh	1.38	Diameter=0.75, Length=1.5

DENSITIES OF MATERIALS

MATERIAL	DENSITY (kg/m^3)
Balsa	140
Plywood	545
Spruce	500

APPENDIX C

-WING SPAR DEFLECTION AND STRESS THEORY

- V-N DIAGRAM CURVE THEORY

APPENDIX C: STRUCTURES THEORY

C.1: Wing Spar Deflection and Stress Analysis

In this analysis, the wing spar is assumed to be the only load carrying component. The wing divided in half and cantilevered at the midpoint (the point of attachment to the fuselage). It was assumed that each half behaved the same, and that each half of the wing supported exactly half of the total load.

The wing flight load was assumed to be parabolic and of the form

$$w(x) = -Ax^2 + Bx + C$$

with A, B, and C as constants and x the length in inches from the fuselage root (x=0) to the wing tip (x = L). With the boundary conditions that $\frac{dw}{dx}$ @ (x=0) equals 0, and w(L) = 0, and knowing that the total area under the curve must equal the load factor (n) times the weight, the constants A, B, and C can be found. By this analysis, B = 0 for all load conditions.

The shear, bending moment, and deflection graphs can be found using the integration method found in Reference C.1, p. 415. This method begins with the fourth order equation:

$$EI\frac{d^4\delta}{dx^4} = -w(x)$$

Integrating gives:

$$EI\frac{d^3\delta}{dx^3} = V(x) = -1/3\,Ax^3 + Cx + D \qquad (\text{Note: } B = 0)$$

$$EI\frac{d^2\delta}{dx^2} = M(x) = -(1/4)(1/3)Ax^4 + (1/2)Cx^2 + Dx + E$$

$$EI\frac{d\delta}{dx} = -(1/5)(1/4)(1/3)Ax^5 + (1/3)(1/2)Cx^3 + (1/2)Dx^2 + Ex + F$$

$$EI\delta = -(1/6)(1/5)(1/4)(1/3)Ax^6 + (1/4)(1/3)(1/2)Cx^4 + (1/3)(1/2)Dx^3 + (1/2)Ex^2$$
$$+ Fx + G$$

The following boundary conditions were used to solve for the constants D, E, F, and G:

$$@ \, x = 0 \, : \, \delta = 0$$

$$@ \, x = 0 \, : \, d\delta/dx = 0$$

$$@ \, x = L \, : \, V = 0$$

$$@ \, x = L \, : \, M = 0$$

Given these, the following values were reached for the 3g loading condition:

$$A = 1.52 \times 10^{-4}$$

$$B = 0$$

$$C = 0.268$$

$$D = (1/3) \, A \, L^3 - CL$$

$$E = (1/4)(1/3)A \, L^4 - (1/2)C \, L^2 - DL$$

$$F = 0$$

$$G = 0$$

The values for the Modulus of Elasticity (E) for the graphite and steel shafts were found by testing the individual members. This test involved clamping the rod at one end and applying a point load at a known moment arm. By applying different loads, an estimation of E can be found by measuring the tip deflection. With the solution to the deflection of the tip given by:

$$\delta = - \frac{PL^3}{3EI}$$ (Ref. C.1, p. 598)

and knowing P(load), L, δ, and I, the Modulus can be estimated.

After finding the load, shear, and bending moment diagrams, the resultant stresses in the wing spar can be found by:

$$\sigma = \frac{M \, y}{I}$$

Finding the maximum stress then allows calculations for the margins and factors of safety for any flight loading condition.

C.2: V-N Diagram Curves

The stall limit lines of the V-N diagram (Figure 9.1) were found using the following relation:

$$n_{max/min} = \frac{1}{2} \rho \frac{S}{W} C_{L_{max/min}} V^2$$

where $\rho = 3.3769 \times 10^{-3}$ lb sec^2/ft^4, $C_{L_{max}} = 1.03$, $C_{L_{min}} = -0.5$, S = 7.5 ft^2 and Weight = 5.1 lbs .

The gust lines were found by the analysis from Reference C.2, p. 466-7. The vertical gust velocity was set at 10 ft/s in accordance with the DR&O of Recent Future, Inc. The following relation was then used to find the load lines:

$$n = 1 \pm \frac{K_g U_{gust} V a}{498(W/S)}$$

Here, a = the slope of the airplane normal force coefficient (C_L/rad) . Kg is a gust alleviation factor designed to modify the assumption of a "sharp-edged" gust. Kg is based on the airplane mass ratio in the following relation:

$$\mu = \text{airplane mass ratio} = \frac{2(W/S)}{\rho \, c \, a \, g}$$

$$Kg = \frac{0.88 \, \mu}{5.3 + \mu} \qquad \text{(Ref. C.2, p. 467)}$$

References:

C.1: Beer, Ferdinand P. and E. Russell Johnston, Jr. Mechanics of Materials. New York: McGraw-Hill Book Company, 1981.

C.2: McCormick, Barnes W. Aerodynamic, Aeronautics, and Flight Mechanics. New York: John Wiley & Sons, 1979.

APPENDIX D

PRIMARY DELIVERABLES
FIGURES & TABLES

Side View

Engine

Passenger Passenger

Speed Controller

Battery Battery
Battery Battery

Aileron Servo

Receiver & Power Pack

Rudder & Elevator Servo

Passenger Passenger Passenger Passenger

Wing Carrythrough

Top View

Engine

Passenger Passenger

Speed Controller

Battery Battery
Battery Battery
Battery Battery

AileronServo

Receiver

Power Pack

Elevator Servo

RudderServo

Passenger Passenger Passenger Passenger
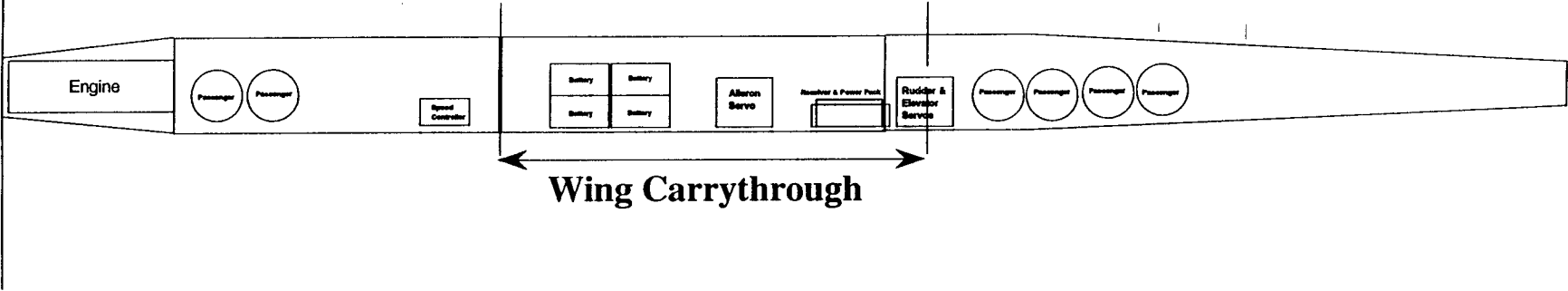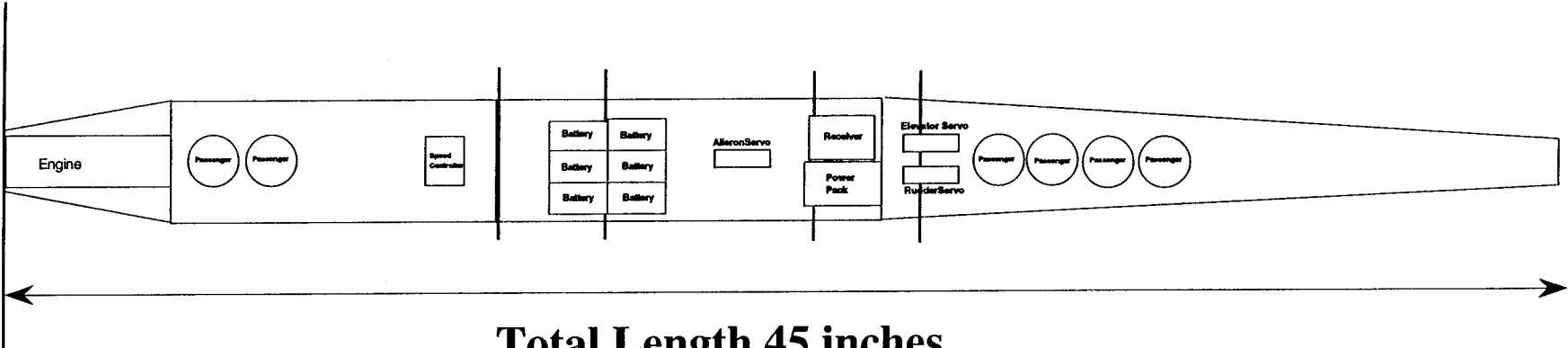
Total Length 45 inches

3 View External View

Weight & Balance Diagram
(scale: 1 inch = 5.77 inches)

CG located at 29% MAC

● indicates component center of gravity
(exact component locations shown in table 6.1)

Passengers
Rudder/
elevator
Receiver/
Power pack
Servo
Aileron
Batteries
Speed
Controller
Pilot/copilot
Engine

D - 3

Table 6.1: Detailed Weight Breakdown

Component	Weight (oz)	Location (inches from nose)
Propulsion:		
engine (incl mount & gearbox)	10.30 (known)	3.00
propeller	1.552 (known)	0.0
batteries	22.10 (known)	17.35
avionics battery pack	2.00 (known)	24.25
speed controller	1.80 (known)	12.75
Structure:		
Wing	17.02 (est.)	17.93
Fuselage sections		
engine	1.97 (est.)	4.19
front	3.95 (est.)	9.63
middle	4.24 (est.)	20.00
tail	6.67 (est.)	35.38
Vertical Tail	1.31 (est.)	39.40
Horizontal Tail	2.76 (est.)	39.40
Avionics:		
elevator servo	0.74 (known)	26.50
rudder servo	0.74 (known)	26.50
aileron servo	0.74 (known)	21.25
receiver	0.95 (known)	24.25
Landing Gear:		
Main gear tires	1.16 (est.)	15.42
Main gear struts	3.20 (est.)	16.37
Tail gear tire	0.14 (est.)	41.60
tail gear strut	0.23 (est.)	41.42
	———	
Empty Total	83.57	
Payload (passengers)	0.53 (known)	
	———	
Total	84.10	

Figure 9.1: V-N Diagram

Figure 5.2: Determining the Most Efficient Three-Bladed Propeller

Figure 5.2: Determining the Most Efficient Three-Bladed Propeller

10 - 8

Efficiency (Cruise) = .82

11 - 7
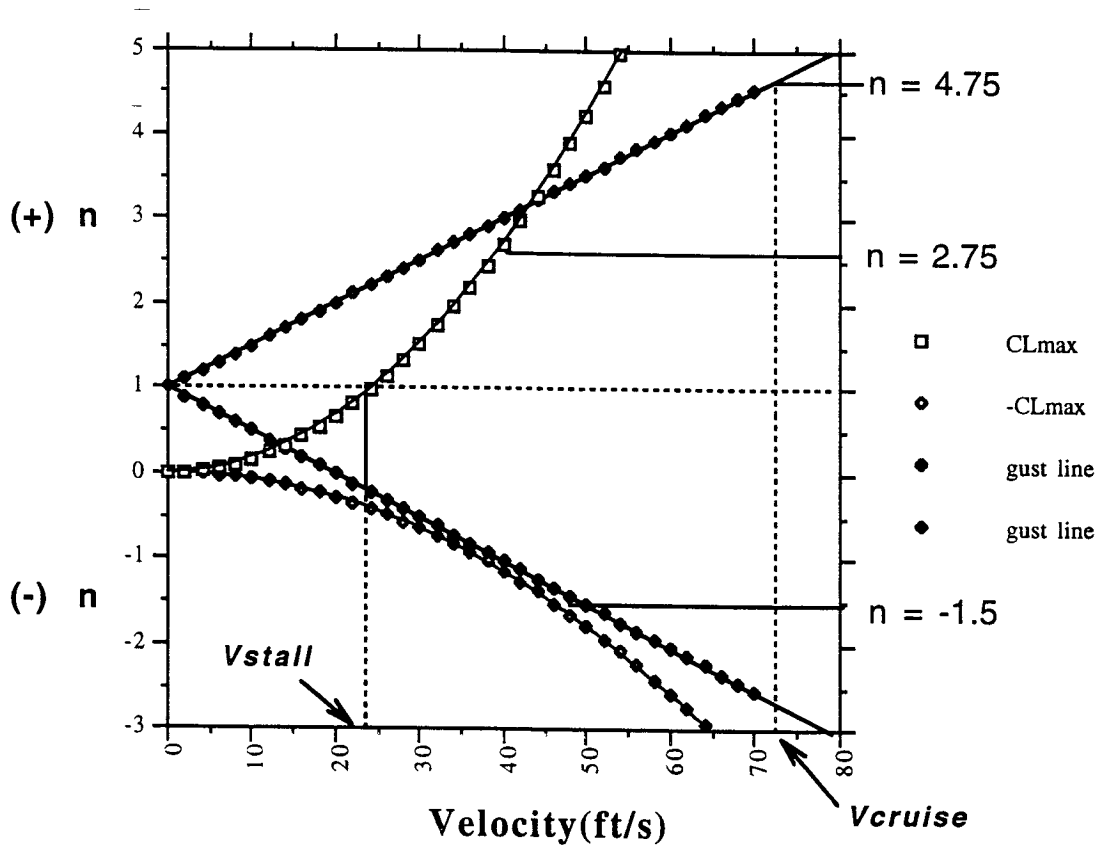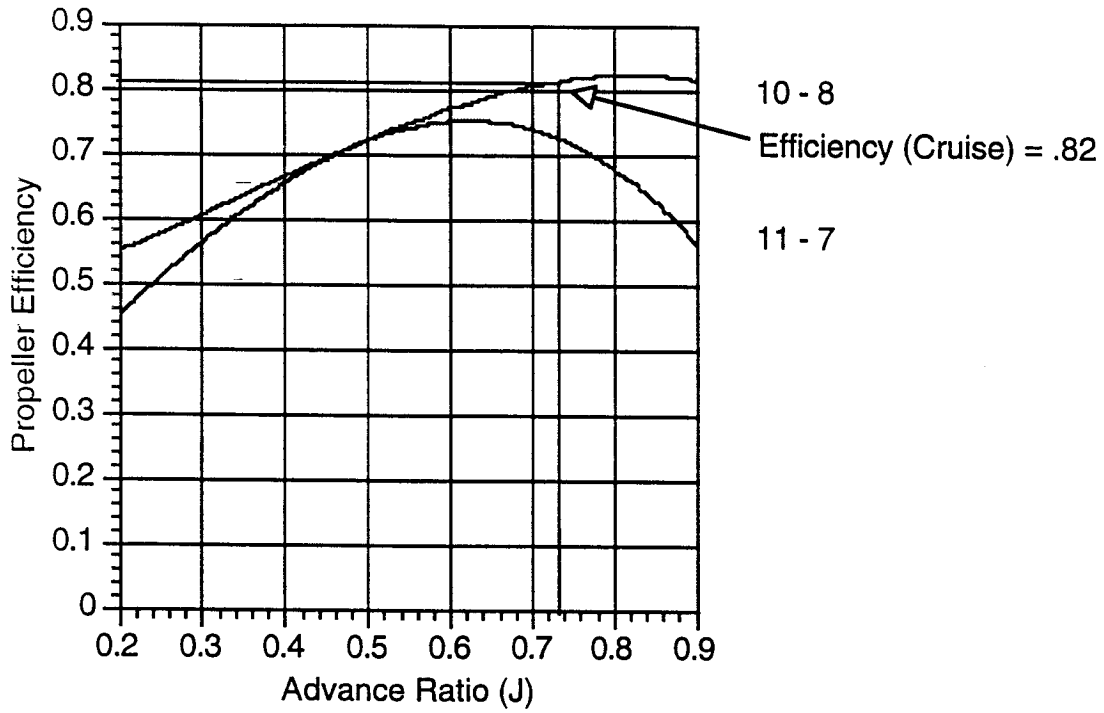
Figure 8.2 Power Required and Power Available Curves With Respect to Velocity
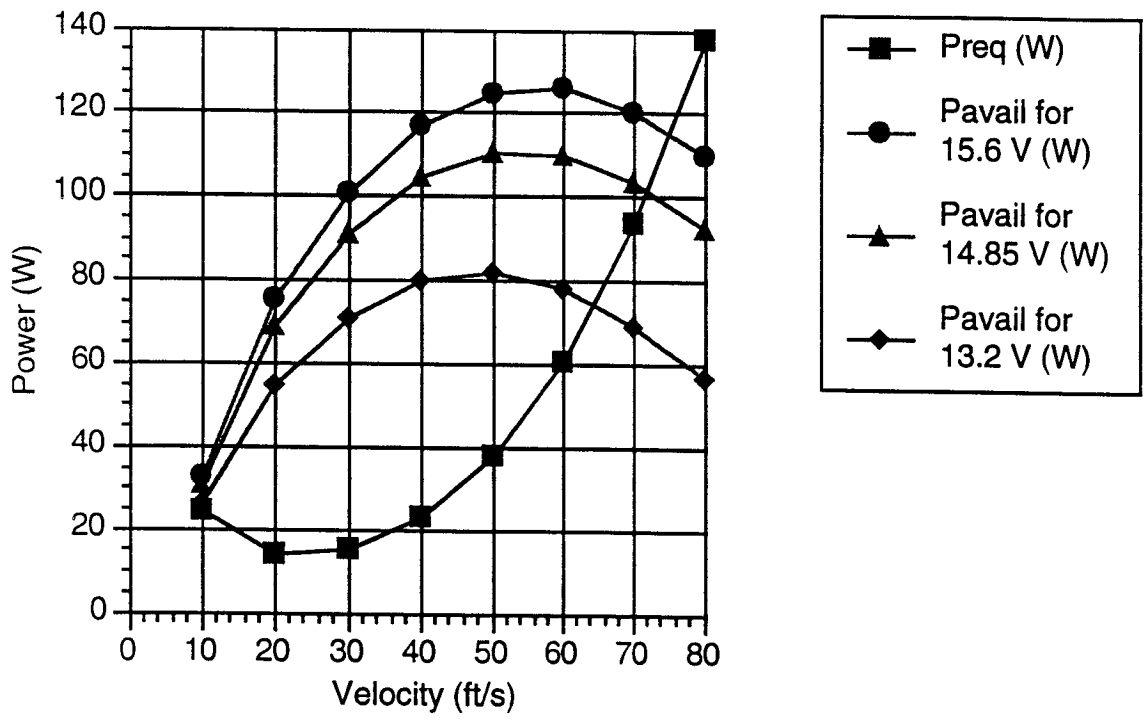
Figure 8.6: Effects of Payload on Range
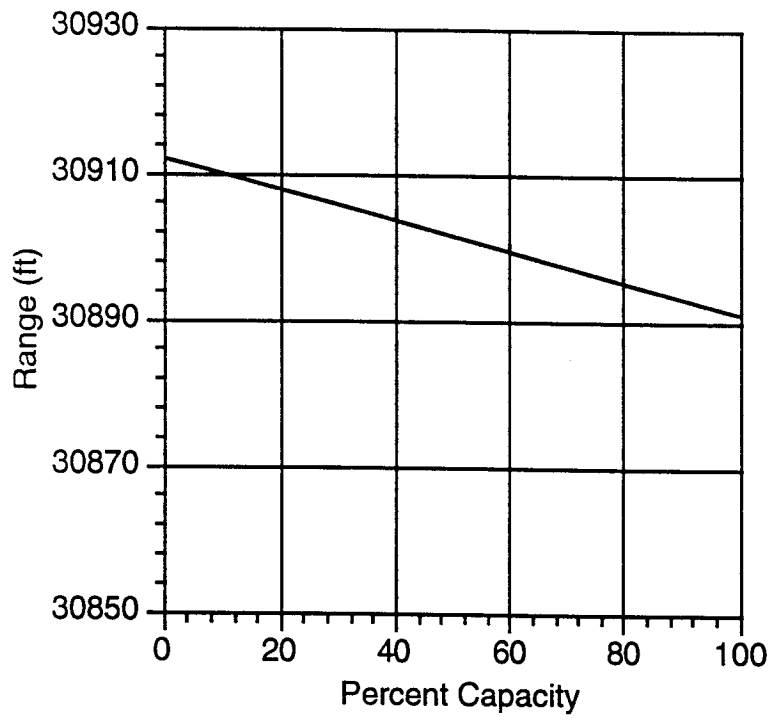
Airfoil Lift Curve (DF101)
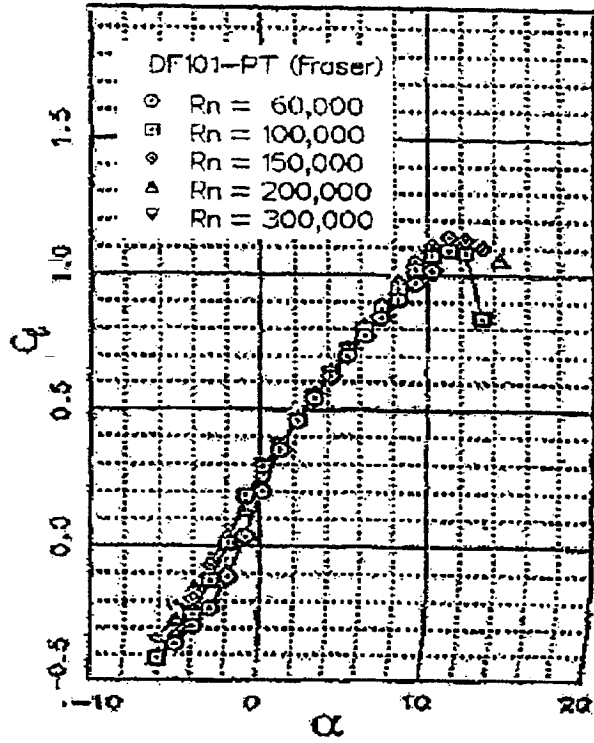
Figure 4.4: Lift Curve Slope for Complete Configuration Aircraft
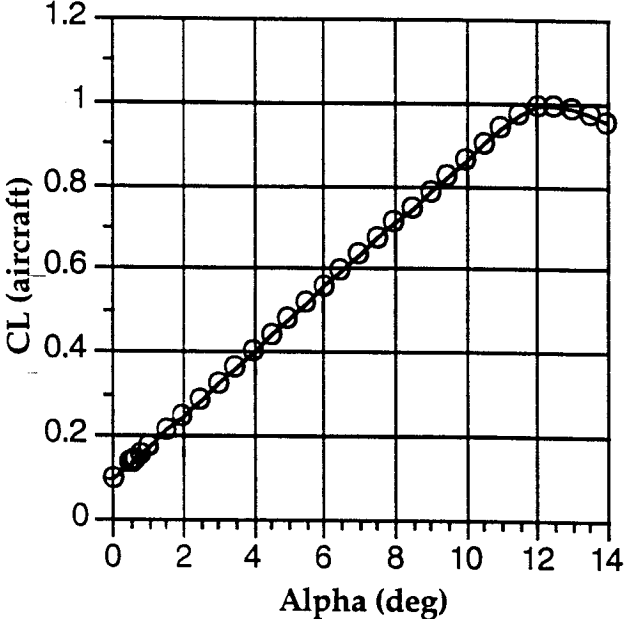
Figure 4.5

Complete Aircraft Configuration Drag Polar

Table 4.2: Contribution of Each Component

Component	$C_{D\pi}$	$S\pi$ (sq. in.)	Data Source
Wing	0.0070	1080.5	Reference 4.6
Fuselage	0.110	9.625	Reference 4.6
Horizontal Tail	0.0080	224.0	Reference 4.6
Vertical Tail	0.0080	71.5	Reference 4.6
Landing Gear-Tires (Main)	1.1	1.875	Reference 4.5
Landing Gear-Struts (Main)	1.1	1.125	Reference 4.5
Landing Gear-Tire (Tail)	1.1	0.9375	Reference 4.5
Landing Gear-Strut (Tail)	1.1	0.5	Reference 4.5
Interference	15%		Reference 4.6

Figure 4.7: Comparison of High and Low Speed Cruise Efficiency

L/D max

L/D high-speed cruise

L/D

Angle of Attack (deg)
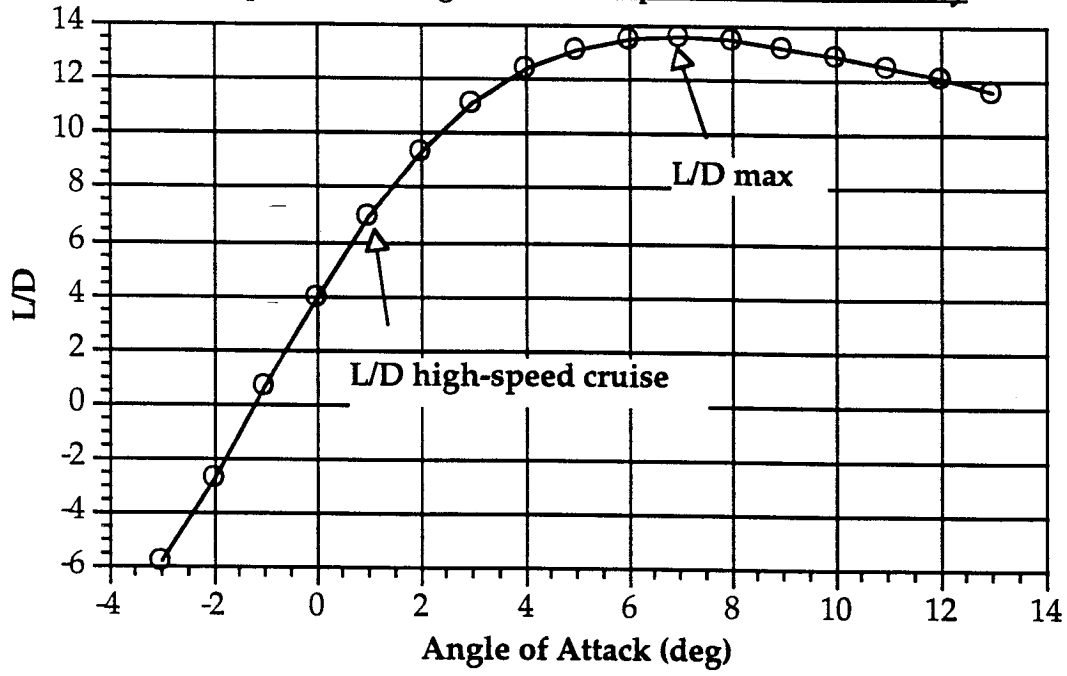
Sensitivity of Longitudinal Static Stability
to Center of Gravity Position

NP @ xc.g. = 19.5" from l.e.

Design point @ xc.g. = 17.9" from l.e.

Legend:
- design -1"
- design - 2"
- design + 1"
- design + 2"
- NP
- design pt

CM

Angle of Attack (deg)
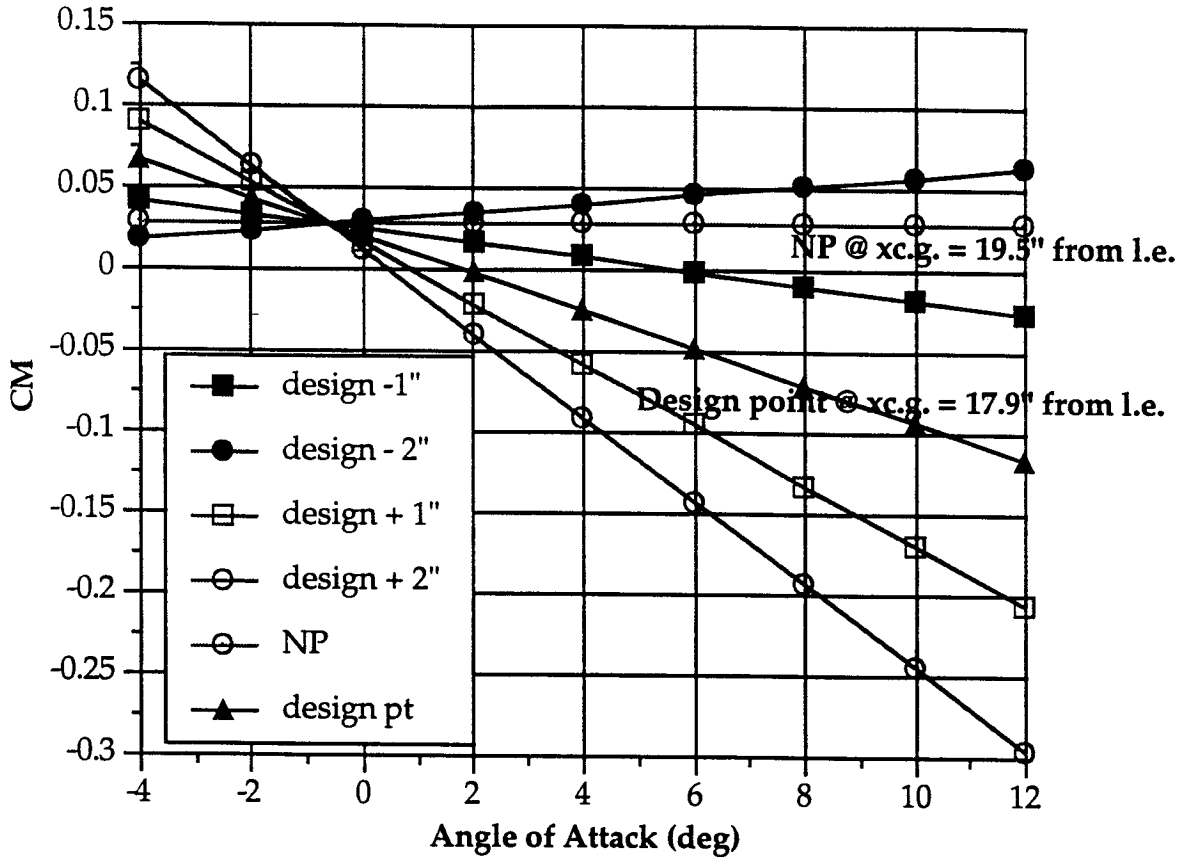
APPENDIX E

- PROP 123 PROGRAM

- TAKEOFF PERFORMANCE
  PROGRAM

- RADIO PILOTED VEHICLE
  SPREADSHEET

PERFORMANCE ESTIMATE

Fractional rad,	X:	0.30	0.45	0.60	0.70	0.75	0.80	0.85	0.90	0.9!
Radial position,	r:	1.50	2.30	3.00	3.50	3.80	4.00	4.30	4.50	4.8(
Blade chord,	C:	0.80	0.90	0.90	0.80	0.80	0.70	0.60	0.60	0.5(
Thickness,	In:	0.10	0.10	0.10	0.10	0.10	0.10	0.10	0.10	0.1(
Thickness ratio,	T:	0.15	0.15	0.15	0.15	0.15	0.15	0.15	0.15	0.1!
Blade Angle, Beta:		40.50	29.40	23.20	20.20	18.90	17.80	16.80	15.90	15.1(
Geometric Pitch, GP:		8.10	8.00	8.10	8.10	8.10	8.10	8.00	8.00	8.1(
Solidity,	S:	0.154	0.165	0.166	0.154	0.145	0.134	0.124	0.113	0.09!

THRUST, POWER, EFFICIENCY, AND VELOCITIES

J:	0.320	0.380	0.430	0.490	0.540	0.600	0.660	0.710	0.770	0.820	0.880
Ct:	0.162	0.153	0.135	0.124	0.113	0.101	0.088	0.073	0.058	0.042	0.035
Cp:	0.081	0.087	0.088	0.086	0.083	0.078	0.073	0.065	0.055	0.045	0.039
eta:	0.639	0.661	0.665	0.704	0.740	0.769	0.794	0.803	0.809	0.777	0.810
Mt:	0.962	0.497	0.311	0.270	0.253	0.238	0.227	0.217	0.208	0.200	0.207
RPM:	13500	11489	10000	8852	7941	7200	6585	6067	5625	5242	4909

Thrust Distribution: (dCt/dX vs. X and J)

X	J: 0.32	0.38	0.43	0.49	0.54	0.60	0.66	0.71	0.77	0.82	0.8
0.30	0.06	0.07	0.07	0.06	0.05	0.05	0.04	0.03	0.03	0.02	-0.(
0.45	0.12	0.16	0.13	0.12	0.10	0.10	0.08	0.07	0.05	0.03	-0.(
0.60	0.29	0.22	0.21	0.19	0.17	0.15	0.14	0.11	0.09	0.06	0.(
0.70	0.28	0.26	0.24	0.22	0.21	0.18	0.17	0.14	0.11	0.08	0.(
0.75	0.29	0.28	0.25	0.24	0.22	0.19	0.17	0.14	0.12	0.09	0.(
0.80	0.30	0.28	0.26	0.25	0.22	0.20	0.18	0.15	0.12	0.09	0.(
0.85	0.31	0.28	0.26	0.25	0.22	0.20	0.18	0.15	0.12	0.09	0.(
0.90	0.29	0.28	0.27	0.24	0.22	0.20	0.18	0.15	0.12	0.09	0.:
0.95	0.41	0.37	0.27	0.23	0.20	0.18	0.16	0.13	0.11	0.09	0.:

Torque Distribution: (dCq/dX vs. X and J)

X	J: 0.32	0.38	0.43	0.49	0.54	0.60	0.66	0.71	0.77	0.82	0.8
0.30	0.005	0.005	0.006	0.006	0.006	0.005	0.005	0.004	0.003	0.002	0.0(
0.45	0.009	0.012	0.012	0.012	0.012	0.011	0.010	0.009	0.007	0.005	-0.0(
0.60	0.020	0.021	0.021	0.020	0.020	0.019	0.018	0.015	0.013	0.010	0.0:
0.70	0.026	0.026	0.025	0.025	0.024	0.023	0.022	0.019	0.016	0.013	0.0:
0.75	0.027	0.027	0.027	0.027	0.026	0.024	0.023	0.020	0.017	0.014	0.0:
0.80	0.028	0.028	0.028	0.028	0.027	0.025	0.024	0.021	0.018	0.015	0.0:
0.85	0.029	0.029	0.028	0.028	0.027	0.026	0.024	0.022	0.019	0.016	0.0:
0.90	0.029	0.029	0.029	0.028	0.027	0.026	0.024	0.022	0.019	0.016	0.0:
0.95	0.022	0.027	0.028	0.027	0.025	0.024	0.022	0.020	0.018	0.016	0.0:

Angles of Attack (Degrees)

X	J: 0.32	0.38	0.43	0.49	0.54	0.60	0.66	0.71	0.77	0.82	0.8
0.30	17.40	15.80	14.40	8.30	6.20	4.60	3.00	1.50	0.00	-1.40	-2.(
0.45	18.50	15.60	7.50	6.30	4.80	3.50	2.20	0.90	-0.30	-1.50	-2.(
0.60	13.40	7.10	6.20	5.00	4.10	2.90	1.90	0.80	-0.20	-1.20	-1.:
0.70	7.30	6.40	5.30	4.30	3.50	2.60	1.60	0.70	-0.20	-1.10	-1.(
0.75	6.60	6.00	5.00	4.30	3.30	2.40	1.50	0.60	-0.20	-1.10	-1.(
0.80	6.50	5.50	4.60	4.00	3.10	2.20	1.40	0.50	-0.30	-1.10	-1.(
0.85	6.10	5.20	4.30	3.60	2.80	2.10	1.20	0.40	-0.30	-1.10	-0.!
0.90	5.50	4.70	4.20	3.30	2.60	1.80	1.10	0.30	-0.40	-1.20	-0.!
0.95	11.70	8.60	4.60	3.00	2.20	1.30	0.70	0.00	-0.60	-1.20	-0.:

Reynolds Number (millions)

X	J: 0.32	0.38	0.43	0.49	0.54	0.60	0.66	0.71	0.77	0.82	0.8
0.30	0.07	0.06	0.06	0.05	0.05	0.04	0.04	0.04	0.04	0.04	0.:

```
 INPUT DATA FILE NAME
final5.3
 \SE - groupb
 JT =    5.300000
SREF =    7.500000
RHO = 2.3779999E-03
CLTO =  0.7067000
CDTO =  5.0285000E-02
CLMAX =   1.030000
SMAX =    200.0000
MU = 5.0000001E-02
DIA = 0.8333300
BVOLTS =   15.60000
KT =   1.084000  —
KV = 7.8599999E-04
RARM =  0.1200000
RBAT =  0.1060000_
FUSAMP =   20.00000
GEARAT =    2.210000
DT = 4.9999999E-03
TMAX =    40.00000
NJ =             12
```

```
J      CT        CP
  0.0000000      0.2160000      7.2999999E-02
  0.3200000      0.1620000      8.1000000E-02
  0.3800000      0.1530000      8.6999997E-02
  0.4300000      0.1350000      8.8000000E-02
  0.4900000      0.1240000      8.6000003E-02
  0.5400000      0.1130000      8.2999997E-02
  0.6000000      0.1010000      7.8000002E-02
  0.6600000      8.8000000E-02  7.2999999E-02
  0.7100000      7.2999999E-02  6.4999998E-02
  0.7700000      5.7999998E-02  5.5000000E-02
  0.8200000      4.1999999E-02  4.5000002E-02
  0.8800000      3.5000000E-02  3.9000001E-02
V TAKEOFF =    28.82565
MAX CURRENT DRAW(amps) =    34.51328
MAX MOTOR POWER(hp) =  0.3681070
MAX MOTOR POWER(watts) =    274.5018
STATIC THRUST (lb)=     3.643918
STATIC CURRENT DRAW (amps)=    13.05882
STATIC PROP RPS=     121.2879
```

```
TIME FOR RUN(SEC) =    1.664999
V AT TO (FT/SEC) =    28.85473
DISTANCE(FT) =    25.38705
BATTERY DRAIN(mahs) =    6.266935
ADVANCE RATIO AT TO =  0.2891954
THRUST(LB) AT TO =    2.734873
LIFT(LB) AT TO(BEFORE ROTATION) =    5.221001
DRAG(LB) AT TO(BEFORE ROTATION) =   0.3714985
FRICTION(LB) AT TO(BEFORE ROTATION) =   3.9499761E-03
CURRENT DRAW AT TO (AMPS) =    13.95164
```

```
STOP
```

eta-J fit				
a1=	0.465360			
a2=	0.277390		Nm Choice(rpm)=	15515
a3=	0.919545			
a4=	-0.884540			
Cq-J fit			OUTPUTS	
b1=	0.0017008	-0.003904	CL=	0.11460059
b2=	0.059101	0.092960	CD=	0.02247312
b3=	-0.0810014	-0.145030	Preq(W)=	**101.471638**
b4=	0.020632	0.059333	J=	0.73842641
			eta=	0.8154406
INPUTS			Cp=	0.05999999
Ra(ohm)=	0.120000		Nprop(rpm)=	7020.36199
Rbat(ohm)=	0.106000		Pmotorout[a](W)=	131.101884
kv(V/rpm)=	0.000786		Pmotorout[b](W)=	131.101884
kt(in.-oz/a)=	1.084000		Pavail(W)=	101.560509
etag=	0.950000		ia(a)=	11.7470127
Tloss(in.-oz)=	1.310200		ROC(ft/s)=	0.01236824
rho(slugs/ft3)=	0.002378		Nm[a](rpm)=	**15515**
AR=	7.200000		Nm choice(rpm)=	**15515**
span(ft)=	7.350000			
CD0=	0.021722		Time	429.045251
load factor=	1.000000		Cool Time =	429.045251
weight(lb)=	5.300000		Range (ft) =	30891.2581
efficiency=	0.773000			
V actual(V)=	14.845000			1400
dprop(ft)=	0.833330		ROC (ft/s)=	0.01236824
gear ratio=	2.210000		Thrust (lb) =	1.41056263
velocity(ft/s)=	72.000000			

APPENDIX F

- INCIDENCE ANGLES AT HIGH-SPEED CRUISE

- STEADY ROLL RATE EQUATION

INCIDENCE ANGLES AT HIGH-SPEED CRUISE

Before solving the equations for the necessary coefficients, however, it was first necessary to determine the incidence angles for the wing and the tail. This was accomplished by writing the force and moment equations for the aircraft in flight at its high-speed cruise configuration.

$$C_L = C_{Low} + \frac{S_t}{S}C_{L\alpha t}\alpha_t + C_{L\alpha w}\alpha_w + C_{L\delta e}\delta e = \frac{2W}{\rho V^2 S}$$

$$C_M = C_{Macw} + C_{Low}\left(\frac{Xcg}{c} - \frac{Xac}{c}\right) + C_{M\alpha w}\alpha_w + \frac{S_t}{S}C_{M\alpha t}\alpha_t + C_{M\delta e}\delta e = 0$$

In doing so, one notices that these represent a system of two equations in the unknowns i_w and i_t expressed as functions of known aerodynamic coefficients by writing

$$\alpha_w = \alpha_{FRL} + i_w$$

$$\alpha_t = \alpha_{FRL} - \varepsilon + i_t$$

These equations can be solved simultaneously to yield the incidence angles required for the aircraft to be trimmed at zero angle of attack of the fuselage reference line, and thus at a minimum drag configuration.

STEADY ROLL RATE EQUATION

The roll moment created by the ailerons stems from the incremental lift force produced by the deflection of the control surface. Using strip theory, this incremental lift and corresponding moment can be estimated assuming a constant lift distribution across the span of the control surface and is given as the control power of the ailerons:

$$Cl_{\delta_a} = \frac{2C_{L\alpha_w}\tau}{S_w b_w} \int_{y_1}^{y_2} cy\,dy$$

This control power was subsequently used to determine the steady roll rate of the aircraft, which can be estimated by considering equation 8.100 of Reference 7.2:

$$Cl_{\delta_a}\delta_a + Cl_{\bar{p}}\bar{p} = 0$$

This equation effectively represents the balance that must exist between the roll moment produced by the ailerons and that produced due to the damping term in order for the aircraft to complete a steady rolling manuever. Solving the above equation for the dimensionless roll rate, $\bar{p}$, gives

$$\bar{p} = \frac{Pb}{2V} = -\frac{Cl_{\delta_a}}{Cl_{\bar{p}}}\delta_a$$

which can be subsequently solved for the dimensional roll rate, P, given the span and velocity of the aircraft through the turn.

APPENDIX G

MANUFACTURING PLAN

Appendix G: MANUFACTURING PLAN

G.1: Introduction

With the concept and goals of *Icarus* established, it is imperative to actually build a prototype that meets the theoretical specifications. Special attention will be given to the weights of individual components and of the overall aircraft. In order to meet the stated goal of high speed, minimization of weight is extremely important. Organization, thoughtful planning, and efficiency are demanded by the goal of producing a relatively low-cost aircraft. This plan will attempt to meet these two goals. It will provide a detailed description of the methods and parts used in the manufacturing process, and it will organize the work involved in the production of the Icarus prototype.

G.2: Organization and Cost Accounting

Two main structural components -- wing and fuselage -- will be manufactured separately. These two parts are designed to be easily attached and removed; creating them separately will not create a problem in building the whole prototype. A team of three will be assigned to the wing and a team of two will build the fuselage. This division of labor will allow specialization and allow each team to work at their own pace. The two teams will be given detailed suspense dates for their component to ensure that steady progress is maintained. These suspense dates are included at the end of this appendix.

Cost accounting will be accomplished through the use of team time cards. An example of these cards is also included at the end of this section. Each team will record the date, work time, and accomplishments made at each session. A running total of the labor hours (hence the cost) will be kept.

Cost control will be facilitated by a detailed initial plan and layout of all wood pieces. This plan will allow Recent Future, Inc. to cut a large volume of wood at one sitting. Optimizing the use of the "Heavy Machinery" (Scroll Saw and Drill Press) will minimize tooling costs, thus saving money in the overall cost of the aircraft. Table I shows the projected use of each tool.

Table I: Projected Use of Heavy Machinery

Tool:	Use:
Scroll Saw	Cut (4) Airfoil templates Cut Engine mount plywood firewall Cut Middle sections of fuselage (balsa) Cut (4) 3x3.5 inch plywood sections Cut fuselage truss spars (balsa and spruce)
Drill Press	Cut holes in airfoil ribs Cut holes in fuselage mid-section

G.3: Special Construction Materials

Glue:

Two types of glue will be used in the construction of *Icarus*. The main glue for wood to wood attachment is Super Jet Cyanoacrylate (CA) glue. Attachments of wood to steel will be formed with a two part Devcon 5 minute Epoxy. This glue, specially made for metal and wood, will provide the high bond strength necessary for structural integrity.

Covering:

Monokote will be used to cover the airplane. This heat shrink material will maintain the aerodynamic shape and provide extra tensile strength. It will also provide the distinctive coloring and design that will set *Icarus* apart in the showroom. The Monokote will be applied by heat activation from an iron and the steady hand of Recent Future, Inc.'s team leader.

G.4: Primary Construction Components

Wing:

The wing is the single biggest and most complicated structure in the prototype design. Therefore, the wing will be the limiting factor in the construction time. Recent Future, Inc. will build two wings: one will be used for structural testing and the other will be attached to the prototype. The test component wing will not have ailerons and will not support landing gear.

The wing is composed has 24 airfoil ribs spaced at approximately four inches intervals. These ribs will maintain the wing's aerodynamic shape. The ribs will be cut from 1/8 inch balsa wood sheeting. Two templates will be made using the desired airfoil shape and excess from the balsa boards. These templates will then be used to trace the outline of the rest of the airfoils. The templates will also serve as the inner two airfoil sections. The airfoils will be cut from the balsa sheeting with scissors or a standard utility knife. They will be attached to either the main steel shaft or to the tip spruce spars by CA glue.

The main load carrying component of the wing will be a thin-walled steel shaft. This component was purchased from a subcontractor and thus has a set geometry (48 inch span). Two templates will be joined by plywood sections and then attached to the center of the shaft. This plywood will provide the attachment point of the wing to the fuselage.

Since the entire length of the wing is 88 inches, spruce spars will be used to extend the steel shaft. The ends of the shaft will be pressed to form a flat surface on the top and bottom. 25 inch spruce spars will then be epoxied directly to the steel shaft using Devcon two-part epoxy.

The wing will also have a curved leading edge spar, two thin upper spars, and a trailing edge spar. The leading and trailing edge spar will help support the

aerodynamic loads, and the upper spars will be used to help maintain wing shape. Ailerons will be integrated into the trailing edge spar, with control rods extending to the fuselage.

Fuselage:

A full scale blueprint of the fuselage has been developed to guide the planning of each component. Since the starboard and port sides of the fuselage are identical, each will be made in the same fashion. The middle section of the fuselage will be cut from balsa wood boards. This section will provide the support for the middle and back of the fuselage as it is being built.

Spruce spars will run the 45 inch length of the fuselage. These will be glued directly to the middle section. The rest of the fuselage structure will be formed from a balsa truss, glued to the main spars. Balsa spars will also form the top and bottom of the fuselage.

A plywood firewall will form the front face of the fuselage. This firewall will act as the engine mount. The rest of the components in the airplane will be positioned using spars and velcro tape. A plywood firewall will also be located in the back of the fuselage. This will provide the point of attachment for the tail dragger back wheel. Both firewalls will be attached to the spruce longerons. This connection of two hardwoods will ensure the integrity of the joint. Hardwood will never be attached solely to balsa wood, for the soft balsa will easily deform or break under the loads experienced by each firewall.

Tail Surfaces:

The horizontal tail will be made with 1/8 inch balsa airfoil ribs fashioned around a spruce main spar. The main spar will be located at the aerodynamic center of the horizontal tail ($\approx$ 0.25 c). The main spruce spars will be attached to the

plywood firewall in the rear of the airplane. This will connect the load bearing component of the tail to the strongest component in the rear of the fuselage. The trailing edge will be made from pre-formed, triangular balsa spars. This edge will be connected to a control servo to allow elevator deflection. Monokote will provide the hinge that connects this surface to the rest of the tail. This type of joint not only minimizes weight, it also provides an airtight connection between surfaces; this facet will reduce the drag of the horizontal tail.

The vertical tail will consist of a balsa wood truss. The trailing edge will be made in the same fashion as the elevator in the horizontal tail. This surface will provide the rudder control needed by the aircraft. The rudder will also be linked to the rear tail wheel. This linkage will allow both surfaces to be controlled by one servo motor.

Wing Group

9 April: All hardwood cut -- **Use of Scroll Saw**

All Airfoil Sections Cut, Middle Sections Drilled -- **Use of Drill Press**

13 April: Center Structure finished for both Test and Wing component

14 April: Main landing gear shaped

Spruce Spars attached to Test Component

15 April: Spruce Spars attached to Wing component

17 April: All structure of Test Component completed

Ribs attached to Wing Component

Landing Gear attached to Wing component

18 April: Test Component Monokoted

Ailerons Integrated into Wing Component

19 April: Test Component Validation Test

20 April: Wing Component Completed: Monokote finished

21 April: Rollout

24 April: All external design finished

25 April: Taxi Test

27 April: Indoor Test Flight

Fuselage Group

9 April: Firewalls cut -- **Use of Scroll Saw**

Vertical and diagonal side spars cut -- **Use of Scroll Saw**

Holes in middle fuselage cut -- **Use of Drill Press**

12 April: Fuselage sides completed

15 April: Sides joined, firewalls installed

17 April: Horizontal Tail completed

All internal components fixed

19 April: Vertical Tail completed

20 April: All control surfaces tested, All Monokote finished

21 April: Rollout

24 April: All external design finished

25 April: Taxi Test

27 April: Indoor Test Flight

Fuselage Team Time Card:

Bryan Farrens
Macy Hueckel

Date	Total Hrs	Labor (Hrs *10)	Description	Tooling Cost: (TO+$/mn*mn)	Total Cost:

Appendix H

Flight Validation, Component Test
and
Manufacturing Hours

Flight Validation Testing Review
April 21-27, 1994
The Icarus-Rewaxed

Summary:
The technology demonstrator was completed on schedule. Initial taxi
tests indicated flaws in the landing gear design and installation.
Modifications were made and the taxi performance improved. A
number of short flights were achieved but the handling and control
characteristics of the aircraft limited the ability to fly in the
constrained Loftus test environment.

Taxi Testing Results: April 21, 1994
Ground handling was severely limited by the flexibility of the
landing gear. It was discovered that a glue joint had failed where the
main gear was attached to the main wing spar.

Taxi Testing Results: April 26, 1994
Ground handling of the aircraft was significantly improved with
modifications to the landing gear design. Steering was acceptable
although there appeared to be significant ground friction due to the
alignment of the gear. All the members of the design team were able
to control the aircraft. All the taxi tests were conducted well below
anticipated flight speeds.

Flight Testing Results: April 27, 1994
The final data sheet for the technology demonstrator is attached. A
number of take-offs, attempted take-offs and aborted flights were
conducted. The aircraft was impressive with respect to its robust
structure. It impacted the ground at a wide variety of orientations
and speeds. Initial problems appeared to be due to wing warp which
was reduced through reshrinking the wing covering. All the take-offs
were accomplished by accelerating to a speed at which the aircraft
lifted off from the on-ground attitude. Take-off distances appeared
to exceed the design goals.

In-flight the aircraft was very difficult to handle in the constrained
Loftus test environment. The ailerons were not effective and full
rudder control was needed to marginally complete an 180° turn. The
lack of wing dihedral and the physical limits on aileron deflection did
not allow for any "fixes" to improve this handling problem. Steady
level flight was acceptable and the aircraft was very responsive in
pitch.

Wing Component Static Load Test, April 19, 1994
Spring 1994
Icarus Rewaxed

Summary:
A wing component was tested to failure. The wing was completed
(excluding ailerons) and attached to a rigid centerbody in a manner
similar to the actual fuselage attachment. The weight of the wing as
tested was not provided.

The wing failed when a total load of 36.4 lb was applied. At this load
there was significant wing deformation and twist. It was difficult to
maintain the loading above the main spar. When the wing bent and
twisted under the highest loads, the "sandbags" slipped toward the
tips and thus increased the bending moments (i.e. altered the
spanwise load distribution.) As the wings began to twist excessively
(trailing edge down) there appeared to be a failure in a number of
ribs near the root and wing failed in torsion. The ribs were "crushed"
and separated from the main spar. The main spar (steel shaft) did
not fail nor undergo any plastic deformation.

1-g Load Distribution:
The approximation to the 1-g load was applied starting at the root.
The load was based upon an assumed aircraft weight of 5.2 lb. but
due to the nature of the loading, it was incremented in 5.7 lb steps.
The spanwise locations where the loads were applied started 2" from
the root and were spaced at 6" intervals. The 1-g load was applied
first and then the 2-g condition was applied by increasing the load
starting at the root. This processes continued until the wing failed.
The wing failed when the total load applied to the wing was 36.4 lb,
and this occurred as the loading was being increased from 6 to 7 g's.

Spanwise location (distance from root in inches)	Load (lb)
2	.5
8	.5
14	.5
20	.4
26	.35
32	.3
38	.2
44	.1

Wing Tip Deflection:

The tip deflection was measured as the load was increased. The tip deflection is presented for even increments in load factor and the last data point taken before failure.

Total Load (lb) - Both wings	Tip Deflection (in)
5.7	1.25
11.4	3.0
17.1	5.0
22.8	6.25
28.5	8.5
34.2	12.5

Additional Information:

Aircraft Weight = 5.2 lb (estimate at this time)
Wing Weight = 17.5 oz

Comparison Between Design and Actual Aircraft Data

	Design Value	Actual Value
Wing Span	88 in	88 in
Wing Area	7.5 ft²	7.5 ft²
Vertical Tail Area	178.2 in²	178.2 in²
Horizontal Tail Area	224 in²	224 in²
Wing Structural Weight (Monokote)	17.1 oz	26.45 oz ← wing plus main landing gear
Wing Structural Weight (no Monokote)	13.0 oz	14.3 oz
Fuselage Structural Weight (Monokote)	14.90 oz	?
Fuselage Structural Weight (no Monokote)	14.00 oz	?
Vertical Tail Weight (Monokote)	1.31 oz	1.41 oz
Vertical Tail Weight (no Monokote)	0.99 oz	—
Horizontal Tail Weight (Monokote)	2.76 oz	2.43 oz
Horizontal Tail Weight (no Monokote)	1.96 oz	—
Landing Gear Weight	4.93 oz	(included in wing)
Propeller Type	Zingali 10-8	Zingali 9-3
Propeller Weight	1.552 oz	1.552 oz
Total Aircraft Weight (post-construction)	5.26 lbs	5.59 lbs
Total Aircraft Weight (post-flight)	5.26 lbs	
CG Location (post-construction)	17.83 in from nose	
CG Location (post-flight)	17.83 in from nose	
Weight of Batteries	22.1 oz	23.67 oz

Please list any other deviations of the technology demonstrater from the original
design.

– the actual batteries we used were different than we designed. This was because the manufacturer
sent the wrong ones. The batteries will offer 0.2 oz more per battery.

	DESIGN	ACTUAL	
MAN HOURS	140 ~ aircraft	175 75 hrs	see back for cost →
	25 ~ component testing		

	Design	Actual
Tooling Cost	$ 100	$ 76.65
MATERIALS COST	$ 168	$ 165 350 ← bought after $ 515
Labor	$ 1400	1757.5
waste		

Wing Team Time Card:

Matt Barrents
Brian Capozzi
Keri Ramsey

ON OFF

Date	Total Hrs	Labor (Hrs *10)	Description	Tooling Cost: (TO+$/mn*mn)	Total Cost:	
04/07			Cutting airfoil template, fuselage section, LE. ↳ Scroll saw !!			11:30 12:15
"			Layout airfoils			11:30 11:4
4/8	(21) 5 min 20 min 15 min		belt sander first airfoils " " jigsaw			Drill Press on
4/9	30 20 min		jigsaw belt sander			
4/9	DAN 4 hrs 15 min		Drill Press (5 min) Jigsaw (5 min)			
4/9	DAN : 4 hrs MATT 3½ hr KERI .7½ hrs		Belt Sander (20 min) Drill (1) JIG SAW (5 min)			
4/11	KERI: 4½ hrs DAN: 3 hrs MATT 4 hrs Bryan 3 hrs		Drill (1 min) JIG (2 min) Sander (5 min)			
4/12	Group 1½ hrs		JIGSAW 15 MIN SANDER 10 MIN			
4/13			JIGSAW 15 MIN SANDER 15 MIN			
4/14	Keri 2 hrs					

Hub
" - "
" - 2.5
" - 6
Dan - 6
Macy - 3.5
Bry - 3
Macy - 3

Group = 5

Macy 2
Bry 2
Keri 1.5

4/13 NIGHT   DAN   2.5
              MATT   2.5
              BRYAN 2.5
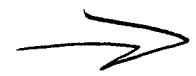
4/16/94)   DAN   8 hRS   DAN   5 hrs
                            DRILL PRESS (10 MIN)   MACY   5 hrs
                            Sander (20 min)   BRYAN 3 hrs
                            JIGSAW (10 min..

4/17/94   DAN   2 ½ hRS
                            JIGSAW (5 min)

                KERI   3 hrs
                MACY   1 hR
                BRYAN   3   SANDER   10 MIN
                                              JIGSAW   15 MIN

4/18/94   KERI   5½   JIGSAW   20 min
                                     SANDER   20 min
             BRIAN   5½

             MACY   5
             BRYAN   3

4-20-94   DAN   3 hrs   JIGSAW   15 MIN
                               SANDER   15 MIN
             MACY   3
             BRYAN   3

4-22   Keri 2.5
             Macy 2.5

4-23   Keri 1
             Macy 1
             Bri- 2
             Matt -1
             Bry 1
             Dan 1